

**Requirement of β 1 integrin for endothelial function,
ischemia-induced blood vascular adaptation
and cardioprotection**

Inaugural-Dissertation

zur Erlangung des Doktorgrades
der Mathematisch-Naturwissenschaftlichen Fakultät
der Heinrich-Heine-Universität Düsseldorf

vorgelegt von

Carina Henning
aus Menden (Sauerland)

Düsseldorf, Juni 2020

aus dem Institut für Stoffwechselphysiologie
der Heinrich-Heine-Universität Düsseldorf

Gedruckt mit der Genehmigung der
Mathematisch-Naturwissenschaftlichen Fakultät der
Heinrich-Heine-Universität Düsseldorf

Berichterstatter:

1. Prof. Dr. Eckhard Lammert
2. Prof. Dr. Ulrich Flögel

Tag der mündlichen Prüfung: 06. August 2020

Table of contents

Summary	1
Zusammenfassung	2
1. Introduction	4
1.1. The cardiovascular system	4
1.1.1. Physiology of the cardiovascular system	4
1.1.2. Femoral and coronary vasculature	8
1.1.3. Cardiovascular diseases	9
1.2. Blood vascular growth and remodeling	12
1.2.1. Collateral circulation existence and function	12
1.2.2. Arteriogenesis	14
1.3. Mechano-signaling in the endothelium	17
1.3.1. Influence of hemodynamic changes	17
1.3.2. Mechanotransduction via β 1 integrin signaling	18
1.4. Aims of the thesis	20
2. Experimental procedure	22
2.1. Mouse lines	22
2.1.1. Genotyping	22
2.2. <i>In vivo</i> and <i>ex vivo</i> procedure	24
2.2.1. Flow-mediated vasodilation (FMD)	24
2.2.2. Hindlimb ischemia	24
2.2.3. Myocardial ischemia	25
2.2.4. Osmotic pumps implantation for proliferation detection	26
2.2.5. Pimonidazole treatment	26
2.2.6. Magnetic resonance imaging (MRI)	26
2.2.7. Echocardiography	27
2.2.8. Triphenyl tetrazolium chloride (TTC) staining	27
2.2.9. Microfil® perfusion of the coronary vasculature	28
2.2.10. Tissue isolation	28
2.3. Immunohistochemistry	29
2.3.1. Equilibration, embedding and cryosectioning	29
2.3.2. Immunostaining	29
2.3.3. Microscopy and image analysis	30
2.4. Magnetic-activated cell sorting (MACS) of ECs	30
2.5. Molecular and biochemical methods	31

2.5.1. Quantitative real-time PCR.....	31
2.5.2. Western blotting	32
2.5.3. Enzyme-linked immunosorbent assay (ELISA).....	33
2.6. Statistical analysis.....	34
2.7. Personal contribution.....	34
3. Results.....	36
3.1. Role of endothelial cell-specific β1 integrin in hindlimb ischemia.....	36
3.1.1. Endothelial β 1 integrin is required for flow-mediated vasodilation (FMD).....	36
3.1.2. Endothelial β 1 integrin is required for ischemia-induced arterial and capillary vessel growth	38
3.2. Transient, repetitive myocardial ischemia reperfusion.....	42
3.3. Role of β1 integrin functionality in Repl/R.....	45
3.3.1. Repl/R-induced cardiac endothelial cell proliferation is impaired by β 1 integrin blockage.....	45
3.3.2. Repl/R-induced blood vascular growth is reduced by β 1 integrin blockage.....	47
3.3.3. Repl/R-induced cardioprotection is sensitive to β 1 integrin blockage.....	49
3.4. Role of endothelial cell-specific β1 integrin in Repl/R.....	53
3.4.1. Quantification of β 1 integrin KO efficiency in cardiac endothelial cells	54
3.4.2. Repl/R-induced cardiac endothelial cell proliferation is controlled by endothelial β 1 integrin	55
3.4.3. Repl/R-induced blood vascular growth is partially influenced by endothelial β 1 integrin	56
3.4.4. Repl/R-induced cardiac protection is impaired by endothelial β 1 integrin deletion	58
3.5. Myocardial ischemia-induced hepatocyte growth factor secretion is regulated by β1 integrin	59
3.6. Role of β1 integrin in permanent myocardial ischemia.....	61
3.6.1. Permanent myocardial ischemia-induced vascular adaptation is regulated by endothelial β 1 integrin	62
3.6.2. Maintenance of cardiac function and survival after permanent myocardial ischemia requires endothelial β 1 integrin	64
4. Discussion.....	66
4.1. Role of β1 integrin in transmission of hemodynamic changes	66
4.2. Role of β1 integrin in vascular adaptation	68
4.2.1. Impact of β 1 integrin for cardiac endothelial cell proliferation.....	69
4.2.2. Impact of β 1 integrin for arteriole and capillary formation.....	70
4.3. Role of β1 integrin in cardioprotection.....	73

4.4. Clinical relevance of targeting β 1 integrin	74
4.5. Conclusion	76
Supplementary information	78
Reference	79
Publications	92
Abbreviations.....	94
List of figures	97
Declaration	99
Danksagung	100

Summary

The cardiovascular system, which includes the heart, all types of blood vessels and the blood, guarantees the optimal supply of all organs and tissues with oxygen, nutrients and other vital metabolites. Dysfunction or weakening of this fundamental network can be life-threatening and is mostly caused by cardiovascular diseases (CVDs) like coronary artery diseases (CADs) or peripheral vascular diseases (PVDs), in which the blood supply is disrupted. However, in some cases the blood vascular system is able to adapt in a protective way by providing blood supply from a collateral circulation. Therefore, it is of huge clinical interest to gain knowledge in the field of vascular growth and remodeling, helping to develop alternative treatments for patients with CVDs.

Hemodynamic changes are believed to be essential in terms of blood vessel adaptation. They occur directly upon artery restriction and occlusion, and can be sensed by mechanosensitive receptors, like integrins. Related to this, the here presented study analyzed the relevance of the subunit $\beta 1$ integrin for endothelial function, for ischemia-induced vascular growth as well as for cardioprotection in different clinically relevant *in vivo* mouse models for CVDs. In this context, $\beta 1$ integrin signaling was inhibited by intravenous injection of specific blocking antibodies as well as by endothelium-specific depletion of the *Itgb1* gene, both in adult mice. First, investigations in a hindlimb ischemia model showed $\beta 1$ integrin to be essential for endothelial function, which was measured by flow-mediated vasodilation (FMD). However, the flow velocity was not changed by manipulation of $\beta 1$ integrin expression. Further experiments in the hindlimb ischemia model could demonstrate that endothelial $\beta 1$ integrin is also needed for long-term vascular adaptation. Those results were strengthened by additional findings from two different adult myocardial ischemia models. Here in the first model, transient coronary artery occlusions contributed to cardiac endothelial cell proliferation, arteriole growth and subsequent cardioprotection in a $\beta 1$ integrin dependent manner. Finally, integrin signaling was further investigated in an acute myocardial ischemia model, in which the relevance of endothelial $\beta 1$ integrin became even more significant. Here, it was proven that the presence and functionality of endothelial $\beta 1$ integrin is strictly needed for preservation of cardiac function and protection from fatal cardiac rupture after myocardial infarction (MI).

Taken together, this thesis provides evidence and new insights for the essential role of endothelial $\beta 1$ integrin in terms of endothelial function, cardioprotective vascular adaptation and protection from cardiac death upon MI. Therefore, results exhibit clear clinical relevance, and targeting endothelial $\beta 1$ integrin in the future might be promising for patients with CVDs.

Zusammenfassung

Das Herz-Kreislaufsystem, welches aus dem Herzen, allen Arten von Blutgefäßen und dem Blut besteht, gewährleistet eine optimale Versorgung aller Organe und Gewebe mit Sauerstoff, Nährstoffen und weiteren überlebensnotwendigen Metaboliten. Eine Funktionsstörung oder Schwächung dieses elementaren Systems kann lebensbedrohlich sein und wird oft durch kardiovaskuläre Erkrankungen, wie koronare Herzerkrankungen oder periphere Gefäßerkrankungen, verursacht, die die Blutversorgung beeinträchtigen. In manchen Fällen ist das Blutgefäßsystem allerdings in der Lage, sich anzupassen, was auf eine schützende Weise wirkt, indem es Blut aus einer Kollateralzirkulation bereitstellt. Daher ist es von bedeutender klinischer Relevanz, weitere Erkenntnisse auf dem Gebiet des Blutgefäßwachstums und -umbaus zu erhalten, um alternative Therapieansätze für Patienten mit kardiovaskulären Erkrankungen zu entwickeln.

Es wird angenommen, dass hämodynamische Veränderungen im Hinblick auf Blutgefäßanpassungen essentiell sind. Sie treten unmittelbar bei Arterienverengung und -verschluss auf und können von mechanosensitiven Rezeptoren, wie den Integrinen, wahrgenommen werden. Im Zusammenhang dessen wurde in dieser Arbeit die Relevanz der Untereinheit $\beta 1$ Integrin für die Endothelfunktion, für das Ischämie-induzierte Blutgefäßwachstum, wie auch für die Kardioprotektion in verschiedenen klinisch relevanten *in vivo* Mausmodellen für kardiovaskuläre Erkrankungen analysiert. Hierbei wurde die Signalweiterleitung des $\beta 1$ Integrin Rezeptors durch intravenöse Injektion eines spezifischen blockierenden Antikörpers unterbunden sowie durch einen endothel-spezifischen Verlust des *Itgb1* Gens in erwachsenen Mäusen verursacht. Als Erstes zeigten Untersuchungen in einem Hinterlaufsischämie-Modell, dass endotheliales $\beta 1$ Integrin notwendig ist für die Endothelfunktion, was durch flussvermittelte Vasodilatationsmessungen ermittelt wurde. Dabei wurde die Flussgeschwindigkeit durch Beeinflussung der $\beta 1$ Integrin Expression allerdings nicht verändert. Weitere Experimente im Hinterlaufsischämie-Modell konnten zeigen, dass endotheliales $\beta 1$ Integrin auch für die langfristige vaskuläre Anpassung notwendig ist. Darüber hinaus konnten diese Befunde in zwei weiteren adulten Myokardischämie-Modellen bestätigt werden. Mit Hilfe des ersten Modells konnte gezeigt werden, dass vorübergehende Verschlüsse eines Herzkranzgefäßes zur Proliferation von Herzendothelzellen, zum Wachstum von Arteriolen und der anschließenden Kardioprotektion, in Abhängigkeit von $\beta 1$ Integrin beitragen. Schließlich wurde die Integrin-vermittelte Signalweiterleitung in einem weiteren Modell für akute Myokardischämie untersucht, indem die Relevanz von endothelialelem $\beta 1$ Integrin noch deutlicher wurde. Hiermit konnte nachgewiesen werden, dass die Anwesenheit und die Funktionalität von endothelialelem $\beta 1$ Integrin zur Aufrechterhaltung der Herzfunktion und dem Schutz vor einer tödlichen Herzruptur, in Folge eines Herzinfarktes, zwingend erforderlich ist.

Zusammengefasst erbringt diese Arbeit Belege und neue Erkenntnisse zur essentiellen Rolle von endothelialelem $\beta 1$ Integrin für die Endothelfunktion, für die kardioprotektive Gefäßanpassung und für den Schutz vor einem Myokardinfarkt-bedingtem Herztod. Daher zeigen die dargelegten Daten klare klinische Relevanz und die Anvisierung von $\beta 1$ Integrin könnte zukünftig für Patienten mit kardiovaskulären Erkrankungen vielversprechend sein.

1. Introduction

1.1. The cardiovascular system

1.1.1. Physiology of the cardiovascular system

The circulatory system of the body forms a network of connecting vessels and is separated into the blood circulatory system, also called cardiovascular system and the lymphatic system (Pugsley and Tabrizchi, 2000; Urner et al., 2018). The cardiovascular system enables blood circulation and is furthermore divided into the systemic circulation, which provides the organism with oxygen and nutrients to ensure vital metabolic processes (Fig. 1.1), and the pulmonary circulation, where the gas exchange in the lungs happens.

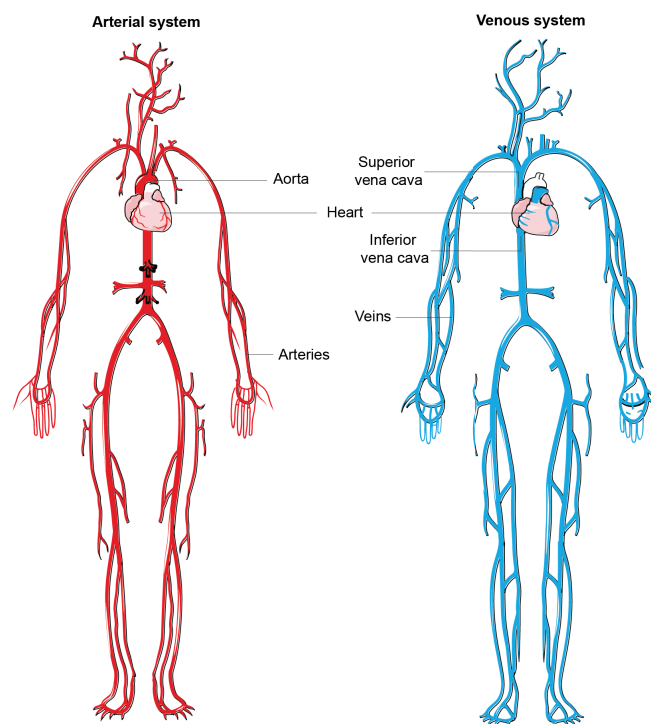


Figure 1.1: Schematic illustration of the cardiovascular system.

Separation of the blood circulatory system in (left) the arterial and (right) the venous part, only showing the systemic circulation. The heart is located in the centrum, the *inferior mediastinum*, from which the aorta emerges and separates into smaller arteries and arterioles, running into the periphery. Smaller venules and veins from the periphery merge into the superior and inferior vena cava back to the heart. Modified from Servier Medical Art, subpoint "Cardiovascular system" and used under the terms of the free-to-use Creative Commons Attribution 3.0 Unported License, <https://smart.servier.com>

Also, other metabolites like carbon dioxide, hormones and waste products are transported via the cardiovascular system (Campbell et al., 2009; Lammert and Zeeb, 2014; Moyes and Schulte, 2008). The heart, all types of blood vessels and the blood itself belong to this complex system and are formed early in embryonic development due to their central role for survival and organ homeostasis (Baldwin, 1996; Brand, 2003; Breier, 2000; Moorman et al., 2003).

The heart is placed within the thoracic cavity, located in the *inferior mediastinum*, surrounded and protected by the rib cage, next to the right and left lobe of the lung (Treuting and Dintzis, 2012). It is characterized by its conical shape, with its lower part, the apex, located to the left side of the thorax (Treuting and Dintzis, 2012). For protection, the heart is embedded into the pericardium, a connective sac-like tissue surrounding the heart and further separated into the fibrous and serous pericardium (Lange, 2013). The pericardium is essential to hold the heart in place while moving, but also allows the heart to expand and contract during every single heartbeat. Furthermore, the pericardium produces pericardial fluid to reduce friction between the surface of the heart and the pericardium itself (Moyes and Schulte, 2008). The inner layer of the pericardium, the epicardium is directly connected to the myocardium, which is the middle layer of the heart wall and the largest one. With its cardiac muscle fibers, the myocardium is responsible for the contractive function of the heart. Followed by the innermost and thinnest layer of the heart wall, named endocardium (Moyes and Schulte, 2008). Endocardial cells line the ventricles and stay in direct contact to the blood, pumped by the ventricles. Due to these characteristics endocardial cells show high similarity to endothelial cells, which represent the innermost layer of all blood vessels (Misfeldt et al., 2009).

In general, the physiological function of the heart is to contract regularly to supply all organs, tissues and cells with fresh blood to maintain their metabolic function (Campbell et al., 2009; Lammert and Zeeb, 2014; Moyes and Schulte, 2008). To ensure the function a mammalian heart is separated into four chambers, the left and right atrium as well as the left and right ventricle. Furthermore, the right heart side is separated by a septum from the left side (Lammert and Zeeb, 2014; Moyes and Schulte, 2008; Treuting and Dintzis, 2012). The chambers are additionally divided by cardiac valves, which prevent backflow of blood. The tricuspid valve is located between the right atrium and the right ventricle, while the bicuspid or mitral valve separates the left atrium from the left ventricle. Furthermore, the arteries leaving the heart and the ventricles are divided by semilunar valves. The pulmonary valve is located between the right ventricle and the pulmonary artery, while the aortic valve separates the left ventricle from the aorta (Lammert and Zeeb, 2014; Moyes and Schulte, 2008).

The pumping process of the heart is ensured by coordinated contraction of cardiac muscle fibers located in the myocardium, mainly performed by cardiomyocytes, representing the central subgroup of cardiac cells (Talman and Kivela, 2018). But the heart is also composed of other cell types, like cardiac fibroblasts, blood and lymphatic endothelial cells, and peri-vascular cells, like smooth muscle cells (SMCs) or pericytes (Talman and Kivela, 2018; Xin et al., 2013; Zhou and Pu, 2016). Those other cell types are essential for the maintenance of the heart homeostasis as they provide components for the extracellular matrix, or guarantee and regulate blood supply in form of the cardiac vasculature (Talman and Kivela, 2018).

To pump blood into the circulatory system, the heart relaxes and the ventricles are filled with blood, which is called diastole. This is followed by the systole, in which the ventricles contract and the blood is pumped into the body via the main arteries (Lammert and Zeeb, 2014; Moyes and Schulte, 2008). From here the blood is transported through the blood vascular system to the regions of demand. The aorta, the largest artery in the body, carries the blood away from the heart and separates into smaller arteries, arterioles and finally into capillaries, the smallest blood vessels, where the gas and nutrient exchange takes place. Afterwards, the blood flows back to the heart through venules, veins and the vena cava (Lammert and Zeeb, 2014; Moyes and Schulte, 2008; Urner et al., 2018). In general, arteries carry the blood away from the heart. In the systemic circulation, arteries transport oxygen-rich blood into the body's periphery, while in the pulmonary circulation arteries provide oxygen-deficient blood for gas exchange in the lungs. In contrast, veins transport blood back to the heart. In the systemic circulation blood coming from the periphery is low in oxygen levels, whereas in the pulmonary circulation veins carry oxygen-rich blood to the heart (Campbell et al., 2009; Lammert and Zeeb, 2014; Moyes and Schulte, 2008).

Arteries are characterized by thicker vessel walls than veins as they are exposed to a higher blood pressure generated by the heart's contraction. Due to lower blood pressure and gravity, most of the veins, especially in the limbs, have valves to prevent backflow of blood (Campbell et al., 2009; Lammert and Zeeb, 2014; Moyes and Schulte, 2008). Despite these differences all blood vessels are characterized by an inner lumen, in which the blood passes through. The blood vessel wall consists of three layers (Fig. 1.2), the *tunica intima*, which is the innermost layer made of endothelial cells (ECs) and a basal lamina. The *tunica media* forms the middle layer, surrounding the *tunica intima* and consists of SMCs and elastic fibers, mainly elastin. Contraction and relaxation of the SMC layer causes vasoconstriction and vasodilation, which regulates the blood flow. The outer layer of blood vessels is called *tunica externa* and is formed by layers of collagen tissue for stabilization (Lammert and Zeeb, 2014; Moyes and Schulte, 2008).

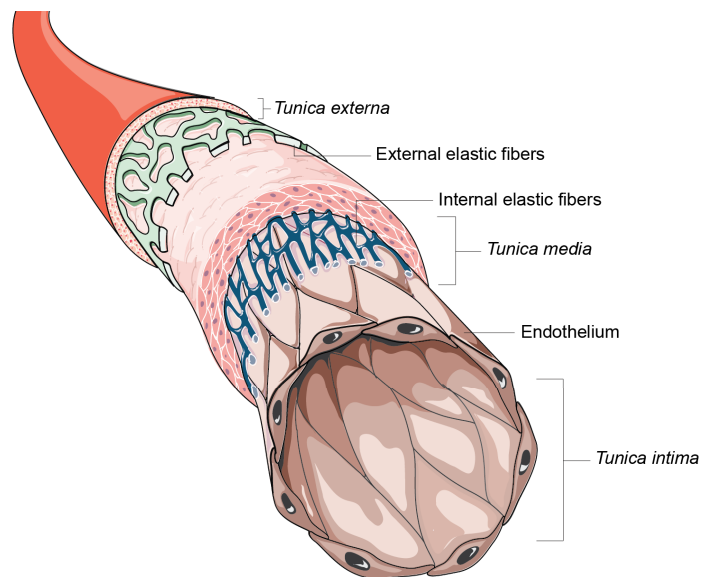


Figure 1.2: General structure of blood vessels.

Separation of blood vessels into three layers. The *tunica intima*, the innermost layer, formed by the endothelium and the basal lamina, the *tunica media*, surrounded by internal and external elastic fibers, and the outer layer, the *tunica externa*. Modified from Servier Medical Art subpoint “Cardiovascular system” and used under the terms of the free-to-use Creative Commons Attribution 3.0 Unported License, <https://smart.servier.com>

The thickness of the individual layers differs between blood vessel types. However, capillaries are only composed of the *tunica intima* and surrounded by contractile pericytes (Aird, 2007b; Lammert and Zeeb, 2014; Moyes and Schulte, 2008). Capillaries are forming networks, named capillary beds, and due to their thin vessel walls an optimal exchange of oxygen and nutrients between blood and tissue is ensured. Three different kinds of capillary types are known: continuous, fenestrated and sinusoidal capillaries that all differ in the structure of their *tunica intima* (Aird, 2007a; Moyes and Schulte, 2008). In capillaries, ECs are connected with each other via tight-junctions to form a monolayer of cells. Continuous capillaries are characterized by the presence of tight-junctions connecting the ECs. Furthermore, they miss fenestrae, which are small pores in the plasma membrane. Due to their tight connection, the exchange of substances is limited to few molecules that can pass the vessel wall. Therefore, continuous capillaries are found in the blood-brain barrier (Moyes and Schulte, 2008). Fenestrated capillaries are built up similar to the continuous capillaries with the only exception of their numerous presence of fenestra. Small molecules and fluid can pass the pores easily, which facilitates the exchange between blood and tissue (Moyes and Schulte, 2008). ECs in sinusoidal capillaries are loosely connected with each other, have less tight-junctions, large intercellular gaps and a discontinuous basement membrane (BM) to allow the exchange of large molecules. Sinusoidal capillaries are found in highly specialized organs, like the liver or spleen (Aird, 2007a; Moyes and Schulte, 2008).

As described, the cardiovascular system is highly complex with its different components, and is specialized in its function to maintain vital processes of the organism. Therefore, the successful interaction and adjustment of all components together, termed by the heart, all blood vessels and the blood, are essential for the physiology and homeostasis of all organs. Damage or disruption of one or more components could contribute to imbalance and pathological conditions.

1.1.2. Femoral and coronary vasculature

With every heartbeat blood is pumped into the systemic circulation via the aorta. After leaving the heart, the aorta is later divided into the thoracic and abdominal aorta. Finally, the abdominal aorta branches into smaller arteries, the right and left common iliac artery, which in turn separate into the external and internal iliac artery (Hwang, 2017; Swift and Bordoni, 2020). As a continuation of the external iliac artery, the common femoral artery arises, which distributes blood into the lower extremities, as the thigh and calf. The common femoral artery afterwards branches into the deep femoral artery, also known as the *profunda femoris* and the superficial femoral artery. The *profunda femoris* with its further branches, supplies the main part of the hip and the thigh, while the superficial femoral artery ensures the transport from oxygen-rich blood to the entire calf (Reardon et al., 2004; Swift and Bordoni, 2020).

The here presented network of vessels describes only a small section of the peripheral blood vasculature, which includes all blood vessels except for the coronary vasculature. The arteries of the coronary vasculature ensure the heart's own blood supply with oxygen and nutrients. Two main coronary arteries arise directly from the *sinus aortae*, the right coronary artery (RCA) and the left coronary artery (LCA) (Fig. 1.3). More precisely, the RCA starts in the *sinus aortae dexter* and the LCA directly above the aortic valve in the *sinus aortae sinister* (Lange, 2013; Treuting and Dintzis, 2012). After arising from the *sinus aortae dexter*, the RCA branches into the posterior descending artery, also called *ramus interventricularis posterior*, and the right marginal artery or *ramus marginalis dexter*. On the left side of the aortic root the LCA is early divided into the left circumflex artery (LCX), or *ramus circumflexus*, and the left anterior descending artery (LAD), also known as *ramus interventricularis anterior* (Lange, 2013; Treuting and Dintzis, 2012).

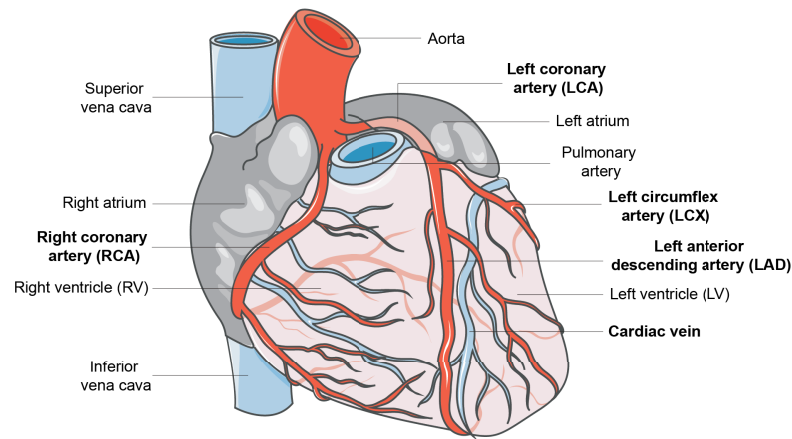


Figure 1.3: Schematic image of the coronary vasculature.

Heart showing both ventricles and atria, the beginning of the vena cava, the pulmonary artery and the aorta. The aorta supplies the heart via two main coronary arteries, the right (RCA) and the left coronary artery (LCA). Illustration of the early branch of the LCA into the left circumflex (LCX) and the left anterior descending artery (LAD). Most cardiac veins run in parallel to the arteries. Modified from Servier Medical Art subpoint “Cardiovascular system” and used under the free-to-use Creative Commons Attribution 3.0 Unported License, <https://smart.servier.com>

After branching into coronary capillaries, the oxygen-deficient and nutrient-poor blood is transported back into coronary veins, which mainly run parallel to the arteries. They fuse together in the *sinus coronarius*, which ends in the right atrium and delivers the blood back into the pulmonary circulation (Bilazarian et al., 1991; Lange, 2013; Treuting and Dintzis, 2012).

The anatomy of the coronary vasculature can differ between humans, which was first described decades ago (Banchi, 1904). These days, three dominant types are known. The right-dominant circulation type is the most prominent one and is characterized by the right coronary artery continuing into the posterior descending artery. Secondly, the left-dominant type is defined, when the posterior descending artery is actually an extension of the circumflex artery. And lastly, the co-dominant or balanced type exists, where the circumflex and right coronary artery both supply the posterior descending artery with blood (Fuster et al., 2001; Lange, 2013; Shriki et al., 2012; Treuting and Dintzis, 2012; Villa et al., 2016).

1.1.3. Cardiovascular diseases

The cardiovascular system is involved in a variety of pathological conditions, called cardiovascular diseases (CVDs). CVDs include all diseases affecting the heart and the blood vessels, like coronary artery diseases (CADs), stroke, peripheral vascular diseases (PVDs), cardiomyopathies as well as rheumatic and congenital heart diseases (Collaborators, 2018). All CVDs together represent the leading cause of death globally (Di Angelantonio et al., 2019). In 2017, around 17.8 million people died due to CVDs, and it is predicted that in 2030 the

number of fatalities will reach over 24 million cases (Collaborators, 2018; Di Angelantonio et al., 2019; Fuster et al., 2011). Well known risk factors for CVDs include unmodifiable factors like age, gender or a genetic predisposition as well as modifiable factors, which are dependent on the person's lifestyle, like hyperglycemia, hyperlipidemia, smoking or physical inactivity. Also a combination of both, such as in pathological conditions like hypertension or diabetes mellitus, which can be caused by genetic, environmental and lifestyle factors, plays an important role in the development of CVDs (Fuster et al., 2011; Lu et al., 2015; Piepoli et al., 2016; Yu et al., 2018).

Especially CVDs affecting the coronary vasculature, known as coronary artery diseases (CADs), coronary heart diseases (CHDs) or ischemic heart diseases (IHDs) represent the deadliest form, as around 9 million deaths were caused by CADs in 2017 (Collaborators, 2018). CADs arise due to a reduction of blood flow in the coronary arteries. A narrowing or a complete blockage of a coronary artery results in an insufficient oxygen and nutrient supply of the myocardium, defined as ischemia (Lange, 2013; Thygesen et al., 2012). A myocardial infarction (MI), or a heart attack is the consequence of long-lasting ischemia (Thygesen et al., 2012). Prolonged ischemia of 20 to 30 minutes induces myocardial cells death, meaning that the heart tissue gets necrotic and is irreversibly damaged (McCorry et al., 2019). Such an event can lead to death, or depending on the area affected, contributes to complications like arrhythmias, cardiogenic shock, pericarditis, myocardial rupture or heart failure (McCorry et al., 2019). The frequency of blockage varies between the branches of the coronary arteries. The LAD is the most affected one as it is blocked in around 50% of cases, followed by the RCA and finally the LCX, which are both less affected (McCorry et al., 2019).

The presence of a MI is often attended by typical symptoms like chest pain, shortness of breath, sweating, nausea, fatigue and anxiety, and can be detected by an electrocardiogram (ECG) (Lu et al., 2015). Thereby, it can be distinguished between a STEMI (ST elevation myocardial infarction) or an NSTEMI (non-ST elevation myocardial infarction). The presence of a STEMI results from a complete thrombogenic blockage of a coronary artery and is characterized by a ST-segment elevation higher than the baseline signal (Kingma, 2018; Lu et al., 2015; Manari et al., 2009). In contrast, NSTEMIs do not show this typical elevation, moreover, they represent a depression, which can be explained by an incomplete blockage of a coronary artery or the occurrence of a coronary artery spasm (Kingma, 2018; Manari et al., 2009). Furthermore, an additional method to diagnose a MI is the detection of released troponin I, troponin T and creatine kinase (CK-MB) from dying cardiac cells into the blood stream (Knuuti et al., 2020; Lu et al., 2015; Roffi et al., 2016).

The most common cause of CVDs is the development of atherosclerosis, which begins years before and is characterized by the enrichment of lipids and fibrous particles in large and medium-sized arteries (Ambrose and Singh, 2015; Libby et al., 2019; Lusis, 2000). Atherosclerosis starts in an initial phase, in which the *tunica intima*, the inner lining of the

arteries gets irritated and damaged, mostly due to risk factors like smoking, hypertension, hyperglycemia or hyperlipidemia. The resulting endothelial cell damage and dysfunction facilitates the permeability and accumulation for plasma components like low-density lipoprotein (LDL) (Hansson and Hermansson, 2011; Hansson and Libby, 2006). Other apolipoprotein B-containing lipoproteins like very low-density lipoproteins, intermediate density lipoproteins or lipoprotein(a) are involved in the process of atherosclerotic plaque formation as well (Ference et al., 2017; Goldstein and Brown, 2015; Libby et al., 2019; Wolf and Ley, 2019). The enrichment of lipoproteins and their processing during oxidation, lipo- and proteolysis and aggregation, initiates the second, inflammatory phase of atherosclerosis (Lusis, 2000). Circulating monocytes and lymphocytes are recruited by the release of chemokines like monocyte chemoattractant protein-1 (MCP-1), also known as C-C motif chemokine ligand 2 (CCL2), CCL5, C-X-C motif chemokine ligand 10 (CXCL10) and C-X3-C motif chemokine ligand 1 (CX3CL1). These trigger the migration of monocytes, T-cells and dendritic cells into the *tunica intima* (Hansson and Hermansson, 2011; Zernecke et al., 2008).

Monocytes in the intima convert into macrophages, take up the oxidized LDL via their scavenger receptors, and start phagocytosing them. In a next step, known as foam cell formation, the macrophages turn into foam cells, die and release the highly oxidized lipids into the intima, visualized as fatty streaks (Hansson and Libby, 2006; Insull, 2009; Lange, 2013). In contrast, it was shown that high-density lipoprotein (HDL) appears to be protective, as it inhibits the oxidation of LDL and helps removing cholesterol (Lusis, 2000). As the core of the atheroma is growing due to lipid, cholesterol and immune cell accumulation, a fibrous cap made of SMCs and collagen is build up too (Hansson and Libby, 2006). All these processes together lead to a narrowing of the artery but not yet to a full occlusion. The growing plaque is constantly exposed to the inner blood flow, which can lead to a rupture of the fibrous cap. Therefore, the plaque gets thrombogenic meaning thrombocytes accumulate and agglutinate, which can lead to a complete blockage of the artery, resulting in a MI, stroke or peripheral artery occlusion (Hansson and Libby, 2006; Lange, 2013; Libby, 2013).

As the incidence and the mortality rate of CVDs is practically high and will still rise in the next years, research in this field is of main relevance for the entire society. To study and to understand the processes and signaling pathways in pathological conditions, mouse models are used due to their genetic and physiological similarities to humans (Perlman, 2016; Rosenthal and Brown, 2007). Even for the research on CVDs, mouse models were developed and established in the science community. To study the outcomes or the influences of an acute MI, different myocardial ischemia models were generated, in which the LAD is temporary or permanently occluded (Lindsey et al., 2018). Similar to the human situation, mice own two main coronary arteries, the RCA and the LCA, with comparable branches (Treuting and Dintzis, 2012). In mice, the LAD is the easiest accessible coronary artery for surgeries and is also the

most blocked artery in humans. Additionally, other CVDs like stroke or PVDs are investigated in mouse models as well. For experimental stroke studies a transient middle cerebral artery occlusion (tMCAO) is performed, in which the right internal carotid artery is occluded via an insertion of a transluminal suture (Clark et al., 1997; Liu and McCullough, 2014). Another model to examine the impacts of pathological ischemia is the hindlimb ischemia, in which the femoral artery is occluded. Induction of hindlimb ischemia mimics conditions of PAD and exists as an established model for research on adult vascular growth and remodeling *in vivo* (Limbourg et al., 2009; Niiyama et al., 2009). Especially studies on the latter are essential for the investigation of revascularization strategies in the context of CVDs.

1.2. Blood vascular growth and remodeling

1.2.1. Collateral circulation existence and function

To reduce the high numbers of patients affected by CVDs, current prevention strategies are based on changes towards a healthy lifestyle, such as diet adaptation, exercise increase and smoking cessation, as well as medical treatment to lower blood lipid levels with statin intake and to regulate hypertension (Piepoli et al., 2016; Virani et al., 2020). Furthermore, a natural or endogenous prevention system exists, called collateral circulation, in which an alternative blood supply is provided to compensate a blockage of a major artery (Faber et al., 2014). Collaterals are anastomotic artery-to-artery connections, and they exist in different regions of the organism like in the brain, the heart or lower extremities (Faber et al., 2014; Jamaiyar et al., 2019; Meier et al., 2013). More than 60 years ago the presence of collaterals in the human heart was observed in studies that made clear that coronary arteries were no end arteries (Baroldi et al., 1956; Fulton, 1956; Meier et al., 2013). It is believed that a well-developed and functional collateral network can protect from ischemia injury like in CADs or PADs (Fig. 1.4) (Faber et al., 2014; Gloekler and Seiler, 2007; McDermott et al., 2014; Seiler, 2010). Especially in patients under life-threatening conditions like during a MI, the existence of coronary collaterals can improve the outcome, as they can limit infarction size, maintain cardiac function, support cardiac remodeling after an ischemic heart event and most importantly reduce mortality rates (Cohen and Rentrop, 1986; Habib et al., 1991; Jamaiyar et al., 2019; Kodama et al., 1996; Zimarino et al., 2014). Furthermore, the development and the extent of a wide coronary collateral circulation differs individually, and is likely to be dependent on genetic predisposition, exercise training and the occurrence of CADs (Gloekler and Seiler, 2007). In some clinical trials it was observed that one third of patients with CADs showed sufficient collateralization to prevent a myocardial ischemic event, comparable to one fifth to one quarter in people without CADs (Pohl et al., 2001; Wustmann et al., 2003).

Several decades ago, Fulton observed collaterals or anastomoses in normal and diseased hearts and determined larger ones in the presence of CADs (Fulton, 1963; Seiler et al., 2013). Thus, slow and partial constriction or occlusion of coronary arteries as in the case of CADs can initiate the process of collateral formation under pathological conditions (Jamaiyar et al., 2019). Moreover, further studies showed a correlation between the presence of angina pectoris and collateral recruitment. Angina pectoris, or short angina, can be a symptom of CADs, often caused by coronary narrowing mainly due to formation of atherosclerotic plaques, and is noticed by chest tightness and pain (Abrams, 2005; Balla et al., 2018; Bergheanu et al., 2017). Decades ago research could show that patients with history of angina could represent a well-developed coronary collateral network (Billinger et al., 2002; Fujita et al., 1987; Fulton, 1964; Piek et al., 1997). Furthermore, chronic angina before a MI reduces infarction size compared to shorter periods or absence of angina (Herlitz et al., 1993).

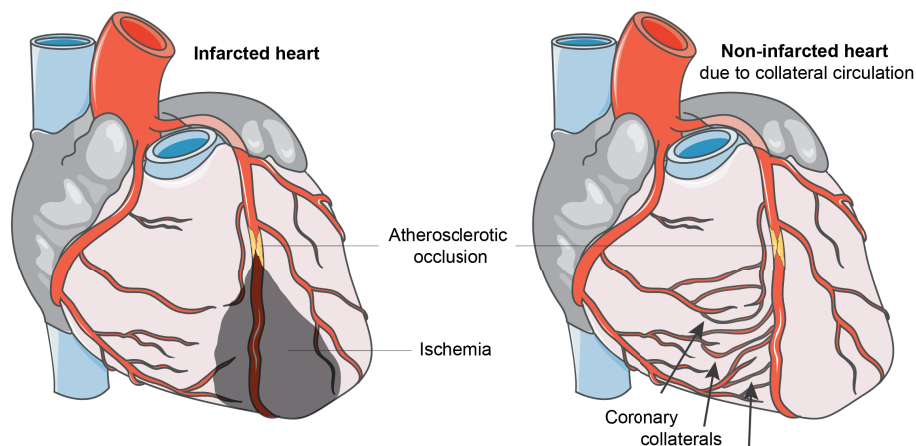


Figure 1.4: Schematic illustration of coronary collaterals.

Hearts showing the main coronary arteries, in which an artery is occluded by an atherosclerotic plaque. (left) Upon total artery blockade the supplied myocardium suffers from ischemia (gray area) and the heart region gets infarcted. (right) By the growth of a well-developed and functional coronary collateral circulation the myocardium stays non-infarcted. Arrows indicate the presence of coronary collaterals. Based on review (Gloekler and Seiler, 2007) and modified from Servier Medical Art subpoint “Cardiovascular system” and used under the free-to-use Creative Commons Attribution 3.0 Unported License, <https://smart.servier.com>

Physiological changes, as during exercise training, also improve the collateralization of the heart. It was shown that months of endurance training could increase the collateral flow index, which serves as degree of collateralization in normal and stenosed vessels (Zbinden et al., 2007; Zbinden et al., 2004). Furthermore, another study demonstrated the benefit of moderate and high-intensity training on the collateral flow index in patients with CADs as well (Möbius-Winkler et al., 2016). These findings point in the same direction as previously

reviewed that patients diagnosed with CADs can effectively improve coronary collateral development by exercise training (Fujita and Sasayama, 2010; Heaps and Parker, 2011). Moreover, the degree of collateralization is dependent on genetic factors and the influence of other diseases. For instance, people affected by the metabolic disorder, diabetes mellitus, show impaired collateral formation in the coronaries as well as in the peripheral vasculature (Abaci et al., 1999; Hinkel et al., 2017; Ruitter et al., 2010; Shen et al., 2018).

A functional compensative collateral network is influenced by many factors, but a native or a pre-existing collateral circulation is embryonically and postnatally developed in different species and organs (Faber et al., 2014). The formation of native collaterals is called collaterogenesis and defines the grade of a native collateral circulation in adults (Chalothorn and Faber, 2010; Clayton et al., 2008; Faber et al., 2014; Lucitti et al., 2012; Zhang et al., 2019). At this stage, native collaterals need to remodel and to enlarge to get functional as alternative blood supply to the stenosed ischemic area (Jamaiyar et al., 2019). This increase happens slowly over time, which can take decades. Thus, the development and remodeling of collaterals require vascular growth, including immune cell infiltration, endothelial and smooth muscle cell proliferation as well as extracellular matrix (ECM) degradation and rearrangement (Meier et al., 2013; Schaper, 2009; van Royen et al., 2009).

1.2.2. Arteriogenesis

Different models and mechanisms of blood vascular growth exist during development, adulthood and disease conditions. During early embryonic development, the first blood vessels are formed *de novo* by vasculogenesis, a process in which angioblasts, vascular progenitor cells, differentiate into endothelial cells (Carmeliet and Jain, 2011; Potente et al., 2011). After initial induction of a primitive vascular labyrinth, vessels sprout out into a vascular network via angiogenesis. The sprouting of vessels is mainly initiated by hypoxic conditions in the tissue and achieves a greater capillarization (Carmeliet and Jain, 2011; Persson and Buschmann, 2011; Potente et al., 2011). Furthermore, arteriogenesis represents a third form of blood vessel formation. During development, arteriogenesis is characterized by SMC recruitment, specification of endothelial cells (ECs), formation of the arterial vessel wall and branching of the arterial tree. But also the formation of native or pre-existing collaterals is defined by this term (Simons and Eichmann, 2015). Furthermore, in adulthood, arteriogenesis is termed as adaptation process to pathological conditions during artery occlusions. Mainly two distinct types of adult arteriogenesis are known.

The first type is the “classical” form of arteriogenesis, which is forced by hemodynamic changes inducing increased shear stress in the collateral network. Thus, pre-existing collaterals expand and enlarge (Heil and Schaper, 2004; Schaper, 2009; Simons and Eichmann, 2015; Simons and Ware, 2003). Shortly after artery restriction or occlusion a pressure gradient develops, leading to shear stress-dependent endothelial nitric oxide synthase (eNOS) activation and vasodilation as acute response (Cai and Schaper, 2008; Hofer et al., 2013). During acute vasodilation, circumferential wall stress (CWS) increases, adhesion molecules like vascular cell adhesion molecule-1 (VCAM-1) and intercellular adhesion molecule-1 (ICAM-1) are upregulated, and monocytes are recruited by MCP-1. Those monocytes migrate and release extracellular scaffold digesting proteases. Furthermore, the endothelium starts secreting growth factors, including basic fibroblast growth factor (bFGF), platelet derived growth factor-B (PDGF-B) and transforming growth factor beta 1 (TGF- β 1). Growth factor secretion induces EC and SMC proliferation, which is essential for collateral expansion and remodeling days after the acute response (Carmeliet, 2000; Conway et al., 2001; Meier et al., 2013; Simons and Eichmann, 2015; van Royen et al., 2001; van Royen et al., 2009).

The second type is the *de novo* formation of arterioles, which is an arterialization of capillaries in the skeletal muscle. These capillaries expand and become covered with mural cells (Faber et al., 2014; Mac Gabhann and Peirce, 2010; Simons and Eichmann, 2015).

Recently, another mechanism of collateral formation was published, called artery reassembly, in which arterial ECs migrate away from arteries to capillaries, and reassemble to collateral arteries (Das et al., 2019). However, this process is mainly restricted to the neonatal stage in mice and is nearly absent in the adult scenario.

So far, the underlying mechanism of blood vascular growth and remodeling is studied in different animal models. However, in contrast to larger animal studies, murine models allow pharmacologic as well as genetic manipulation of possible key molecules involved in these processes. The induction of hindlimb ischemia (HI) is the most common model for peripheral ischemia vascular adaptation and can be used to investigate adult angio- and arteriogenesis simultaneously (Limbourg et al., 2009; Meisner et al., 2013; Simons and Eichmann, 2015). Therefore, the femoral artery is surgically ligated, distal to the origin of the deep branch. This ligation builds up a pressure gradient and leads to an increase of blood flow into the pre-existing collaterals of the thigh (Limbourg et al., 2009; Schaper, 2009). Due to these hemodynamic changes, shear stress rises to the inner vessel wall of the collaterals and triggers the processes of collateral remodeling and expansion, meaning arteriogenesis is induced (Hofer et al., 2013; Limbourg et al., 2009; Schaper, 2009). Whereas, the thigh stays mainly perfused due to fast collateral adaptation, the calf remains ischemic (Henning et al., 2019; Limbourg et al., 2009). As arteriogenesis occurs relatively independent from hypoxia, femoral

artery ligation causes a local and prolonged hypoxia in the calf. Due to this hypoxic condition, angiogenesis, the sprouting of capillaries, is initiated via hypoxia inducible factor-1 α -vascular endothelial growth factor-A (HIF-1 α -VEGF-A) upregulation (Carmeliet, 2000). This means that post hindlimb ischemia, arteriogenesis occurs in the thigh, and angiogenesis in the calf (Heil et al., 2006; Henning et al., 2019; Limbourg et al., 2009; van Royen et al., 2009). However, the adaptation processes by ischemia induction can quickly disappear if the affected artery is reopened again (Fulton, 1964; Heil and Schaper, 2004).

Furthermore, the integration of mouse models to analyze coronary vascular growth is of huge clinical relevance as revascularization strategies due to stenting and bypass surgeries are often not applicable, and the induction of coronary vascular growth might be an alternative cardioprotective mechanism following an ischemic heart event (Das et al., 2019). In the past, some researchers studied arterial vessel growth in the injured mouse heart and tried to gain knowledge of the mechanism behind (Das et al., 2019; He et al., 2017; Ingason et al., 2018; Jamaiyar, 2020; Lavine et al., 2013; Miquerol et al., 2015; Tang et al., 2018; Zhang and Faber, 2015).

Two main adult mouse models of ischemia-induced cardiac vascular growth were used. In the first model, transient LAD occlusions contribute to myocardial repetitive ischemia reperfusion (Repl/R). This procedure was able to induce coronary growth in form of small arterioles and arteries with cardioprotective properties (Lavine et al., 2013). The described model was used to mimic the temporary ischemic events of stuttering angina, often appearing in patients with CADs, and which are discussed as important trigger for coronary collateralization (Lavine et al., 2013). In the second model, a permanent LAD occlusion was applied to induce *de novo* formation of coronary collaterals as mice lack pre-existing collaterals in the heart (Zhang and Faber, 2015).

Even though the research on coronary collateralization in murine hearts is ongoing, the cellular and molecular pathways behind are still poorly understood and conclusions from other organ or tissue studies, as the hindlimb or the brain, cannot be fully transferred to the myocardial situation. It is conceivable that arteriogenesis can be induced under ischemic or hypoxic conditions in the myocardium, and different signaling molecules could play a role (Heil et al., 2006; Jamaiyar et al., 2019).

1.3. Mechano-signaling in the endothelium

1.3.1. Influence of hemodynamic changes

It is strongly believed that physical forces released by hemodynamic changes reflect initial triggers and are essential in the processes of adult blood vascular remodeling and growth (Heil et al., 2006; Heil and Schaper, 2004; Schaper, 2009; Schaper and Scholz, 2003). More than a century ago, Thoma described a connection between vessel diameter and blood flow in the artery of chick embryos (Heuslein and Blackman, 2015; Schaper and Scholz, 2003; Thoma, 1893). Afterwards, the knowledge about the driving forces of arteriogenesis raised, and changes in shear stress pattern were identified as key regulators (Heuslein and Blackman, 2015; Schaper, 2009). Circumferential wall stress (CWS) and fluid shear stress (FSS) are known as remodeling forces in this scenario (Schaper and Scholz, 2003). After an artery occlusion a pressure gradient develops within the vasculature of the affected tissue. In the presence of anastomosed vessels this pressure gradient develops an increase in blood flow velocity, which initiates enhanced FSS to the collaterals. Consequently, FSS is dependent on blood flow velocity and the internal radius of the collateral vessel (Schaper and Scholz, 2003). Furthermore, arterial occlusion causes vasodilation, which may lead to increased CWS (Cai and Schaper, 2008; Schaper, 2009; Simons and Eichmann, 2015). Thus, CWS relates to the inner pressure and vessel wall thickness, and influences collateralization additionally, for instance by smooth muscular growth (Schaper and Scholz, 2003). FSS and CWS are both important shear stress factors for arteriogenesis, but CWS appears to be the stronger force, as it stays over one thousand times higher (Heil and Schaper, 2004; Schaper, 2009; Schaper and Scholz, 2003). Hereby, maximal outgrowth and manifestation of collateral vessels is dependent on the duration and magnitude of shear stress (Eitenmuller et al., 2006; Meisner et al., 2013; Schierling et al., 2009). With those adaptation processes the vascular system tries to provide adequate blood flow to the occluded tissue, and it is hypothesized to stop, when shear stress is reduced due to this vascular remodeling (Heuslein and Blackman, 2015; Murray, 1926).

Indication of shear stress by artery occlusion can be measured in different ways. For instance, endothelium-dependent flow-mediated vasodilation (FMD) measurements in ultrasound investigation provide a non-invasive tool to analyze arterial response and endothelial function due to short artery occlusion (Charakida et al., 2010; Welters et al., 2017). In clinic, it is an established method to analyze endothelial dysfunction correlating with atherosclerosis, cardiovascular risk or the presence of diabetes (Bonetti et al., 2003; Charakida et al., 2010; Schuler et al., 2014). To measure FMD in mice the femoral artery is occluded for 5 min. After reopening, blood flow velocity rises, shear stress increases and causes vessel

dilation in the healthy artery. Based on the measurement of the vessel diameter before and after femoral artery occlusion, the FMD can be calculated (Henning et al., 2019; Schuler et al., 2014). With the additional inclusion of flow velocity, corresponding wall shear stress influence can be determined as well (Henning et al., 2019; Schuler et al., 2014). However, this mouse model is mainly designed to detect hemodynamic changes and subsequent endothelium response in the bigger femoral artery rather than in the smaller collaterals. To measure direct shear stress changes in mouse collaterals, researchers established a trans-illuminated laser speckle flowmetry (LSF) system (Meisner et al., 2013). With this, they could show for the first time in mice that femoral artery occlusion causes blood velocity and shear stress increase in hindlimb collaterals. It was demonstrated that the shear stress level was elevated around 2-folds through the length of the collaterals, and that the flow direction was reversed in some collateral segments upon femoral artery ligation (Heuslein and Blackman, 2015; Meisner et al., 2013). This imaging technique helps to investigate how shear stress changes influence collateralization processes in the hindlimb model (Meisner et al., 2013). In contrast, the detection of hemodynamic changes in the mouse coronary vasculature is potentially detectable, but quite difficult due to size and resolution limitation.

1.3.2. Mechanotransduction via β 1 integrin signaling

Changes in blood flow behavior are directly recognized by the endothelium. But how artery occlusion-induced hemodynamic changes and corresponding increase in shear stress levels are signaled into the endothelium is not yet exactly known. In the mechanism of shear stress transmission, transcription factors like Kruppel-like factor 2 (KLF2) and endothelial cell-specific junctions like platelet endothelial cell adhesion molecule-1 (PECAM-1) and VE-cadherin as well as receptors like vascular endothelial growth factor receptor 2/3 (VEGFR2/3) play an essential role (Baeyens et al., 2016; Henning et al., 2019; Urner et al., 2018). Changes in mechanical forces can also be sensed by mechanosensitive integrins (Humphrey et al., 2014; Ingber, 1991; Lorenz et al., 2018; Planas-Paz et al., 2012; Ross et al., 2013; Schwartz, 2010; Sun et al., 2019). Integrins are heterodimeric transmembrane glycoprotein receptors, composed of an α and a β subunit, and function as “bridges” between the ECM or rather the basement membrane (BM) and the cytoskeleton in a bidirectional way (Fig. 1.5) (Hynes, 2002; Moreno-Layseca et al., 2019).

Furthermore, integrins lack their own kinase domain, but the cytoplasmic domain is linked via adapter proteins, like talin, vinculin, filamin, α -actinin and the IPP-complex, composed of integrin-linked kinase (ILK), particularly interesting Cys-His-rich protein (PINCH) and parvin, to the cytoskeleton and enable intercellular signaling (Humphrey et al., 2014; Legate et al., 2006). Recently, it was found that ILK impedes the interaction of integrins and

VEGF receptors (Urner et al., 2019). Moreover, integrins are involved in many physiological and pathological processes including cell proliferation, survival and migration but also, more precisely, vessel growth stimulation and secretion of angiocrine factors that are important for organ development and growth (Avraamides et al., 2008; Lorenz et al., 2018; Silva et al., 2008; Somanath et al., 2009).

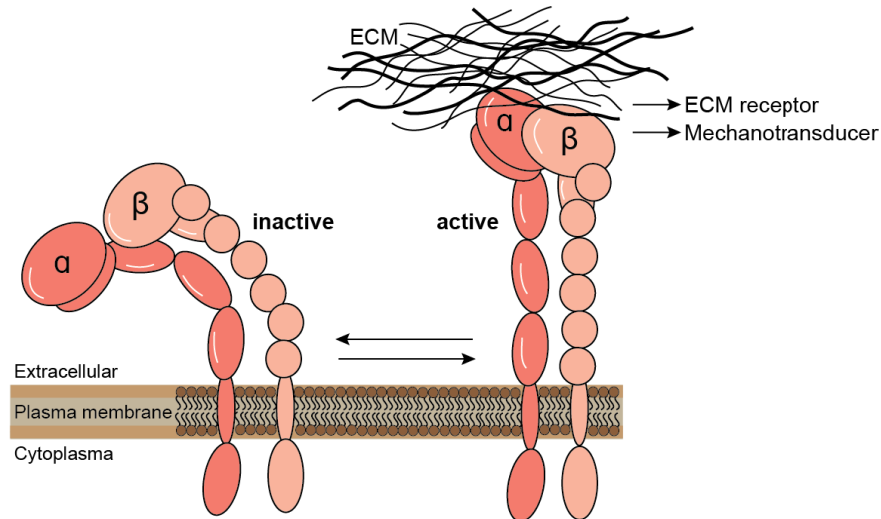


Figure 1.5: Integrin receptor.

Image of an integrin transmembrane receptor, composed of an α and a β subunit, in its inactive and active conformation state, binding to the extracellular matrix (ECM). Integrins can function as mechanotransducer to signal changes in mechanical forces. Original image was drafted by Dr. Jennifer Axnick (Axnick, 2016) based on the reviews (Avraamides et al., 2008; Serini et al., 2008) and with permission used and modified by Carina Henning.

Especially, the subunit $\beta 1$ integrin, the largest subgroup, cooperates with almost all α subunits and is expressed on nearly every cell type, including ECs (Silva et al., 2008). Global deletion of $\beta 1$ integrin gene (*Itgb1*) results in an early embryonic lethality before vascularization is induced (Fassler and Meyer, 1995; Stephens et al., 1995). Even with an endothelial specific knockout (KO), by using *Tie2-* or *VE-cadherin-Cre*, embryonic lethality occurs, and embryos show angiogenic sprouting defects, which implies the essential need of endothelial $\beta 1$ integrin for initial vascular formation and development (Carlson et al., 2008; Lei et al., 2008; Tanjore et al., 2008; Zovein et al., 2010). An impaired vascular phenotype is also detectable postnatally and under pathological conditions. It was shown that endothelial $\beta 1$ integrin is important for stable, non-leaky vessels as well as for acute function in vascular growth and maturation (Yamamoto et al., 2015). $\beta 1$ integrin signaling was also shown to be essential by transmitting hemodynamic changes after carotid or femoral artery ligation, resulting in endothelium activation, vascular remodeling and collateralization (Cai et al., 2009; Henning et al., 2019; Lei et al., 2008). Furthermore, it was shown that $\beta 1$ integrin is present on the basolateral and apical side of the endothelium, which enables possible mechanotransduction and interaction with components of the BM, VEGF receptors or shear stress-mediated activation of eNOS (Henning

et al., 2019; Lorenz et al., 2018; Yang and Rizzo, 2013). Therefore, the presence of $\beta 1$ integrin for the crosstalk of the ECM and the endothelium can be critical in terms of mechanically-forced signaling and is essential for appropriate vascular adaptation and activation of VEGF receptor 2 and 3 (Avraamides et al., 2008; Umer et al., 2018). For instance, patients with diabetes mellitus show changes in the composition and thickness of their vascular ECM, or rather BM, resulting in elevated arterial stiffness and subsequent higher cardiovascular risk (Goldin et al., 2006; Safar, 2018). These changes may contribute to impaired cellular integrin signaling and decreased vascular remodeling, which could be a possible explanation for reduced collateralization in patients with diabetes mellitus (Dincer et al., 2006; Ruitter et al., 2010; Shen et al., 2018).

All these findings suggest $\beta 1$ integrin as key player for blood vessel development and vascular adaptation. In a clinically relevant manner, those adaptation processes could contribute to a well-developed and functional collateral network, which could act in a cardioprotective way in terms of CVDs. For cardiac health it is known that a global heterozygous KO of the *Itgb1* gene impairs the outcome after MI (Krishnamurthy et al., 2006) and overexpression of $\alpha 7\beta 1D$ in cardiomyocyte reduces infarction size after I/R (Okada et al., 2013). However, until now it is poorly investigated whether $\beta 1$ integrin, especially on the endothelium, is actually involved in cardiac vascular adaptation and essential for cardioprotection, in ischemic heart events.

1.4. Aims of the thesis

Remodeling and growth of the adult blood vasculature represents a powerful mechanism to protect from ischemic injury. In this context, transduction of hemodynamic changes via the endothelium is essential, but the relevance of specific mechanosensitive receptors in adult ischemic tissue injury like in the hindlimb or the heart is less investigated. Therefore, the major aim of this thesis was to analyze the role of endothelial $\beta 1$ integrin for endothelial function, ischemia-induced blood vascular adaptation and cardioprotection. To examine the relevance of $\beta 1$ integrin in the endothelium, different *in vivo* mouse models were used, in which a main artery was occluded to induce local ischemia and subsequent vascular changes.

First, short hindlimb ischemia reperfusion in EC-specific $\beta 1$ integrin KO mice was triggered to evaluate the role of endothelial $\beta 1$ integrin for the transfer of shear stress in the endothelium and the acute vascular response. Therefore, the parameters flow velocity and FMD reaction were determined. Additionally, to get insights into the relevance of endothelial $\beta 1$ integrin for ischemia-induced long-term vascular adaptation processes, the femoral artery from EC-specific $\beta 1$ integrin KO animals was permanently occluded. Afterwards, blood

vascular changes were examined by arteriole number and capillary density quantifications in the thigh and the calf.

Since the role of $\beta 1$ integrin in myocardial ischemia with regard to vascular adaptation is mainly unclear, two different myocardial ischemia mouse models were used, in which the LAD was repetitively or permanently occluded. Additionally, to specify the role of $\beta 1$ integrin signaling, wild type mice were treated with blocking antibodies or EC-specific $\beta 1$ integrin KO mice were analyzed in both models. The first myocardial ischemia model, in which the LAD was repetitively occluded, was used to examine $\beta 1$ integrin-dependent EC proliferation and arteriole formation upon ischemia. Furthermore, to discover the role of ischemia locality, morphological changes in the vascular pattern were analyzed in the ischemic and the non-ischemic myocardium. Since the relevance of $\beta 1$ integrin for cardioprotection is less investigated, the first, repetitive myocardial ischemia model was also used to induce cardioprotective benefits, and further analyzed in terms of $\beta 1$ integrin dependency.

Next, the second myocardial ischemia model, in which the LAD was permanently closed, was inserted to strengthen the results and to find out whether $\beta 1$ integrin is essentially needed for vascular adaptation and preservation of cardiac function upon prolonged myocardial ischemia. Finally, this model enabled to analyze the consequences of endothelial $\beta 1$ integrin depletion for the progression of cardiac death after acute MI.

2. Experimental procedure

Some parts of the experimental procedure are substantially described in the publication (Henning et al., 2019) and in the manuscript (Henning et al., 2020, in preparation), which is prepared for publication in a peer-reviewed journal.

2.1. Mouse lines

Several adult mouse lines with different background were used and analyzed in this thesis. To inhibit the signaling pathway of β 1 integrin pharmacologically, a β 1 integrin blocking antibody (BD Bioscience, 555002) was intravenously (i.v.) injected (1 mg/ml, 100 μ l) into the tail vein of 10 to 15 weeks old wild type (wt) male C57BL/6J mice delivered from Janvier. To check antibody application itself, control antibody treatment was performed similarly in the same amount and frequency.

For genetic deletion studies of β 1 integrin in ECs, *Cdh5-Cre^{ERT2}* mice (Benedito et al., 2009; Wang et al., 2010) were mated with homozygous *Itgb1-loxP* mice (Potocnik et al., 2000) to generate endothelial cell specific homozygous *Itgb1* KO mice (*Itgb1^{IECKO}*). *Cdh5-Cre^{ERT2}* mice were used as controls. KOs and controls were both age-matched, male and treated with tamoxifen by intraperitoneal (i.p.) injections (75 mg/kg bodyweight, 100 μ l) for 5 consecutive days.

All listed experiments were performed according to the German animal protection laws (Animal Ethics Committee of the Landesamt für Natur, Umwelt und Verbraucherschutz, North-Rhine-Westphalia).

2.1.1. Genotyping

Tail biopsies of KO and control mice were lysed in lysis buffer containing 78 μ l dH₂O, 2 μ l Proteinase K solution (740 mAnsonU/ml, PanReac AppliChem) and 20 μ l 5x Flexi buffer (Promega) for each sample. Tails were incubated over night at 56°C and 300 rpm, and subsequently centrifuged at 13000 rpm for 10 min before polymerase chain reaction (PCR). Supernatant of lysates were used in the following master mixes:

PCR compound	<i>Cdh5-Cre^{ERT2}</i> (μl)	<i>Itgb1-loxP</i> (μl)
dH ₂ O	12.8	12.8
5x Green Flexi Buffer (Promega)	4	4
MgCl ₂ (25 mM, Promega)	1.2	1.2
dNTPs (10mM, Sigma)	0.4	0.4
Primer forward (100 pmol/μl, Eurofins)	0.2	0.2
Primer reverse (100 pmol/μl, Eurofins)	0.2	0.2
Taq polymerase (5 U/μl, MPI-CGB)	0.2	0.2
Tail lysate	1	1

Listed primer sequences were used to amplify DNA in PCR.

Mouse line	Primer sequence (5' → 3')	Product size
<i>Cdh5-Cre^{ERT2}</i>	Forward: GCC TGC ATT ACC GGT CGA TGC AAC GA Reverse: GTG GCA GAT GGC GCG GCA ACA CCA TT	pos approx. 700 bp
<i>Itgb1-loxP</i>	Forward: AGG TGC CCT TCC CTC TAG A Reverse: GTG AAG TAG GTG AAA GGT AAC	wt approx. 350 bp het approx. 350 bp and approx. 450 bp homo approx. 450 bp

The following temperature program was performed for each gene.

Mouse line	Temperature program
<i>Cdh5-Cre^{ERT2}</i>	1) 94°C for 5 min 2) 94°C for 30 sec 3) 58°C for 30 sec 4) 72°C for 1 min Repeat steps 2) - 4) for 35 cycles 5) 72°C for 5 min 6) 10°C pause

<i>Itgb1-loxP</i>	1) 94°C for 2 min
	2) 94°C for 1 min
	3) 58°C for 1 min
	4) 72°C for 1 min
	Repeat steps 2) - 4) for 35 cycles
	5) 72°C for 10 min
6) 10°C pause	

Resulting PCR products were run on a 1% agarose gel (Bio-Budget Technologies, GmbH) containing 3% SYBR® Safe (Invitrogen) for DNA labeling on 120 V for around 20 min. Subsequently, marked DNA bands were imaged under UV light in a Chemidoc™ XRS Imaging System (Bio-Rad).

2.2. *In vivo* and *ex vivo* procedure

2.2.1. Flow-mediated vasodilation (FMD)

FMD measurements were determined to analyze endothelial function in the femoral artery as previously described (Henning et al., 2019; Schuler et al., 2014). Therefore, male *Itgb1*^{IECKO} mice and corresponding controls were anesthetized with isoflurane (1.5% vol., Piramal Healthcare) and placed on a pre-heated ultrasound investigation table. To induce temporary ischemia in the distal hindlimb a vascular occluder (5 mm diameter, Harvard Apparatus) was placed around the lower hindlimb and the femoral artery was visualized by ultrasound probe arrangement. Accurate positioning was confirmed by pulse wave doppler of the blood vessel and the arterial blood flow. First baseline condition was imaged followed by 5 min occlusion of the vascular occluder. After reopening of the occluder, femoral artery diameter and flow velocity were recorded for max. 150 seconds (s) in 30 s intervals. Images were analyzed off-line by using a semi-automated system as previously described (Heiss et al., 2008). FMD was calculated as:

$$\text{diameter}(\text{post-ischemia}) - \text{diameter}(\text{baseline}) / \text{diameter}(\text{baseline}) * 100$$

2.2.2. Hindlimb ischemia

To analyze structural vascular remodeling processes in the hindlimb of male *Itgb1*^{IECKO} mice and corresponding controls, ligation of the femoral artery was performed as previously described (Henning et al., 2019). Therefore, mice were anesthetized via ketamine (100 mg/kg

bodyweight, KetanestS®, Pfizer Pharma GmbH) and xylazin (10 mg/kg bodyweight, Rompun TM, Bayer Healthcare) by i.p. injections. During surgery respiration was ensured with oxygen-enriched air (O₂ 40%) and isoflurane (1.5% - 2% vol., Piramal Healthcare). Mice were placed on a 37°C pre-heated surgery table, hair of the hindlimb was removed, the skin was disinfected and a small incision was made along the middle of the thigh. The femoral artery was exposed, ligated with two knots distal to the origin of the *arteria profunda femoris* and the artery was severed between the two knots. Wounds were closed with suture and mice could recover from procedure.

2.2.3. Myocardial ischemia

To induce transient episodes of myocardial ischemia in mouse hearts, a closed-chest ischemia reperfusion model was performed as previously described (Dewald et al., 2004; Lavine et al., 2013; Nossuli et al., 2000). For ischemia induction, an occluder was implanted for temporary LAD occlusion. Wt or KO mice received ketamine (100 mg/kg bodyweight, KetanestS®, Pfizer Pharma GmbH) and xylazin (10 mg/kg bodyweight, Rompun TM, Bayer Healthcare), i.p. for anesthesia. During surgery, respiration was ensured with oxygen-enriched air (O₂ 40%) and isoflurane (2% vol., Piramal Healthcare). Mice were placed on a 37°C pre-heated surgery table, the hair was removed and the skin disinfected. The heart was exposed by opening the skin, the muscle layers and the ribs were widened. After identification of the LAD a 7-0 prolene suture (Ethicon, Johnson and Johnson) was placed under the proximal artery. Suture ends were threaded through a 1 mm polyethylene (PE) tube, which later functioned as the occluder. A loose snare was formed with the suture, the thorax was closed again and the suture ends were stored in a subcutaneous pocket until the first ischemia induction. When mice received a permanent LAD occlusion, the LAD was directly closed with 7-0 silk suture (Seraflex®, Serag Wiessner), and hereby ischemia was induced, modified but previously described (Gao et al., 2005).

Some days after implantation, mice for transient LAD occlusions were anaesthetized with isoflurane (3% vol., Piramal Healthcare) and oxygen-enriched air (O₂ 40%). Mice were placed on a 37°C pre-heated surgery plate and isoflurane amount was reduced to 2%. Skin was disinfected and ECG electrodes were placed on fore- and hind feet. After reopening of the skin, suture ends were removed, attached to two magnets and set under tension for 15 or 60 min to occlude the LAD. Success of ischemia induction and subsequent reperfusion was controlled by ST-segment elevation. Ischemia reperfusion (I/R) was performed for 15 min every other day, or in case the infarction size and cardiac function were quantified, an additional 60 min I/R followed.

2.2.4. Osmotic pumps implantation for proliferation detection

For the labeling of proliferating cardiac cells after transient ischemia reperfusion, osmotic pumps (Alzet®, model 1002) filled with 20 mg/ml 5-bromo-20-deoxyuridine (BrdU, Sigma) in PBS (Ca^{2+} , Mg^{2+}) were used. Pumps were i.p. implanted in the first ischemia induction. Therefore, hair from the abdominal skin was removed, the skin was disinfected and a small incision was made in the skin and the peritoneum. One filled osmotic pump was inserted and wounds were closed again.

2.2.5. Pimonidazole treatment

Pimonidazole treatment was performed to determine hypoxic regions in the heart during ischemia induction. For anesthesia, wt mice were i.p. injected with ketamine (100 mg/kg bodyweight, KetanestS®, Pfizer Pharma GmbH) and xylazin (10 mg/kg bodyweight, Rompun TM, Bayer Healthcare). Pimonidazole (60 mg/kg bodyweight, Hypoxyprobe Green Kit, Hypoxyprobe, Inc., Burlingston) solved in PBS (Ca^{2+} , Mg^{2+}) was injected i.p. and the LAD was occluded as described before without reperfusion. Shortly after ischemia induction hearts were isolated, perfused with ice-cold PBS (Ca^{2+} , Mg^{2+}), deep-frozen in nitrogen and embedded in Tissue-Tek O.C.T. (Sakura Finetek GmbH) for cryosectioning.

2.2.6. Magnetic resonance imaging (MRI)

MRI was used to quantify the ischemic area by late gadolinium enhancement (LGE) and to determine cardiac function of the left ventricle (LV) before, 1 day, 7 days and 28 days after 60 min I/R. These measurements were performed in a Bruker AVANCE III 9.4 T Wide Bore NMR spectrometer (Bruker) driven by ParaVision 5.1 as previously described (Bonner et al., 2014; Haberkorn et al., 2017). For analysis, mice were anaesthetized with isoflurane (1.5% vol., Piramal Healthcare). For monitoring vital functions with the M 1025 system (SA Instruments, Stony Brook) ECG electrodes were placed on fore- and hind feet and a pneumatic pillow was placed at the back to record respiration. Values were needed to synchronize cardiac and respiratory motions during H^1 MRI measurements. To quantify the size of the ischemic area, 1 day post 60 min I/R Gd-DTPA (0.2 mmol/kg bodyweight) was i.p. injected before measurements. H^1 cine MR loops in short axis of the heart were taken for cardiac function analysis. Therefore, an ECG- and respiration-gated segmented fast gradient echo cine sequence with steady state precession (FISP) was used. End-diastolic (EDV) and end-systolic volumes (ESV) were determined by manual measuring of the left ventricular borders of the myocardium by means of the ParaVision software (Bruker) region-of-interest (ROI) tool. Base on this, left ventricular ejection fraction (EF) was calculated by difference between EDV and

ESV volumes divided by the EDV. Ischemic area size was quantified by manual selection of LGE-positive area and related to the left ventricular volume.

2.2.7. Echocardiography

Transthoracic echocardiography was performed as previously described (Erkens et al., 2015). Left ventricular cardiac function was analyzed before, 1 day, 7 days and 14 days after permanent myocardial ischemia using a MS-400 scanhead (Vevo 2100, VisualSonics, FUJIFILM). For analysis, mice were anaesthetized with isoflurane (1.5% vol., Piramal Healthcare) and the long and short axis in B and M mode, the mitral valve flow and the aorta ascendens flow were recorded. To calculate EF, EDV and ESV, long axis B mode images were analyzed in the vevo lab software 1.7.1 (VisualSonics).

2.2.8. Triphenyl tetrazolium chloride (TTC) staining

The TTC staining was performed to determine the infarct size as well as the area at risk (AAR), meaning the area affected by the ischemia but without necrosis after the 60 min I/R. Therefore, mice were anesthetized via i.p. injections of ketamine (100 mg/kg bodyweight, KetanestS®, Pfizer Pharma GmbH) and xylazin (10 mg/kg bodyweight, Rompun TM, Bayer Healthcare). After sufficient anesthesia, hearts were exposed via thoracotomy and transferred into ice-cold NaCl solution (0.9%, Braun). Attached organs like the lung und the thymus were carefully removed, the heart was cannulated over the aorta and washed with NaCl solution (0.9%, Braun) to remove remaining blood clots. Afterwards, the LAD was permanently closed with a silk suture and the heart was perfused with 1% evens blue solution (in NaCl) via the aorta. Hearts were removed from the cannula and frozen at -20°C for approximately 1 h. For TTC staining hearts were transversally cut into equal sections until the suture position, transferred into TTC solution containing 8 parts 0.1 M Na₂HPO₄, 2 parts 0.1 M NaH₂PO₄ (pH 7.4) and 10 mg/ml TTC and incubated at 38°C for 5 to 10 min shaking. Finally, heart sections were imaged using a stereomicroscope (Leica MZ6 with Leica KL 1500 LCD) and infarcted area and AAR were measured and analyzed with the software DISKUS (Vers. 4.30.7, Carl H. Hilgers, DISKUS mikroskopische Diskussion).

2.2.9. Microfil® perfusion of the coronary vasculature

To visualize the coronary vasculature, adult mouse hearts were perfused with Microfil® compound (Flow Tech Inc.) as previously described but modified (Zhang and Faber, 2015). Therefore, mice were anesthetized via i.p. injections of ketamine (100 mg/kg bodyweight, KetanestS®, Pfizer Pharma GmbH) and xylazin (10 mg/kg bodyweight, Rompun TM, Bayer Healthcare). To expose the hearts, mice were fixed in a dorsal position, the thorax and abdomen was opened and a small incision was made in the thoracic aorta. Over the thoracic aorta the hearts were washed with PBS (Ca^{2+} , Mg^{2+}) and afterwards fixed with 1% PFA. Microfil® working solution was prepared in a mixture of 40% diluent, 55% compound (here yellow) and 5% curing agent. Finally, the washed and fixed hearts were perfused with working solution until the entire coronary artery network was visualized. After 20 to 30 min, the solution finished polymerization and was stable. Perfused hearts were removed and additionally fixed in 2% PFA over night. Hearts were drained in increasing ethanol concentrations (25%, 50%, 75%, 95% and absolute ethanol, Merck) and optically cleared with methyl salicylate (Sigma Aldrich). Cleared hearts were imaged under a stereomicroscope (Leica MZ6 with Leica KL 1500 LCD).

2.2.10. Tissue isolation

For heart and hindlimb isolation mice were i.p. anesthetized with ketamine (100 mg/kg bodyweight, KetanestS®, Pfizer Pharma GmbH) and xylazin (10 mg/kg bodyweight, Rompun TM, Bayer Healthcare). After sufficient anesthesia, mice were fixed in a dorsal position and a thoracotomy was performed to expose the heart. For immunohistochemical analysis, hearts and hindlimbs were washed over the left and right ventricle with ice-cold PBS (Ca^{2+} , Mg^{2+}) containing 1 μM adenosine (Sigma). Afterwards, tissue was perfused with 4% PFA and transferred to 4% PFA for fixation over night at 4°C. For molecular or biochemical analysis, hearts were exposed, washed with ice-cold PBS (Ca^{2+} , Mg^{2+}) containing protease (cOmplete Protease Inhibitor Cocktail Tablets, Roche) and phosphatase inhibitors (Phosphatase Inhibitor Cocktail, Roche) and the left and right ventricle were separated from each other before freezing into liquid nitrogen.

2.3. Immunohistochemistry

2.3.1. Equilibration, embedding and cryosectioning

For equilibration, hearts and hindlimbs were transferred in 15% and subsequent 30% sucrose solution over night at 4°C shaking. Afterwards, hearts and hindlimbs were embedded in Tissue-Tek O.C.T embedding compound (Sakura Finetek GmbH) and stored at -80°C or directly cryosectioned for immunohistochemical analysis. For hypoxia staining, hearts were cryosectioned in 8 µm thickness, while for remaining immunohistochemical analysis 12 µm thick tissue sections were prepared with a cryostat (Mictrotom HM 560, Thermo Fischer Scientific).

2.3.2. Immunostaining

General tissue staining: After cryosectioning, sections were blocked with blocking solution containing 5% normal donkey serum (NDS, Jackson ImmunoResearch) and 3% bovine serum albumin (BSA, AppliChem) and 0.2% Triton X-100 (AppliChem) for 1 h at room temperature (RT). Afterwards, sections were incubated with primary antibody diluted in blocking solution for 1 h at RT or over night at 4°C. Slides were washed 2 times for 10 min with PBS (Ca²⁺, Mg²⁺) and a last time with PBS (Ca²⁺, Mg²⁺) containing 0.2% Triton X-100. Incubation with secondary antibody followed, containing DAPI (Sigma) diluted 1/1000 for 45 min at RT. Lastly, slides were washed 3 times each for 10 min with PBS (Ca²⁺, Mg²⁺) again and mounted with Fluoroshield™ (Sigma).

Hypoxia staining: After cryosectioning, sections were fixed with acetone for 10 min and incubated with fluorophore-coupled antibodies for hypoxyprobe-fluorescein isothiocyanate-mono-clonal antibody (HP-FITC-MAb), which detects pimonidazole adducts. The remaining procedure to co-stain other proteins was performed as previously described.

Proliferation staining: Sections of mouse hearts, which were treated with BrdU, were incubated in 2 M HCl solution for 30 min at 37°C and subsequently neutralized by incubation with 0.1 M sodiumtetraborate. Afterwards, primary and secondary antibodies were applied as previously described.

The following table shows used primary and secondary antibodies as well as the dilution concentrations.

Primary antibodies	Dilution	Secondary antibodies	Dilution
Goat anti-PECAM-1 (R&D Systems, AF3628)	1/20	Donkey anti-goat/mouse/rat Alexa Fluor 488 (Invitrogen Molecular Probes)	1/500
Mouse anti- α SMA (Sigma, A5228)	1/100	Donkey anti-goat/mouse/rat Alexa Fluor 555 or Cy3 (Invitrogen Molecular Probes or Jackson ImmunoResearch)	1/500
Mouse anti- α SMA-Cy3 (Sigma, C6198)	1/200	Donkey anti-goat/mouse Cy 5 (Jackson ImmunoResearch)	1/500
Rat anti-BrdU (abcam, ab6326)	1/200		
HP-FITC-MAb (Hypoxyprobe Green Kit, Hypoxyprobe, Inc. Burlington, HP6-XXX)	1/50		

All mounted slides were directly imaged or stored at 4°C.

2.3.3. Microscopy and image analysis

After immunohistochemical staining, sections were scanned and imaged using a confocal laser scanning microscope (LSM 710, Zeiss) and subsequently analyzed with the open source program FIJI (ImageJ, NIH). For quantification, the proliferating ECs and the arterioles were counted manually and related to the myocardial or hindlimb area in mm². Capillary density was calculated by counts of capillaries divided by the number of muscular fibers.

2.4. Magnetic-activated cell sorting (MACS) of ECs

ECs of hearts were isolated and purified via magnetic-activated cell sorting (MACS) from adult *Itgb1*^{IECKO} and control mice. All steps were performed according to the manufacturer's protocol from Miltenyi Biotech. Starting with 'Preparation of single-cell suspension from mouse hearts' and followed by 'CD45 MicroBeads' and 'CD31 MicroBeads' coupling. Therefore, hearts were dissociated with a gentleMACS Dissociator (Miltenyi Biotech) and digested with collagenase II (Worthington, CLS-2) and DNase I (AppliChem) solution to generate the single-cell suspension. Afterwards cells were labelled with CD45 MicroBeads (Miltenyi Biotech, 130-

052-301) to remove leukocytes and platelets as those subtypes of immune cells are also positive for the subsequent used EC marker CD31. After labeling, CD45 positive cells were separated in magnetic field and remaining cells were further marked with CD31 MicroBeads (Miltenyi Biotech, 130-097-418) for EC isolation. The remaining EC pellets were used for real-time PCR or Western blot analysis.

2.5. Molecular and biochemical methods

2.5.1. Quantitative real-time PCR

Quantitative real-time PCR was used to determine KO efficiency on RNA level. Therefore, heart EC pellets from MACS were homogenized in 150 µl peqGold TriFast (PepqLab) and total RNA was isolated by performing a single-step acid guanidinium thiocyanate-phenol-chloroform extraction (Chomczynski and Sacchi, 1987). Afterwards, the RNA concentration was determined by using a BioMate™ 3 (Thermo Fisher Scientific), and cDNA synthesis was performed using SuperScript™ II Reverse Transcriptase (Invitrogen by Thermo Fischer Scientific) according to the manufacturer's protocol. For subsequent quantitative real-time PCR analysis, the Brilliant III Ultra-Fast SYBR® Green QPCR Master Mix (Agilent Technologies) and the thermal cycler Stratagene Mx3000P (Agilent Technologies) were used. Samples were analyzed in duplicates or triplicates and the following primers were used:

Primer (Eurofins)	Primer sequence (5' → 3')
Mouse <i>Itgb1</i>	Forward: AAT GCC AAG TGG GAC ACG GG Reverse: TGA CTA AGA TGC TGC TGC TGT GAG C
Mouse <i>Rplp0</i>	Forward: GAT GCC CAG GGA AGA CAG Reverse: ACA ATG AAG CAT TTT GGA TAA TCA
Mouse <i>Hprt</i>	Forward: CAC AGG ACT AGA ACA CCT GC Reverse: GCT GGT GAA AAG GAC CTC T
Mouse <i>β2m</i>	Forward: GAG CCC AAG ACC GTC TAC TG Reverse: GCT ATT TCT TTC TGC GTG CAT

Following temperature protocol was used for quantitative real-time PCR analysis.

Steps	Temperature program
Pre-incubation	1) 95°C for 2 min
Amplification	2) 95°C for 5 sec
	3) 60°C for 20 sec
	Repeat steps 2) - 3) for 40 cycles
Melting	4) 95°C for 1 min
	5) 55°C for 30 sec
	6) 95°C for 30 sec

The endothelial $\beta 1$ integrin KO efficiency in murine hearts were determined by means of the $\Delta\Delta CT$ method, therefore $\Delta\Delta CT$ is defined as CT gene of interest - CT housekeeping gene (Livak and Schmittgen, 2001). Here the genes *Rplp0*, *Hprt* and *$\beta 2m$* were used as housekeeping genes and normalized to *Itgb1* (gene of interest).

2.5.2. Western blotting

For determination of endothelial $\beta 1$ integrin KO efficiency on protein level, sorted EC pellets from MACS were lysed in radioimmunoprecipitation assay (RIPA) buffer, containing 50 mM Tris/HCl (pH 7.4), 150 mM NaCl, 1% IGEPAL, 0.25% Na-deoxycholate, 1 mM EDTA, protease (cOmplete Protease Inhibitor Cocktail Tablets, Roche) and phosphatase inhibitors (Phosphatase Inhibitor Cocktail, Roche). To measure protein content, the Pierce™ bicinchoninic acid (BCA) protein assay Kit (Thermo Fisher Scientific) was performed according to the manufacturer's protocol and equal amounts of protein per sample were used for sodium dodecyl sulfate-polyacrylamide gel electrophoresis (SDS-PAGE) separation. Therefore, β -mercaptoethanol (Roth) was diluted 1/10 in 4x Laemmli buffer (Bio-Rad), mixed with samples and heated at 95°C for 5 min for protein denaturation. After denaturation, proteins were separated to their molecular weight in 4-15% SDS-gels (Bio-Rad) by 180 V for 30 min using a Mini-PROTEAN Tetra Cell (Bio-Rad). For semi-dry protein transfer from SDS-gel to a polyvinylidene fluoride (PVDF) membrane, the Trans-Blot® Turbo™ Mini PVDF Transfer Pack (Bio-Rad) and the Trans-Blot Turbo Transfer System (Bio-Rad) was used. After Western blotting membranes were cut due to the molecular weight of the proteins of interest and blocked for 1 h at RT in blocking solution containing 5% BSA (AppliChem) and 0.5% Tween-20 (AppliChem) diluted in PBS (Ca^{2+} , Mg^{2+}). Afterwards, membranes were incubated with primary antibodies over night at 4°C, washed 3 times for 10 min with PBS (Ca^{2+} , Mg^{2+}) containing 0.5% Tween-20 (AppliChem) followed by incubation with secondary antibodies for 45 min at RT and washed again. Following table shows the used antibodies and their dilution in blocking solution.

Primary antibody	Dilution	Secondary antibody	Dilution
Rat anti- β 1 integrin (Millipore, MAB1997)	1/1000	Donkey anti-rat HRP (Jackson ImmunoResearch)	1/5000
Rabbit anti-GAPDH (Abcam, ab9485)	1/2000	Donkey anti-rabbit HRP (Cell signaling)	1/5000

After the last washing step, membranes were incubated with WesternBright Chemiluminescent Substrate Quantum (Advansta, 171206-34, 1:1) for 1 min in dark and imaged in the ChemieDocTM MP, Imaging System (Bio-Rad). For semi-quantitative band density analysis (performed with FIJI, ImageJ NIH), β 1 integrin levels were normalized to GAPDH protein levels, needed as housekeeping protein.

2.5.3. Enzyme-linked immunosorbent assay (ELISA)

To detect endothelin-1, neuregulin-1 and hepatocyte growth factor (HGF) protein levels in murine plasma and heart tissue, the endothelin-1 Quantikine[®] ELISA Kit (R&D, DET 100), the mouse NRG-1 (Neuregulin 1) ELISA (Novus biologicals, NBP2-68070) and the mouse/rat HGF Quantikine[®] ELISA Kit (R&D, MHG00) was used. Therefore, plasma was collected by retrobulbar isolation of blood. Heparinized blood was centrifuged at 3000 g for 3 min at 4°C and supernatant was removed for plasma protein analysis. Hearts were isolated as described for molecular or biochemical analysis. For tissue lysis, 20-30 mg left ventricular heart muscle, which was exposed to ischemia, in 500 μ l lysis buffer, containing protease (cOmplete Protease Inhibitor Cocktail Tablets, Roche) and phosphatase inhibitors (Phosphatase Inhibitor Cocktail, Roche) diluted in RIPA buffer, was homogenized in a gentleMACS Dissociator (Miltenyi Biotec). After centrifugation at 400 g for 3 min at 4°C to reduce foam, the supernatant was centrifuged a second time at 4000 g for 10 min at 4°C. Protein concentration of the supernatant was determined by using the PierceTM BCA Protein Assay Kit (Thermo Fisher Scientific). Only neuregulin-1 plasma samples were diluted 1/6. Heart tissue samples were diluted to 40 μ g protein per well. Afterwards, plasma and heart tissue samples were loaded on the endothelin-1, neuregulin-1 and HGF ELISA plate and analyzed as duplicates. The general assay procedures were performed according to the manufacturer's protocol. Finally, optical density of each well was detected by using a NanoQuant Infinite M200 Reader (TECAN) and endothelin-1, neuregulin-1 and HGF relative protein amounts were calculated.

2.6. Statistical analysis

To determine statistical significance, Excel (Microsoft) or Prism (GraphPad Inc.) was used as calculation software. Therefore, an unpaired or paired two-tailed Student's *t*-test was used if two groups were compared with each other. Differences in *P* values less or equal 0.05 were considered as statistically significant and the values with two decimal places were shown in the figures or the figure legends. Values are shown in dot plot graphs or as averages of all values per group \pm standard error of the mean (SEM). Survival rates were described in a Kaplan-Meier curve and the significance was calculated with a log-rank test (Mantel-Cox test).

2.7. Personal contribution

Carina Henning performed most of the here described experiments and was supervised by Prof. Dr. Eckhard Lammert.

Anna Branoploski contributed to the cryosectioning, staining and immunohistochemical analysis on numbers of arterioles and capillaries in the hindlimb and arterioles in the heart. Furthermore, Anna Branopolski recorded MR images of the mouse hearts. Carina Henning analyzed the MR images for ischemic area size and cardiac function.

Paula Follert was co-supervised by Carina Henning during her Bachelor Thesis in 2018 and performed experiments to quantify KO efficiency of endothelial cell specific homozygous *Itgb1* KO mice (*Itgb1*^{IECKO}).

Dr. Dominik Schuler performed ultrasound-based flow velocity and FMD measurements as well as hindlimb ischemia surgeries in endothelial cell specific homozygous *Itgb1* KO mice (*Itgb1*^{IECKO}) and their controls. Carina Henning performed most further experimental steps, including tamoxifen injections, harvesting, cryosectioning, staining and immunohistochemical analysis of the hindlimbs.

Aysel Ayhan supported the echocardiographic measurements for permanent myocardial ischemia surgery. Carina Henning measured and analyzed the echocardiographic data for cardiac function.

As Carina Henning and Anna Branopolski were both involved in the project, they share some experimental results for their theses. Carina Henning and Anna Branopolski contributed to equal amounts to the following figures: Fig. 3.3, Fig. 3.4, Fig. 3.5, Fig. 3.6, Fig. 3.12, Fig. 3.13, Fig. 3.21 and Fig. 3.22. Carina Henning contributed to three-quarter and Anna Branopolski to one-quarter to the following figures: Fig. 3.16, Fig. 3.17 and Fig. 3.23.

3. Results

Some parts and illustrations of the results are substantially described in the publication (Henning et al., 2019) and in the manuscript (Henning et al., 2020, in preparation), which is prepared for publication in a peer-reviewed journal.

3.1. Role of endothelial cell-specific $\beta 1$ integrin in hindlimb ischemia

Endothelial $\beta 1$ integrin was reported to hold a central role in embryonic and postnatal vascular development, as its deficiency results in an impaired vascularization (Carlson et al., 2008; Lei et al., 2008; Tanjore et al., 2008; Yamamoto et al., 2015; Zovein et al., 2010). Therefore, in the context of adult vascular remodeling upon artery occlusion, it is conceivable that integrins are able to signal blood flow changes to the endothelium, which is discussed to be the initial trigger for collateralization.

To study the role of endothelium-specific $\beta 1$ integrin for endothelial function and vascular adaptation, an adult hindlimb ischemia model was used. Hemodynamic changes and flow-mediated vasodilation (FMD) were analyzed as acute response to short femoral artery (FA) occlusion. Furthermore, structural vascular remodeling was observed as an increase of arteriole number. Additionally, angiogenesis, indicated by a rise of capillary numbers, was further investigated.

3.1.1. Endothelial $\beta 1$ integrin is required for flow-mediated vasodilation (FMD)

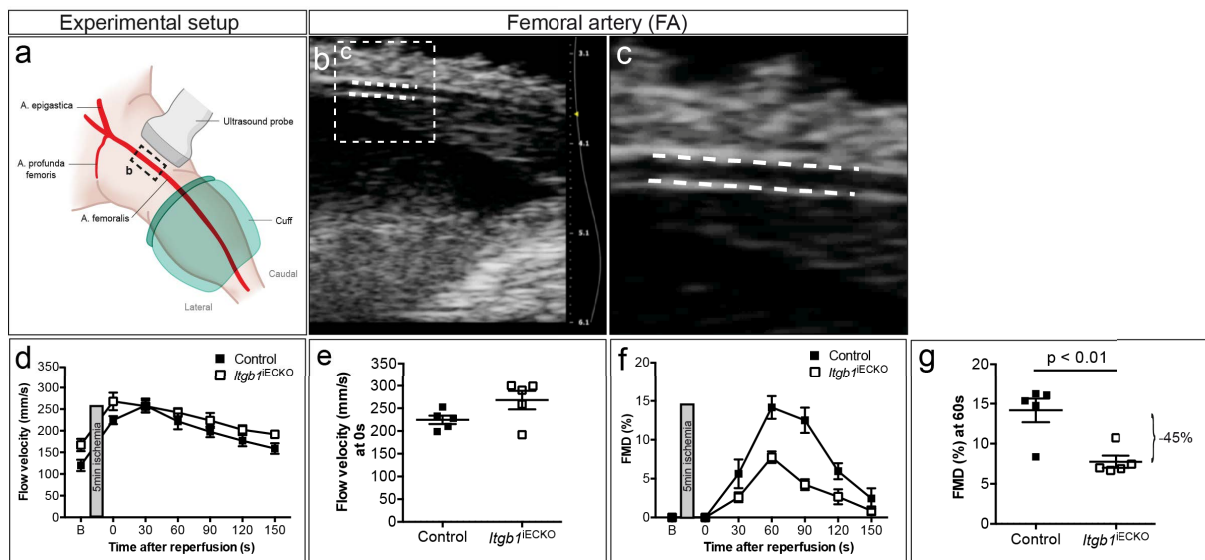
To examine the role of endothelial $\beta 1$ integrin in endothelium function, flow velocity and FMD after 5 min cuff-induced FA occlusion (Fig. 3.1 a-c) was measured, in mice selectively deficient for *Itgb1* gene in ECs. This procedure is comparable to measurements in humans using the brachial artery (Heiss et al., 2008; Henning et al., 2019; Schuler et al., 2014).

EC-specific deletion was generated by crossing tamoxifen-inducible *Cdh5-Cre^{ERT2}* mice (Benedito et al., 2009; Wang et al., 2010) with homozygous *Itgb1-loxP* mice (Potocnik et al., 2000). A LacZ staining of the thigh and gene expression analysis showed successful KO induction in ECs after tamoxifen administration (Henning et al., 2019). Those *Cdh5-Cre^{ERT2}*; homozygous *Itgb1-loxP* mice (referred as *Itgb1^{IECKO}*) were compared to tamoxifen-induced *Cdh5-Cre^{ERT2}* mice (referred as control).

After reopening of the cuff in the lower leg region, reperfusion was induced, followed by an increase in flow velocity and corresponding FMD. Both parameters were measured in *Itgb1^{IECKO}* and control mice over 150 s after short FA occlusion. The increase in flow velocity after reopening was the highest at 0 s in *Itgb1^{IECKO}* mice (Fig. 3 d), but not significantly higher compared to control mice (Fig. 3.1 e). Over the entire measuring period, flow velocity was

largely unaffected in the two groups. Therefore, generation of shear stress, meaning the main trigger for FMD was not substantially influenced by the EC-specific KO of $\beta 1$ integrin. However, the dilation of the artery, indicated by FMD was clearly impaired in *Itgb1*^{IECKO} mice compared to controls. This was shown over the time of measurement as well as at 60 s after reopening, where vasodilation was at the maximum in both mouse lines (Fig. 3.1 f, g).

In conclusion, flow velocity and hence shear stress generation was not substantially influenced by $\beta 1$ integrin deletion in the endothelium, but shear stress signaling was interrupted and subsequent FMD response decreased.



Images and results from this subitem were adapted and recently described in the publication (Henning et al., 2019), Fig. 3 a-c and Fig. 4.

3.1.2. Endothelial $\beta 1$ integrin is required for ischemia-induced arterial and capillary vessel growth

Ligation or permanent occlusion of the FA in mice is a well-established model to study different types of pathological vessel growth simultaneously. Therefore, the *arteria femoris* or FA was permanently closed after the branch of the *arteria profunda femoris* (Fig. 3.2 a), inducing permanent hindlimb ischemia (HI). After several days pre-existing collaterals in the thigh expand and increase to larger ones, whereas in the calf capillaries start growing (Limbourg 2009). Furthermore, arterioles can also develop *de novo* from capillaries (Faber et al., 2014; Mac Gabhann and Peirce, 2010; Simons and Eichmann, 2015). In this model, processes of arterio- and angiogenesis were initiated and histologically analyzed by transversal cross-sections through the thigh and calf (Fig. 3.2 b, c).

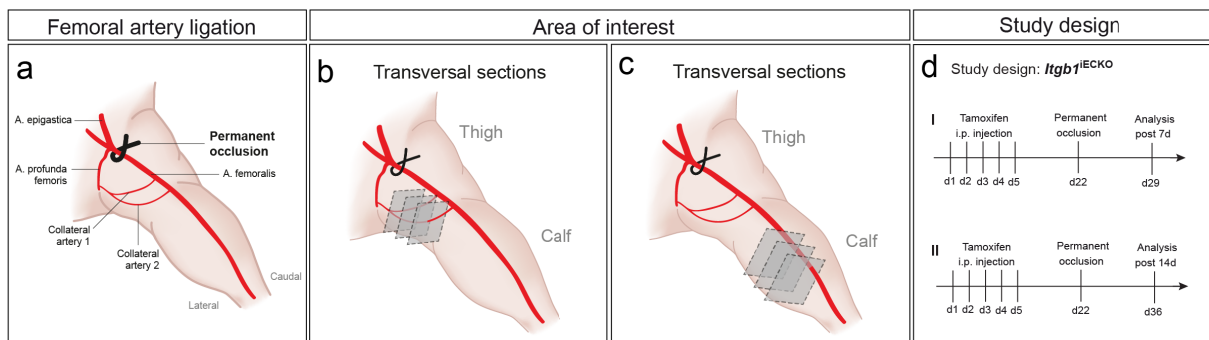


Figure 3.2: Illustration of hindlimb ischemia experiments.

(a) Graphical presentation of permanent FA occlusion, also indicated as FA ligation. The area of interest for histological analysis in (b) the thigh and (c) the calf is visualized by squares with dotted line. (d) Overview of the study design with the endpoint analysis at (I) 7 d and (II) 14 d post permanent FA occlusion. Images (a-c) were drafted by Carina Henning and illustrated by Yousun Koh.

To determine whether those processes were influenced by EC-specific deletion of $\beta 1$ integrin, again *Itgb1*^{IECKO} and control mice were treated equally with i.p. injections of tamoxifen to induce the KO but also to check the influence of *Cre* activity in control mice. Afterwards, the FA was ligated and hindlimbs were isolated 7 days (d) and 14 d post HI for analysis (Fig. 3.2 d I, II).

Vascular adaptation was determined by immunohistochemical analysis of blood vessels, in transversal cross-sections of the thigh and calf. Co-staining of PECAM-1 and α -smooth muscle actin (α SMA) was used to detect changes in arteriole numbers and single PECAM-1 staining was used to identify modifications in capillary density.

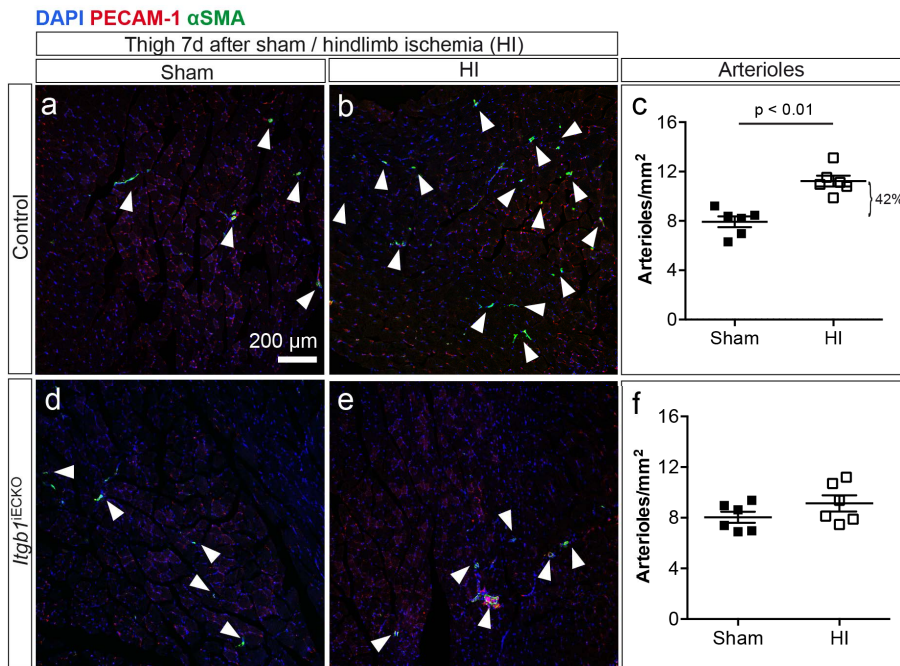


Figure 3.3: Hindlimb ischemia-induced arteriole vessel growth in the thigh is reduced in mice with endothelial cell-specific deletion of *Itgb1*.

(a, b, d, e) Representative immunofluorescence images of the thigh 7 d after hindlimb ischemia (HI) in (a-c) control and (d-f) *Itgb1*^{IECKO} mice. Mice received (a, d) sham or (b, e) HI surgery. Sections were stained for endothelial cells (PECAM-1, red), smooth muscle cells (α SMA, green) and nuclei (DAPI, blue). Arrows indicate arterioles by co-staining of PECAM-1 and α SMA. (c, f) Quantification of arterioles per mm² in (c) control and (f) *Itgb1*^{IECKO} mice. Reported values are means \pm SEM with n = 6 mice per condition. Statistical significance was determined using paired two-tailed Students t-test. Carina Henning, Anna Branopolski and Dr. Dominik Schuler performed the presented experiment.

Notably, before ischemia induction the vessel density of arterioles and capillaries in the thigh and the calf was unchanged by tamoxifen treatment, as well as EC apoptosis was not increased baseline after β 1 integrin KO induction. Consequently, tamoxifen application and therefore EC-specific β 1 integrin KO in adult mice alone did not influence vascular status before permanent FA occlusion (Henning et al., 2019).

Furthermore, 7 d post HI induction, quantification of control mice showed an increase in arteriole numbers in the thighs, compared to thighs without intervention (sham) (Fig. 3.3 a-c). Interestingly, this enhancement was inhibited in *Itgb1*^{IECKO} mice (Fig. 3.3 d-f). In contrast to arteriole number, capillary density in the thighs of control mice was not significantly increased after HI (Fig. 3.4 a-c). Moreover, *Itgb1*^{IECKO} mice also did not show any changes in capillary density by HI compared to sham procedure (Fig. 3.4 d-f). Therefore, results indicate endothelial β 1 integrin to be important for HI-induced arterial growth in the thigh. Furthermore, capillary growth or angiogenesis was barely induced by HI in the thigh of control or *Itgb1*^{IECKO} mice.

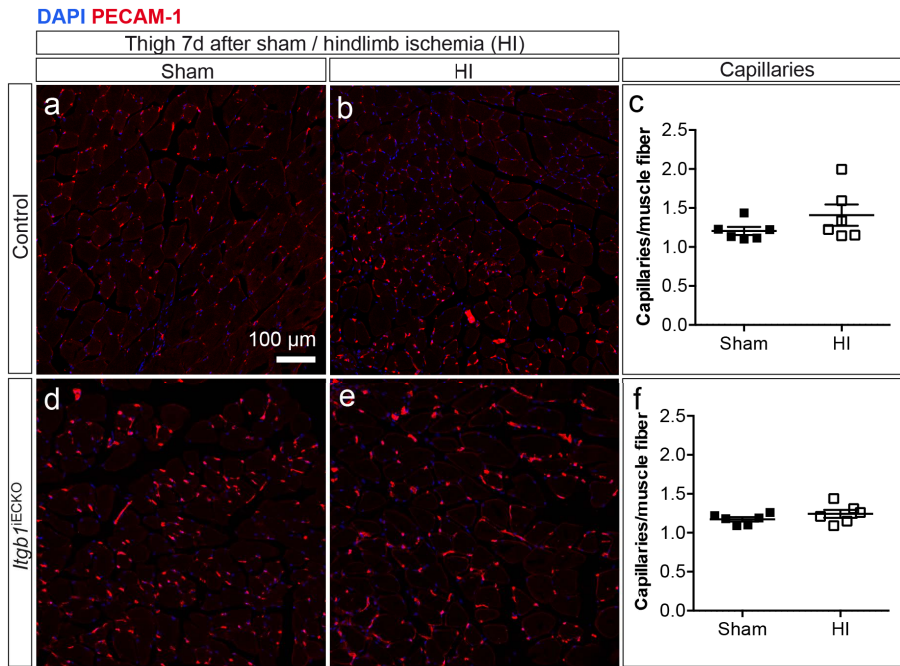


Figure 3.4: Hindlimb ischemia did not induce angiogenesis in the thigh of control and KO mice with endothelial cell-specific deletion of *Itgb1*.

(a, b, d, e) Representative immunofluorescence images of the thigh 7 d after HI in (a-c) control and (d-f) *Itgb1*^{IECKO} mice. Mice received (a, d) sham or (b, e) HI surgery. Sections were stained for endothelial cells (PECAM-1, red) and nuclei (DAPI, blue). (c, f) Quantification of capillaries per muscle fiber in (c) control and (f) *Itgb1*^{IECKO} mice. Reported values are means \pm SEM with $n = 6$ mice per condition. Statistical significance was determined using paired two-tailed Students t-test. Carina Henning, Anna Branopolski and Dr. Dominik Schuler performed the presented experiment.

However, further analysis of the calf showed different vascular adaptation processes to permanent FA occlusion compared to the thigh. In contrast to arteriole growth in the thigh, the increase of arteriole numbers was less distinct and only visualized in a non-significant rise in control mice (Fig. 3.5 a-c). Furthermore, this tendency of elevated arteriole numbers was no longer observed in *Itgb1*^{IECKO} mice (Fig. 3.5 d-f).

However, compared to arteriole formation, the enhancement of capillary density in the calf from control mice was more statistically clear (Fig. 3.6 a-c), whereas this increase was absent in mice with EC-specific deletion of $\beta 1$ integrin. Therefore, results demonstrate that ischemia-induced angiogenesis in the calf is dependent on the presence of endothelial $\beta 1$ integrin.

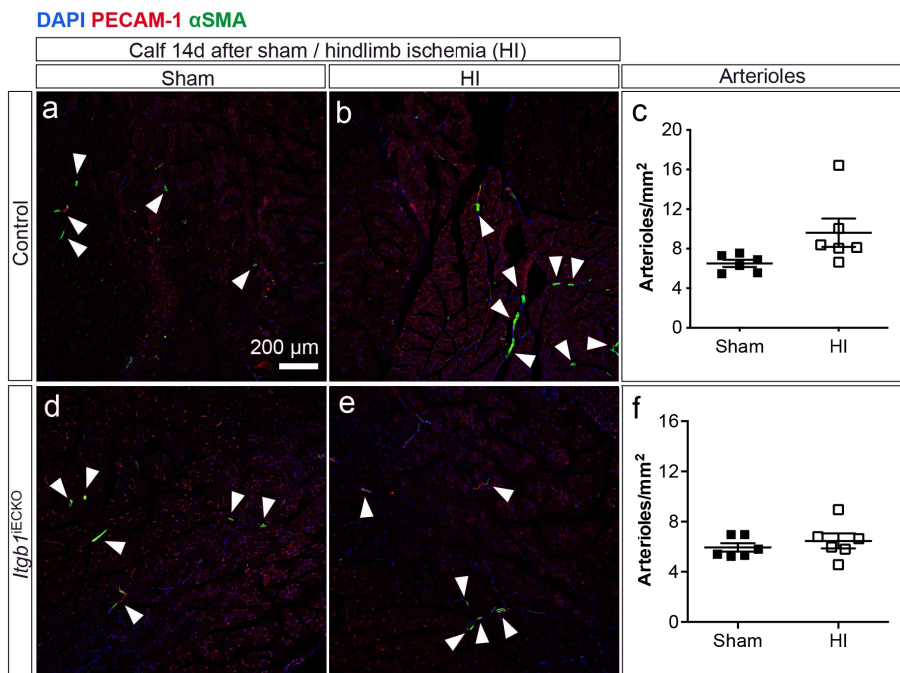


Figure 3.5: Hindlimb ischemia slightly induces arteriole vessel growth in the calf of control mice, but not in KO mice with endothelial cell-specific deletion of *Itgb1*.

(a, b, d, e) Representative immunofluorescence images of the calf 14 d after HI in (a-c) control and (d-f) *Itgb1^{IECKO}* mice. Mice received (a, d) sham or (b, e) HI surgery. Sections were stained for endothelial cells (PECAM-1, red), smooth muscle cells (α SMA, green) and nuclei (DAPI, blue). Arrows indicate arterioles by co-staining of PECAM-1 and α SMA. (c, f) Quantification of arterioles per mm^2 in (c) control and (f) *Itgb1^{IECKO}* mice. Reported values are means \pm SEM with $n = 6$ mice per condition. Statistical significance was determined using paired two-tailed Students t-test. Carina Henning, Anna Branopolski and Dr. Dominik Schuler performed the presented experiment.

Similar results were also observed after antibody-induced inhibition of $\beta 1$ integrin in the same model. Hereby, FA ligation-induced enlargement of pre-existing collaterals, the enhancement of arteriole numbers in the thigh as well as the rise in capillary density in the calf was suppressed by $\beta 1$ integrin blocking antibody administration compared to the treatment with a control antibody (Henning et al., 2019).

Thus, both pharmacological and genetic loss-of-function experiments showed $\beta 1$ integrin to be essential for the signaling in vascular adaptation and therefore this integrin subunit plays a critical role in long-term vascular rearrangement in the thigh and the calf.

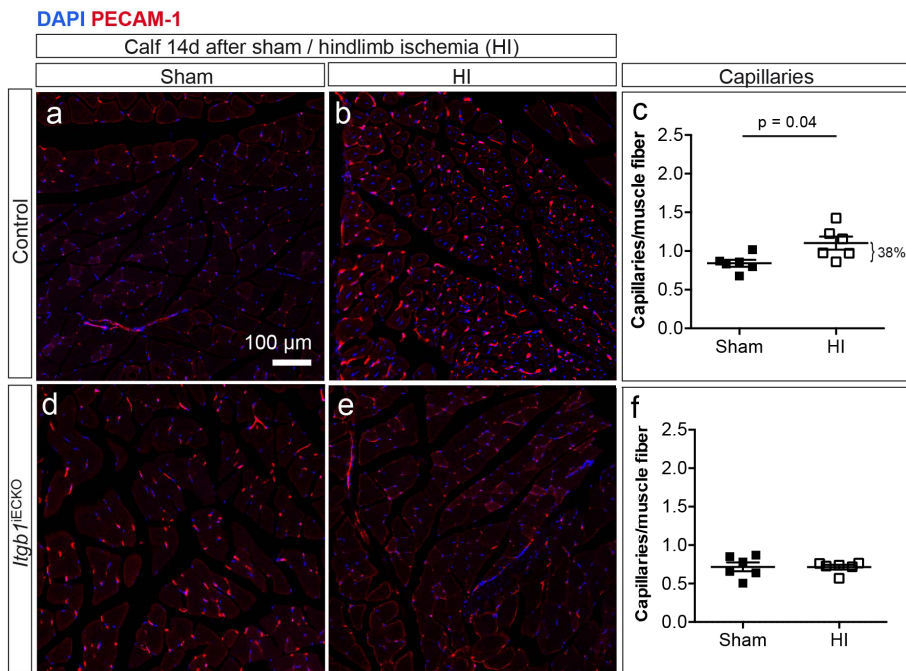


Figure 3.6: Hindlimb ischemia-induced angiogenesis in the calf is reduced in mice with endothelial cell-specific deletion of *Itgb1*.

(a, b, d, e) Representative immunofluorescence images of the calf 14 d after HI in (a-c) control and (d-f) *Itgb1*^{IECKO} mice. Mice received (a, d) sham or (b, e) HI surgery. Sections were stained for endothelial cells (PECAM-1, red) and nuclei (DAPI, blue). (c, f) Quantification of capillaries per muscle fiber in (c) control and (f) *Itgb1*^{IECKO} mice. Reported values are means \pm SEM with n = 6 mice per condition. Statistical significance was determined using paired two-tailed Students t-test. Carina Henning, Anna Branopolski and Dr. Dominik Schuler performed the presented experiment.

Images and results from this section were adapted and recently described in the publication (Henning et al., 2019), Fig. 1 f, l and Fig. 2.

3.2. Transient, repetitive myocardial ischemia reperfusion

Vascular adaptation processes due to ischemia induction can also be initiated in the mouse heart. This represents an effective model to study cellular and molecular signals, which trigger coronary vessel growth with the intention to reflect the situation in humans.

In the past, using a closed-chest myocardial ischemia model, short transient and repetitive periods of ischemia with reperfusion, shortly named Repl/R, were sufficient to cause cardiac vascular remodeling and growth (Lavine et al., 2013). Those periods of LAD occlusions should mimic stuttering angina events, present in patients with CADs and correlating with the development of a cardioprotective well-defined collateral circulation (Billinger et al., 2002; Fujita et al., 1987; Fulton, 1964; Lavine et al., 2013; Piek et al., 1997).

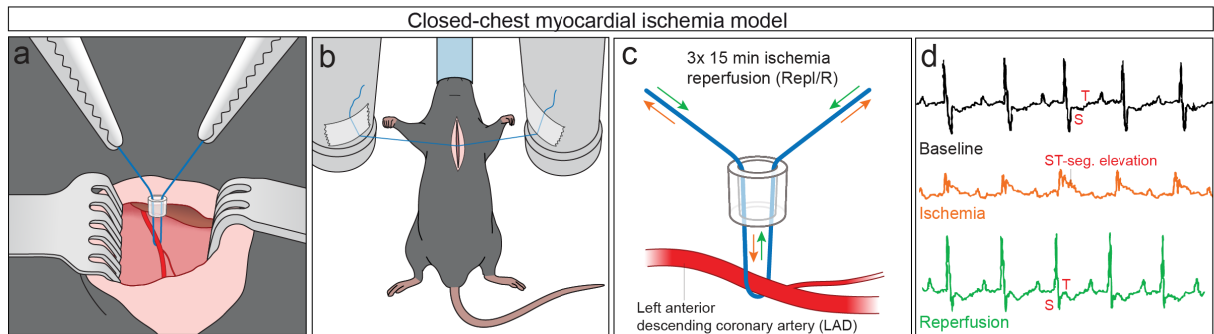


Figure 3.7: Illustration of the closed-chest myocardial ischemia model to induce transient, repetitive myocardial ischemia reperfusion (Repl/R).

(a) View of the occluder implantation where a prolene suture is placed around the proximal left anterior descending coronary artery (LAD) and threaded through a polyethylene (PE) tube, which functions as an occluder. (b) Using this closed-chest model to induce (c) 3x 15 min ischemia by setting the suture ends under tension (orange arrows) and to induce reperfusion by releasing the tension (green arrows). The procedure is shortly called Repl/R. (d) Perfusion changes are recorded by ECG before ischemia, baseline (black line), during ischemia indicated by ST-segment elevation (orange line) and after reperfusion (green line). Images were drafted by Carina Henning and illustrated by Yousun Koh.

For performance, the intervention required a pre-surgery for occluder implantation (Fig. 3.7 a). The occluder temporarily closed the LAD and caused ischemia in the supplying region of the coronary artery. After several days of recovery, in the here described experiments, left myocardial ischemia was induced under closed-chest by pulling tension to the occluder, which interrupted the blood flow through the artery (Fig. 3.7 b, c orange arrows). After 15 min the tension was released and the myocardial tissue was perfused with fresh blood (Fig. 3.7 c green arrows). Here, successful and complete LAD occlusion caused transmural ischemia and ST-segment elevation (STEMI), recorded in ECG measurements (Fig. 3.7 d). The procedure was performed for 3 times every other day and in combination with $\beta 1$ integrin blocking antibody treatment or endothelial $\beta 1$ integrin KO induction (Fig 3.8 a I, II). Furthermore, influence of Repl/R treatment was compared to mice with occluder implantation, but without ischemia induced, referred as RepSham.

Finally, for analysis of morphological changes, transversal cross-sections of the papillary muscle region underneath the occluder were defined as area of interest and histologically investigated by immunofluorescence staining (Fig. 3.8 b). Those sections represent the RV and LV, the main coronary arteries and simultaneously the myocardial tissue, which was exposed to ischemia and which not. (Fig. 3.8 c).

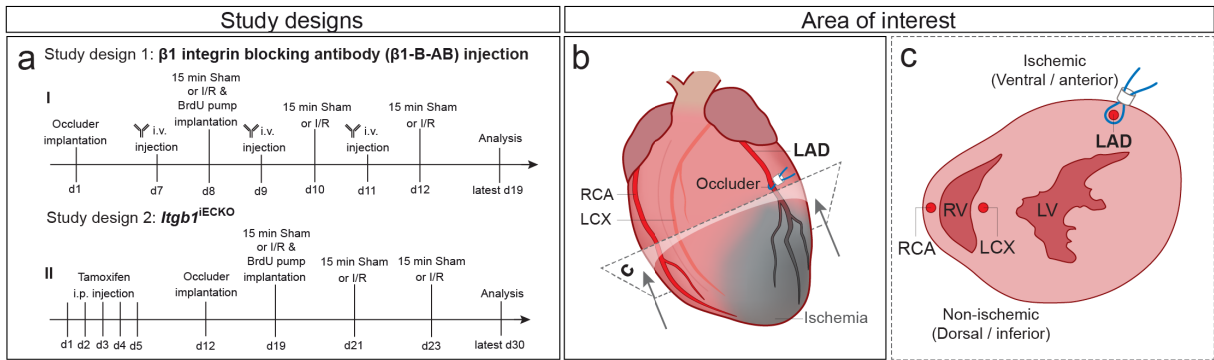


Figure 3.8: Illustration of Repl/R study design and area of interest for histological analysis.

(a) Visualization of study design 1 for (I) i.v. antibody treatment (control (ctrl-AB) or $\beta 1$ integrin blocking antibodies ($\beta 1$ -B-AB)) and study design 2 for (II) EC-specific KO of $\beta 1$ integrin (control or *Itgb1*^{IECKO} mice). (b) Schematic illustration of a mouse heart with implanted occluder and coronary arteries, including the right coronary artery (RCA), the left circumflex artery (LCX) and left anterior descending artery (LAD). Dotted square indicates the cross-section (shown in c) analyzed underneath the occluder. (c) Transversal cross-section, presenting the right (RV) and left ventricle (LV), the coronary arteries as in (b) and the region of ischemic and non-ischemic myocardium after LAD occlusion. Images (b, c) were drafted by Carina Henning and Anna Branopolski and illustrated by Yousun Koh.

Analysis of hypoxia staining showed hypoxic myocardial tissue during LAD occlusion in the left myocardium (referred as ischemic). However, hypoxia was absent in the right and septal myocardium (referred as non-ischemic) (Fig. 3.9 c, d), as well as in control mouse hearts, treated with hypoxic probe and sham procedure (Fig. 3.9 a, b). Therefore, results indicate absence of hypoxia in adult mouse hearts under baseline conditions, but is indeed initiated by LAD occlusion in the area of blocked blood perfusion.

Due to the ischemic and non-ischemic myocardial regions, immunohistochemical analysis was focused on these areas for the detection of blood vascular changes.

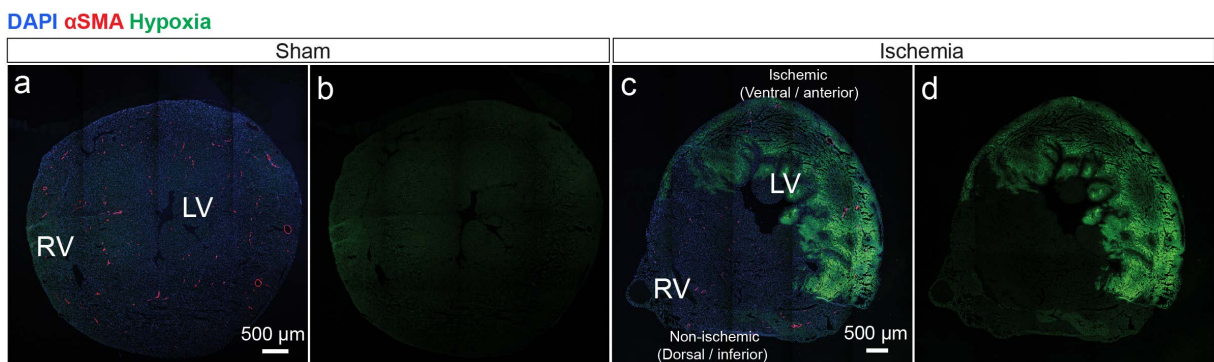


Figure 3.9: LAD occlusion causes hypoxia and therefore ischemia in the left ventricle of the myocardium.

(a-d) Representative immunofluorescence images of the papillary muscular region of mouse hearts treated with hypoxic probe (pimonidazole) before (a, b) sham or (c, d) LAD occlusion (ischemia). Sections were stained for smooth muscle cells (α SMA, red), hypoxia (hypoxic probe, green) and nuclei (DAPI, blue). For orientation the right ventricle (RV) and the left ventricle (LV) is indicated. Carina Henning performed the presented experiment.

3.3. Role of β 1 integrin functionality in Repl/R

Vascular adaptation processes due to Repl/R procedure can be studied on different levels. In this context, ischemia, more specifically, repeated ischemia events can change cellular and molecular homeostasis and enable the organism to adapt. If the ischemic trigger is sufficient in strength, morphological adaptation processes, like vasculature adaptation can be observed. Furthermore, it was shown that coronary vessel growth was accompanied by protection from myocardial infarction (MI) (Lavine et al., 2013).

As in the hindlimb ischemia model, it is conceivable that artery occlusion causes hemodynamic changes and alterations in physical forces, which can be sensed by mechanosensitive receptors, like β 1 integrins (Avraamides et al., 2008; Humphrey et al., 2014; Schwartz, 2010). To verify the relevance of β 1 integrins in ischemia-induced coronary vessel adaptation, mice underwent Repl/R or RepSham procedure and were additionally treated with β 1 integrin blocking antibody (β 1-B-AB) or an isotype-matched control antibody (ctrl-AB). Afterwards, morphological vascular changes and possible cardioprotective properties were analyzed.

3.3.1. Repl/R-induced cardiac endothelial cell proliferation is impaired by β 1 integrin blockage

EC proliferation is discussed to be essential and initial for vascular remodeling and growth (Meier et al., 2013; van Royen et al., 2009). Therefore, to study cardiac EC proliferation due to Repl/R procedure, osmotic pumps were filled with the proliferation marker bromodeoxyuridin (BrdU) and implanted i.p. in the first round of ischemia induction (Fig. 3.8 a, I). To determine the number of proliferating cells, hearts were isolated after surgical intervention, sectioned and stained for BrdU and PECAM-1, to detect proliferating ECs.

Notably, mice treated with ctrl-AB showed an increase in proliferating ECs in the non-ischemic (Fig. 3.10 a-e) as well as the ischemic myocardium (Fig. 3.10 f) after Repl/R compared to RepSham procedure. This increase was particularly stronger in the ischemic myocardium compared to the non-ischemic myocardium.

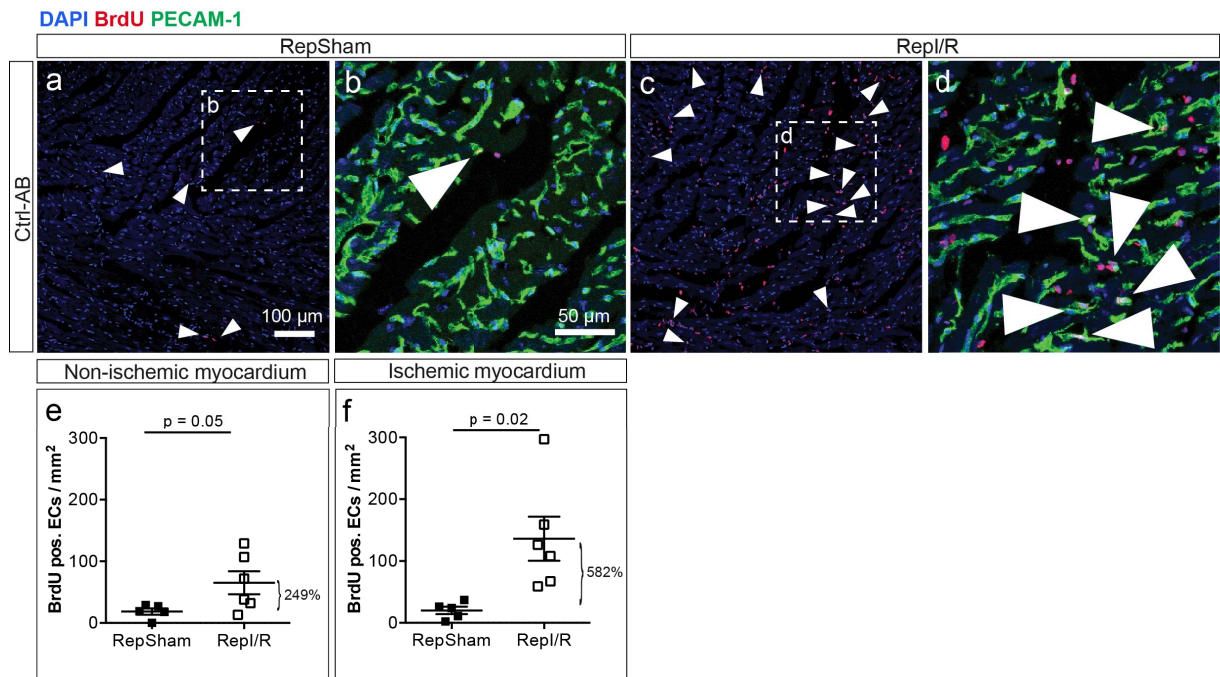


Figure 3.10: Repl/R treatment induces EC proliferation in the ischemic and the non-ischemic myocardium. (a-d) Representative immunofluorescence images of the non-ischemic myocardium of mouse hearts treated with control antibody (ctrl-AB) and (a, b) RepSham or (c, d) Repl/R procedure. Dotted squares indicate zoom in of sections. Sections were stained for proliferation (bromodeoxyuridine (BrdU), red), endothelial cells (PECAM-1, green) and nuclei (DAPI, blue). Arrows indicate proliferating ECs by co-staining of BrdU and PECAM-1. (e, f) Quantification of BrdU positive ECs per mm² in (e) the non-ischemic and (g) the ischemic myocardium. Reported values are means \pm SEM with RepSham n = 5 and Repl/R n = 6 mice. Statistical significance was determined using unpaired two-tailed Students t-test. Carina Henning performed the presented experiment.

Afterwards, cardiac EC proliferation was examined in the response to β 1-B-AB treatment, as previously described (Henning et al., 2019; Planas-Paz et al., 2012). Regarding the prior results, the Repl/R-induced increase in cardiac EC proliferation was inhibited by β 1 integrin blocking in the non-ischemic (Fig. 3.11 a-e) as well as the ischemic myocardium (Fig. 3.11 f).

Concluding, Repl/R procedure alone is sufficient to induce proliferation of ECs in the ischemic and non-ischemic myocardium. Furthermore, this enhancement in EC proliferation was dependent on β 1 integrin functionality as inhibition by blocking AB clearly abolished Repl/R-induced proliferation of ECs.

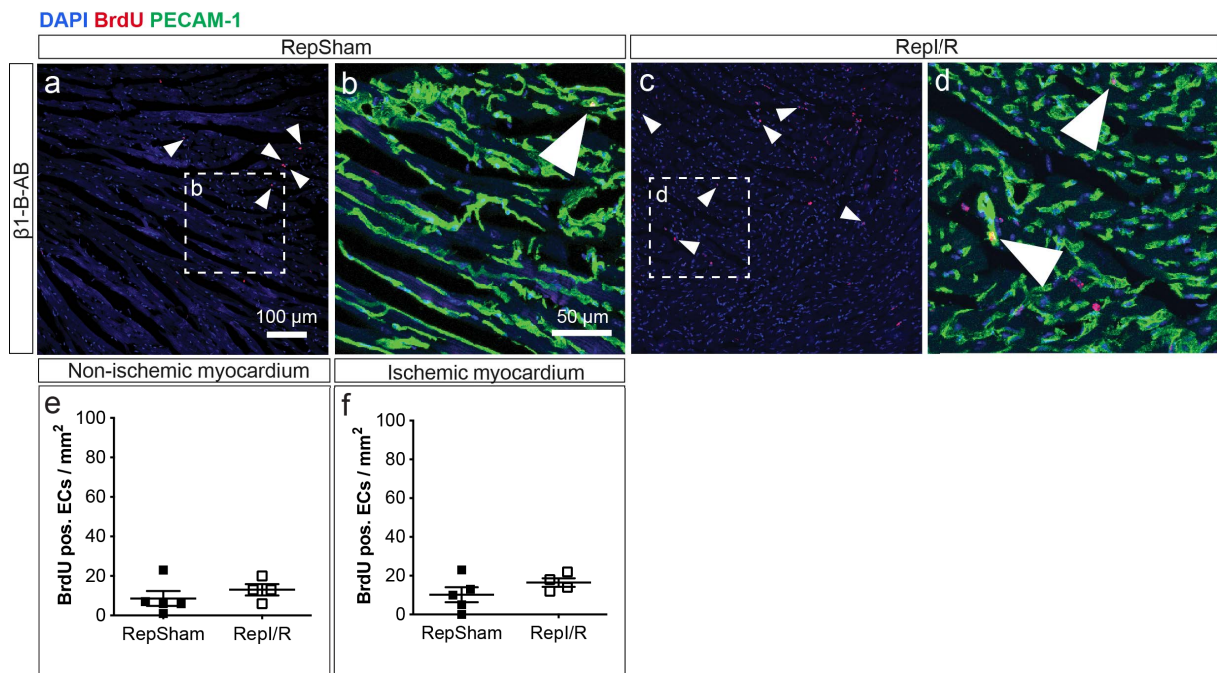


Figure 3.11: Repl/R-induced EC proliferation in the myocardium is inhibited by $\beta 1$ integrin blocking antibody treatment.

(a-d) Representative immunofluorescence images of the non-ischemic myocardium of mouse hearts treated with $\beta 1$ integrin blocking antibody ($\beta 1$ -B-AB) and (a, b) RepSham or (c, d) Repl/R procedure. Dotted squares indicate zoom in of sections. Sections were stained for proliferation (BrdU, red), endothelial cells (PECAM-1, green) and nuclei (DAPI, blue). Arrows indicate proliferating ECs by co-staining of BrdU and PECAM-1. (e, f) Quantification of BrdU positive ECs per mm^2 in (e) the non-ischemic and (g) the ischemic myocardium. Reported values are means \pm SEM with RepSham $n = 5$ and Repl/R $n = 4$ mice. Statistical significance was determined using unpaired two-tailed Students t-test. Carina Henning performed the presented experiment.

3.3.2. Repl/R-induced blood vascular growth is reduced by $\beta 1$ integrin blockage

Structural vascular adaptation happens due to remodeling of pre-existing anastomotic vessel (classical arteriogenesis), but can also occur due to expansion and arterialization of capillaries (*de novo* arteriogenesis) (Faber et al., 2014; Simons and Eichmann, 2015).

To detect ischemia-induced vascular remodeling and growth in mouse hearts, quantification of the arteriole amount was further analyzed after Repl/R treatment. After ctrl-AB application and RepSham or Repl/R intervention, wt mouse hearts were isolated, sectioned and the papillary muscle region underneath the occluder was stained for PECAM-1 and α SMA, to detect arterioles by co-staining of both markers (Fig. 3.12 a-d).

Immunohistochemical analysis represented an increase in the number of arterioles after Repl/R procedure, in the non-ischemic (Fig. 3.12 a-e) as well as the ischemic myocardium (Fig. 3.12 f).

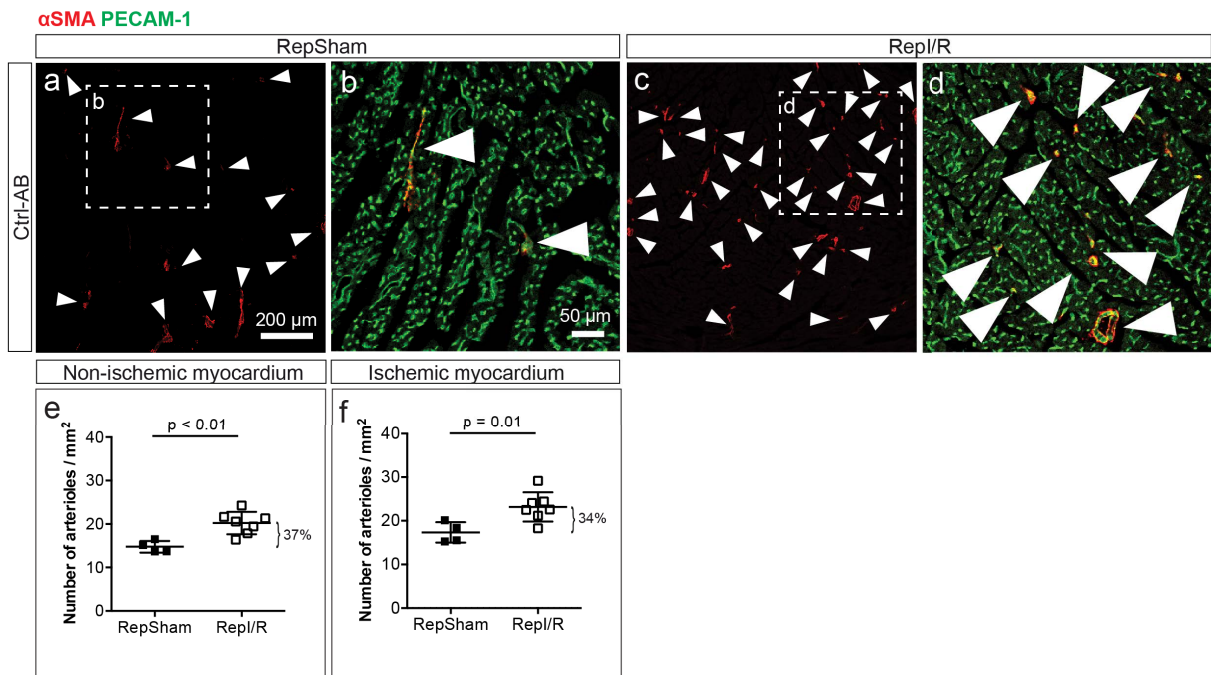


Figure 3.12: RepI/R treatment induces arteriole number increase in the ischemic and the non-ischemic myocardium.

(a-d) Representative immunofluorescence images of the non-ischemic myocardium of mouse heart treated with ctrl-AB and (a, b) RepSham or (c, d) RepI/R procedure. Dotted squares indicate zoom in of sections. Sections were stained for endothelial cells (PECAM-1, green) and smooth muscle cells (α SMA, red). Arrows indicate arterioles by co-staining of PECAM-1 and α SMA. (e, f) Quantification of arterioles per mm² in (e) the non-ischemic and (f) the ischemic myocardium. Reported values are means \pm standard error of the mean (SEM) with RepSham n = 4 and RepI/R n = 7 mice. Statistical significance was determined using unpaired two-tailed Students t-test. Carina Henning and Anna Branopolski performed the presented experiment.

However, this ischemia-induced increase in arteriole number was no longer detectable in mice, which underwent injections of β 1-B-AB. Here, the blocking AB treatment caused an inhibition of arteriole formation in the non-ischemic (Fig. 3.13 a-e) as well as the ischemic myocardium (Fig. 3.13 f) in RepI/R treated mice.

Taken together, these results indicate that short periods of LAD occlusions and subsequent ischemia induction can trigger arteriole formation in the myocardium. Interestingly, this rise was not exclusively dependent on the location of ischemia, as the arteriole number also increased in the non-ischemic myocardium. However, independent from the myocardial region, β 1 integrin function was essential for this process of adult arteriole growth.

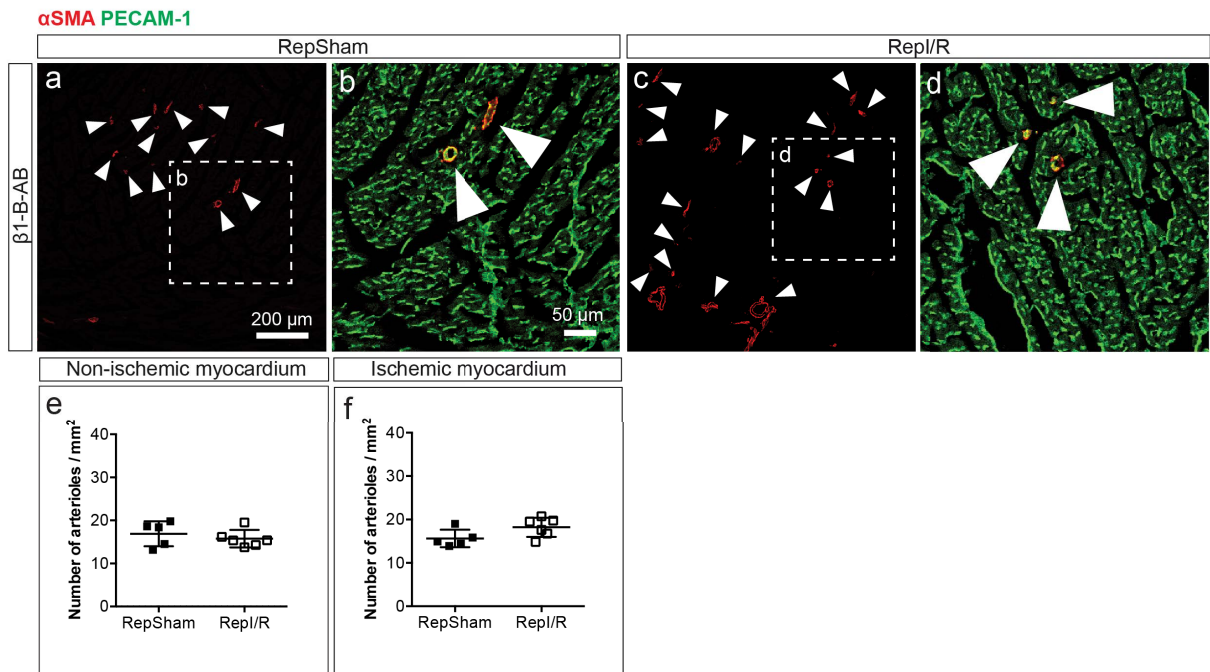


Figure 3.13: Repl/R-induced arteriole number increase in the myocardium is inhibited by β 1 integrin blocking antibody treatment.

(a-d) Representative immunofluorescence images of the non-ischemic myocardium of mouse heart treated with β 1-B-AB and (a, b) RepSham or (c, d) Repl/R procedure. Dotted squares indicate zoom in of sections. Sections were stained for endothelial cells (PECAM-1, green) and smooth muscle cells (α SMA, red). Arrows indicate arterioles by co-staining of PECAM-1 and α SMA. (e, f) Quantification of arterioles per mm^2 in (e) the non-ischemic and (f) the ischemic myocardium. Reported values are means \pm SEM with RepSham n = 5 and Repl/R n = 6 mice. Statistical significance was determined using unpaired two-tailed Students t-test. Carina Henning and Anna Branopolski performed the presented experiment.

3.3.3. Repl/R-induced cardioprotection is sensitive to β 1 integrin blockage

Vascular growth in form of a collateral circulation is described to be protective in case of an ischemia event like a myocardial infarction (MI) in patients with CADs (Faber et al., 2014; Gloekler and Seiler, 2007; Seiler, 2010).

As vascular growth was initiated by repetitive ischemic events, next it was investigated whether cardioprotective properties were additionally detectable with dependency on β 1 integrin functionality. Therefore, mice were treated with RepSham or Repl/R procedure as well as antibody administration. Furthermore, these mice received an additional subsequent 60 min occlusion of the LAD to induce a left ventricular MI. Afterwards, the area of the ischemic myocardium, indicated as area at risk (AAR) and the area of myocardial cell death, indicated as infarction size (INF) was quantified in the left ventricle (LV) by TTC staining (Fig. 3.14 a, b). Results from ctrl-AB treatment showed a non-significant but a tendential reduction in the AAR per LV (Fig. 3.14 c) by Repl/R treatment, whereas the INF per AAR (Fig. 3.14 d) as well as the INF per LV (Fig. 3.14 e) was clearly reduced by Repl/R. Therefore, results indicate that pre-

treatment with Repl/R procedure reduces the size of the damaged myocardial tissue after MI compared to mice without prior Repl/R intervention.

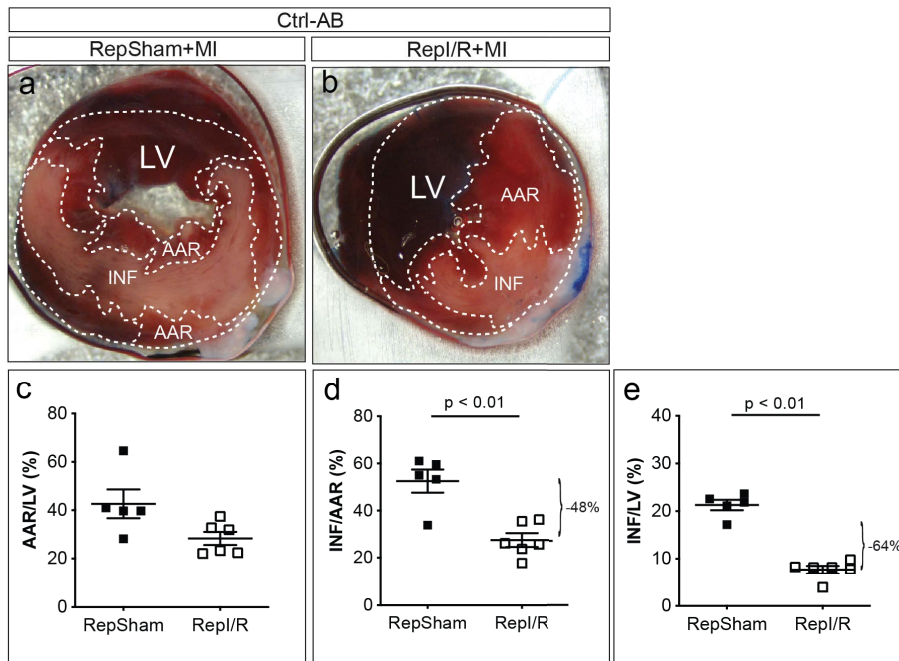


Figure 3.14: Repl/R treatment contributes to infarction size reduction upon myocardial infarction.

(a, b) Representative brightfield images of transversal heart sections after triphenyl tetrazolium chloride (TTC) staining to detect the area at risk (AAR) and the left ventricular infarction size (INF) in mice treated with ctrl-AB and (a) RepSham or (b) Repl/R procedure. Dotted lines indicate the area of the left ventricle (LV), the AAR and the INF. (c-e) Quantification of (c) percentage of AAR per LV, (d) percentage of INF per AAR and (e) percentage of INF per LV. Reported values are means \pm SEM with RepSham $n = 5$ and Repl/R $n = 6$ mice. Statistical significance was determined using unpaired two-tailed Students t-test. Carina Henning performed the presented experiment.

In line with results from Lavine and co-workers, Repl/R procedure was sufficient to induce cardioprotection of the heart indicated by a reduction of left ventricular infarction size (Lavine 2013).

Furthermore, those experiments were compared to mice treated with $\beta 1$ -B-AB. Here, antibody treatment alone, meaning without prior Repl/R treatment, did not influence the ratio of the AAR per LV, INF per AAR and INF per LV compared to ctrl-AB application after MI. Additionally, the treatment with functional $\beta 1$ -B-AB before MI was able to abolish the Repl/R-induced cardioprotective properties (Fig. 3.15 a, b). Within the group of mice, which received $\beta 1$ -B-AB, the percentage of AAR per LV, INF per AAR and INF per LV in RepSham versus Repl/R treatment remained unchanged (Fig. 3.15 c-e). This indicates that the cardioprotective effect of Repl/R, in relation to AAR and infarcted area reduction, is dependent on global $\beta 1$ integrin function.

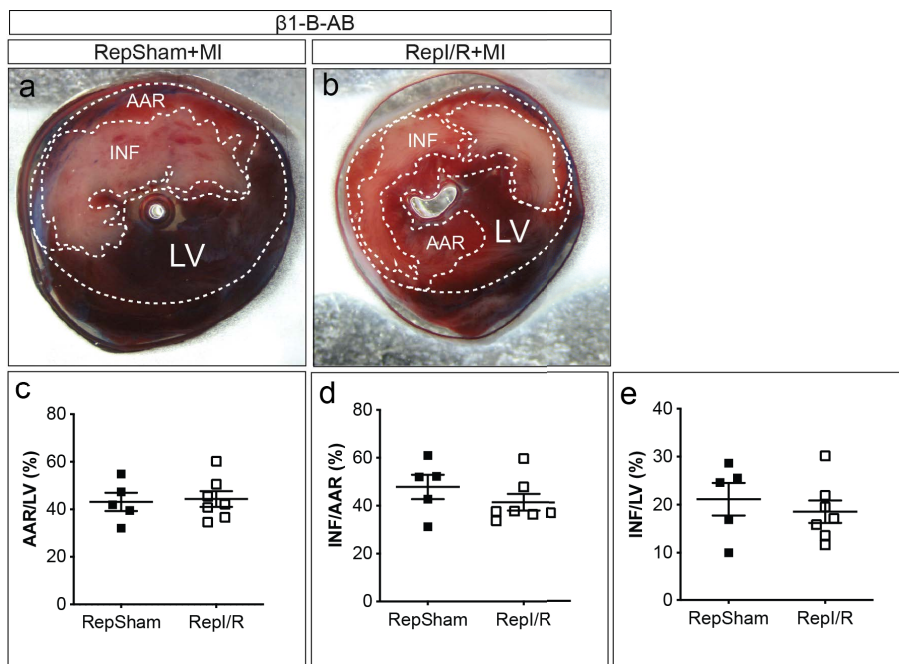


Figure 3.15: Repl/R-induced infarction size reduction is inhibited by β 1 integrin blocking antibody treatment.

(a, b) Representative brightfield images of transversal heart sections after TTC staining to detect the AAR and INF in mice treated with β 1-B-AB and (a) RepSham or (b) Repl/R procedure. Dotted lines indicate the area of LV, AAR and INF. (c-e) Quantification of (c) percentage of AAR per LV, (d) percentage of INF per AAR and (e) percentage of INF per LV. Reported values are means \pm SEM with RepSham $n = 5$ and Repl/R $n = 7$ mice. Statistical significance was determined using unpaired two-tailed Students t-test. Carina Henning performed the presented experiment.

In addition to infarction analysis by TTC staining, cardioprotective characteristics of Repl/R treatment were also investigated in a second examination method by cardiac-specific magnetic resonance imaging (MRI). MRI is a non-invasive imaging technique, in which the ischemic injury of the myocardium and the cardiac function can be analyzed simultaneously in contrast to TTC staining. To quantify the injured area after a prolonged myocardial ischemia, late gadolinium enhancement (LGE) analysis was used. Thereby, gadolinium, previously injected into the mice, accumulates in the damaged heart tissue and is subsequently detectable by H^1 MRI spectrum measurements. The degree of the gadolinium-enriched area indicates the degree of ischemia impact and therefore the degree of damaged myocardium. Cardiac specific MRI is an established technique, also used in the clinical setup as gold standard for tissue characterization and primary endpoint definition (Bonner et al., 2014; Haberkorn et al., 2017; Ibanez et al., 2019).

In the experimental setup the ischemic area (IA) and therefore the resulting infarction size was analyzed 1 d after additional 60 min ischemia reperfusion, referred as MI. Representative MR images are shown in short and long axis view from mice treated with ctrl-AB (Fig. 3.16 a-d). After analysis, results showed a decrease in IA upon Repl/R compared

to RepSham treatment (Fig. 3.16 e). Furthermore, ejection fraction was examined as measure for left ventricular cardiac function (Marwick, 2018). It could be observed that Repl/R procedure constantly preserved cardiac function in the long-term over an observation period of 28 d compared to RepSham treatment (Fig. 3.16 f).

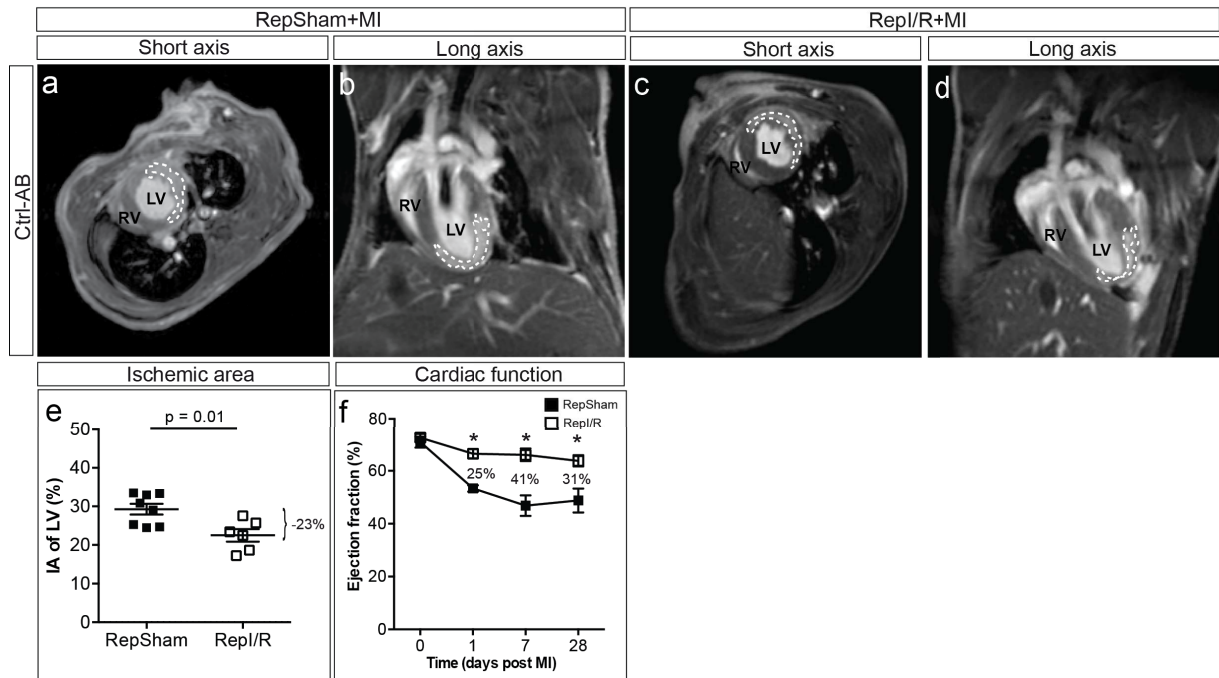


Figure 3.16: Repl/R treatment reduces the ischemic area and preserves cardiac function after MI.

(a-d) Representative magnetic resonance images of mouse hearts treated with ctrl-AB, (a, b) RepSham or (c, d) Repl/R procedure and 60 min ischemia reperfusion, refereed as MI in (a, c) short axis and (b, d) long axis view. Dotted lines indicate the ischemic area by late gadolinium enhancement (LGE) in left ventricle (LV), next to the right ventricle (RV). Quantification of (e) percentage of ischemic area (IA) per LV 1 d post MI and (f) percentage of left ventricular ejection fraction within 28 d. At day 0, independent wt mice without AB injection were used to determine baseline cardiac function. Reported values are means \pm SEM with RepSham $n = 8$ and Repl/R $n = 6$ mice. Statistical significance was determined using unpaired two-tailed Students t-test; hereby listed * p -values are 1 d < 0.01 ; 7 d < 0.01 ; 28 d = 0.01. Carina Henning and Anna Branopolski performed the presented experiment.

Consistent with the results from TTC staining (Fig 3.14) and previous work (Lavine et al., 2013), mice treated with Repl/R procedure exhibit cardioprotection by reduced ischemic area and improved long-term cardiac function after MI.

Furthermore, influence of $\beta 1$ integrin was investigated in the context of Repl/R-induced cardioprotection from myocardial injury. Therefore, mice were treated with $\beta 1$ -B-AB before and during Repl/R or RepSham procedure (Fig. 3.17 a-d). After additional MI the IA was quantified, which remained statistically unchanged between the groups (Fig. 3.17 e). Therefore, results indicate that Repl/R-induced IA reduction was mostly abolished by $\beta 1$ -B-AB treatment, which is comparable to the results from TTC staining (Fig 3.15). Notably, cardiac function was also

critically impaired after administration of $\beta 1$ -B-AB in both groups (Fig 3. 17 f). In conclusion, the cardioprotective property of RepI/R treatment is likely dependent on $\beta 1$ integrin functionality.

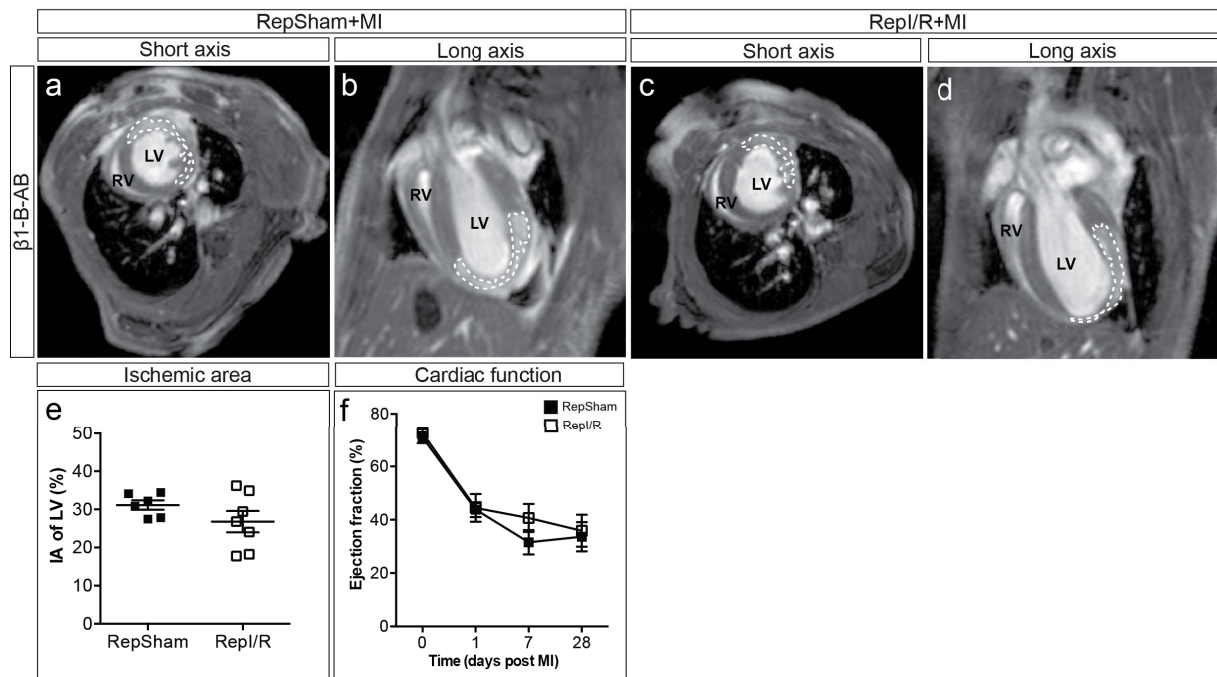


Figure 3.17: RepI/R-induced myocardial protection from MI is sensitive to $\beta 1$ integrin blocking antibody treatment.

(a-d) Representative magnetic resonance images of mouse hearts treated with $\beta 1$ -B-AB and (a, b) RepSham or (c, d) RepI/R procedure before 60 min ischemia reperfusion, refereed as MI in (a, c) short axis and (b, d) long axis view. Dotted lines indicate infarcted area by LGE in LV, next to the RV. Quantification of (e) percentage of IA per LV 1 d post MI and (f) percentage of left ventricular ejection fraction within 28 d. At day 0, independent wt mice without AB injection were used to determine baseline cardiac function. Reported values are means \pm SEM with RepSham n = 6 and RepI/R n = 7 mice. Statistical significance was determined using unpaired two-tailed Students t-test. Carina Henning and Anna Branopolski performed the presented experiment.

3.4. Role of endothelial cell-specific $\beta 1$ integrin in RepI/R

As previously reported, EC-specific deletion of $\beta 1$ integrin results in embryonic lethality, caused by defects in angiogenic sprouting (Carlson et al., 2008; Lei et al., 2008; Tanjore et al., 2008; Zovein et al., 2010). Comprehensibly, the existence and functionality of endothelial $\beta 1$ integrin in adults is also relevant for vascular growth and adaptation under pathological conditions. It was shown that heterozygous depletion of $\beta 1$ integrin in the endothelium results in an abnormal vascular remodeling after external carotid artery ligation (Lei et al., 2008). Furthermore, in a hindlimb ischemia $\alpha 5\beta 1$ integrin was upregulated in collaterals and the here presented results showed endothelial $\beta 1$ integrin to be important for shear stress signaling and ischemia-induced arterio- and angiogenesis (Cai et al., 2009; Henning et al., 2019). However,

the relevance of endothelial $\beta 1$ integrin for adult coronary vessel growth is less investigated and was further addressed.

3.4.1. Quantification of $\beta 1$ integrin KO efficiency in cardiac endothelial cells

To check EC-specific $\beta 1$ integrin KO efficiency in the coronary system, heart ECs from tamoxifen-treated $Itgb1^{iECKO}$ and control mice were isolated by MACS procedure. Analysis of $Itgb1$ gene expression showed an up to 71% reduction in $Itgb1^{iECKO}$ compared to control mice, when gene expression was related to the housekeeping gene $\beta 2M$ (Fig. 3.18 a). By using the housekeeping $Hprt1$, gene expression was also decreased to 67% (Fig. 3.18 b). Furthermore, also a trend in gene expression reduction was visualized in relation to $Rplp0$ (Fig. 3.18 c). Therefore, results indicate a solid downregulation of the $Itgb1$ gene in ECs-specific KO mice. Additionally, investigation in $\beta 1$ integrin protein content showed a strong 70% decline in myocardial ECs from $Itgb1^{iECKO}$ compared to control mice (Fig. 3.18 d, e).

In conclusion, $\beta 1$ integrin was successfully depleted in myocardial ECs.

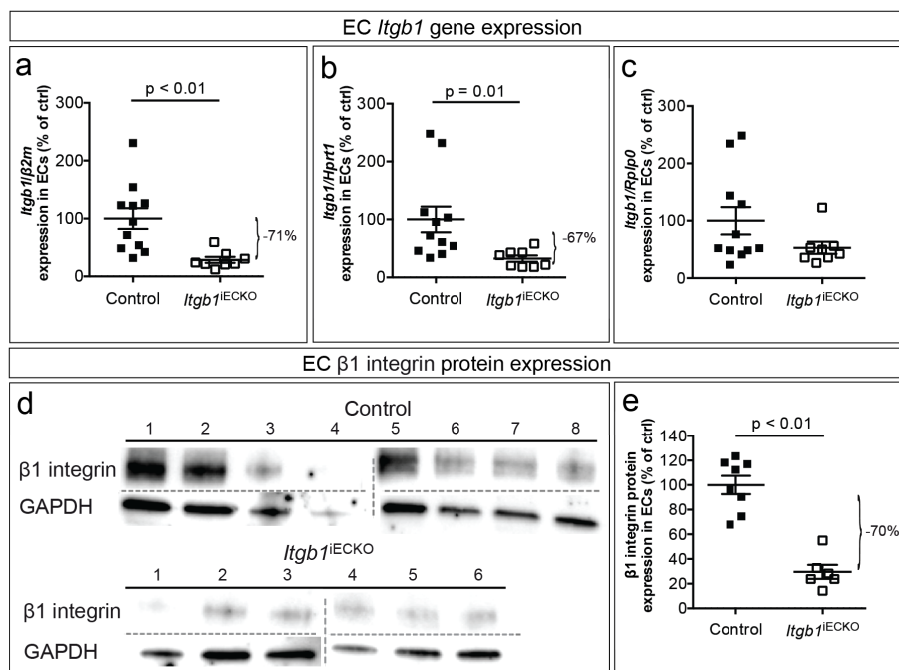


Figure 3.18: Tamoxifen-induced endothelial cell-specific deletion of $Itgb1$ in cardiac ECs from adult mice.

(a-c) Quantification of EC-specific $Itgb1$ gene expression related to (a) $\beta 2M$, (b) $Hprt1$ and (c) $Rplp0$ as housekeeping genes in control and $Itgb1^{iECKO}$ mice. (d) Representative Western blot images showing the detection of EC-specific $\beta 1$ integrin and GAPDH. (e) Semi-quantitative calculation of EC-specific $\beta 1$ integrin protein expression related to GAPDH as housekeeping protein in control and $Itgb1^{iECKO}$ mice. Reported values are means \pm SEM with (a-c) controls $n = 11$ and $Itgb1^{iECKO} n = 8$ and (d, e) controls $n = 8$ and $Itgb1^{iECKO} n = 6$ mice. Statistical significance was determined using unpaired two-tailed Students t-test. Uncropped Western blots are shown in the subitem supplementary information. Carina Henning and Paula Follert performed the presented experiment.

3.4.2. Repl/R-induced cardiac endothelial cell proliferation is controlled by endothelial $\beta 1$ integrin

To examine the role of endothelial $\beta 1$ integrin in Repl/R-induced proliferation of ECs, first control mice were used and analyzed after multiple short myocardial ischemia reperfusion injuries. As previously described, tamoxifen-induced *Cdh5-Cre^{ERT2}* mice, which express the Cre recombinase only in endothelial cells, but hold the wt gene for *Itgb1*, were used as controls.

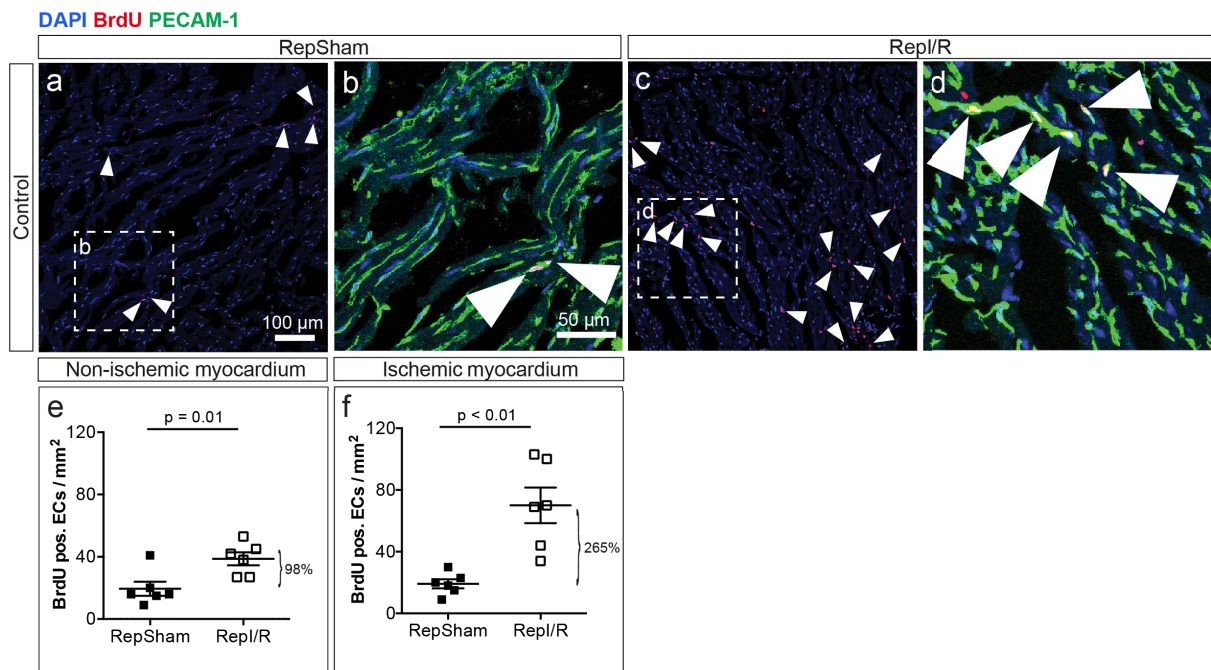


Figure 3.19: Repl/R treatment induces EC proliferation in the ischemic and the non-ischemic myocardium of control mice.

(a-d) Representative immunofluorescence images of the non-ischemic myocardium of control mouse hearts treated with (a, b) RepSham or (c, d) Repl/R procedure. Dotted squares indicate zoom in of sections. Sections were stained for proliferation (BrdU, red), endothelial cells (PECAM-1, green) and nuclei (DAPI, blue). Arrows indicate proliferating ECs by co-staining of BrdU and PECAM-1. (e, f) Quantification of BrdU positive ECs per mm² in the (e) non-ischemic and (g) the ischemic myocardium. Reported values are means \pm SEM with RepSham n = 5 and Repl/R n = 6 mice. Statistical significance was determined using unpaired two-tailed Students t-test. Carina Henning performed the presented experiment.

Corresponding to the wt mice experiments, genetically modified mice received BrdU filled osmotic pumps, which were implanted in the first ischemia, to detect cell proliferation under RepSham and Repl/R intervention. Analysis in control mice indicated an increase in ECs proliferation in the non-ischemic (Fig. 3.19 a-e) and the ischemic myocardium (Fig. 3.19 f). Notably, the rise in proliferating ECs was observed to be greater in the ischemic myocardium compared to the non-ischemic one. Similar to the results from ctrl-AB administration, EC proliferation was triggered independently from the location of ischemia, but was stronger induced under the direct influence of ischemia.

Next, the same analysis was performed in *Itgb1*^{IECKO} mice. To induce EC-specific *Itgb1* gene deletion, animals were treated with tamoxifen and underwent RepSham or Repl/R procedure. Quantification of proliferation by BrdU incorporation revealed no changes in cardiac EC proliferation upon Repl/R compared to RepSham treatment in the non-ischemic (Fig. 3.20 a-e) as well as the ischemic myocardium (Fig. 3.20 f). Thus, the effect of ischemia-induced EC proliferation was abolished by endothelium-specific *Itgb1* gene deletion in both parts of the myocardium.

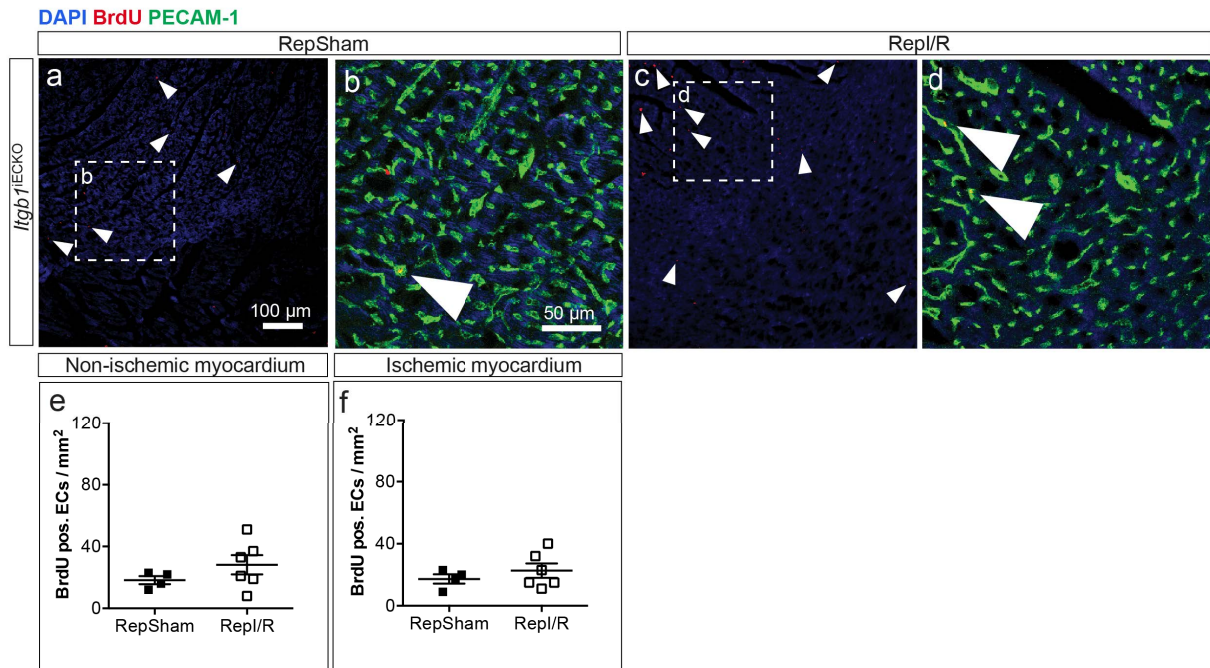


Figure 3.20: Repl/R-induced EC proliferation in the myocardium is inhibited in *Itgb1*^{IECKO} mice.

(a-d) Representative immunofluorescence images of the non-ischemic myocardium of *Itgb1*^{IECKO} mouse hearts treated with (a, b) RepSham or (c, d) Repl/R procedure. Dotted squares indicate zoom in of sections. Sections were stained for proliferation (BrdU, red), endothelial cells (PECAM-1, green) and nuclei (DAPI, blue). Arrows indicate proliferating ECs by co-staining of BrdU and PECAM-1. (e, f) Quantification of BrdU positive ECs per mm² in the (e) non-ischemic and (g) the ischemic myocardium. Reported values are means ± SEM with RepSham n = 4 and Repl/R n = 6 mice. Statistical significance was determined using unpaired two-tailed Students t-test. Carina Henning performed the presented experiment.

3.4.3. Repl/R-induced blood vascular growth is partially influenced by endothelial β1 integrin

Furthermore, and similar to the analysis from antibody treatment, morphologic vascular changes were examined by arteriole number quantification in the myocardium upon Repl/R and RepSham procedure.

After analysis, control mice showed an increase in arteriole number by Repl/R treatment in the non-ischemic (Fig. 3.21 a-e) as well as the ischemic myocardium (Fig. 3.21 f). Therefore, results revealed, as previously detected in ctrl-AB treated wt mice that arteriole formation depends on Repl/R procedure, but is also independently induced from local ischemia influence.

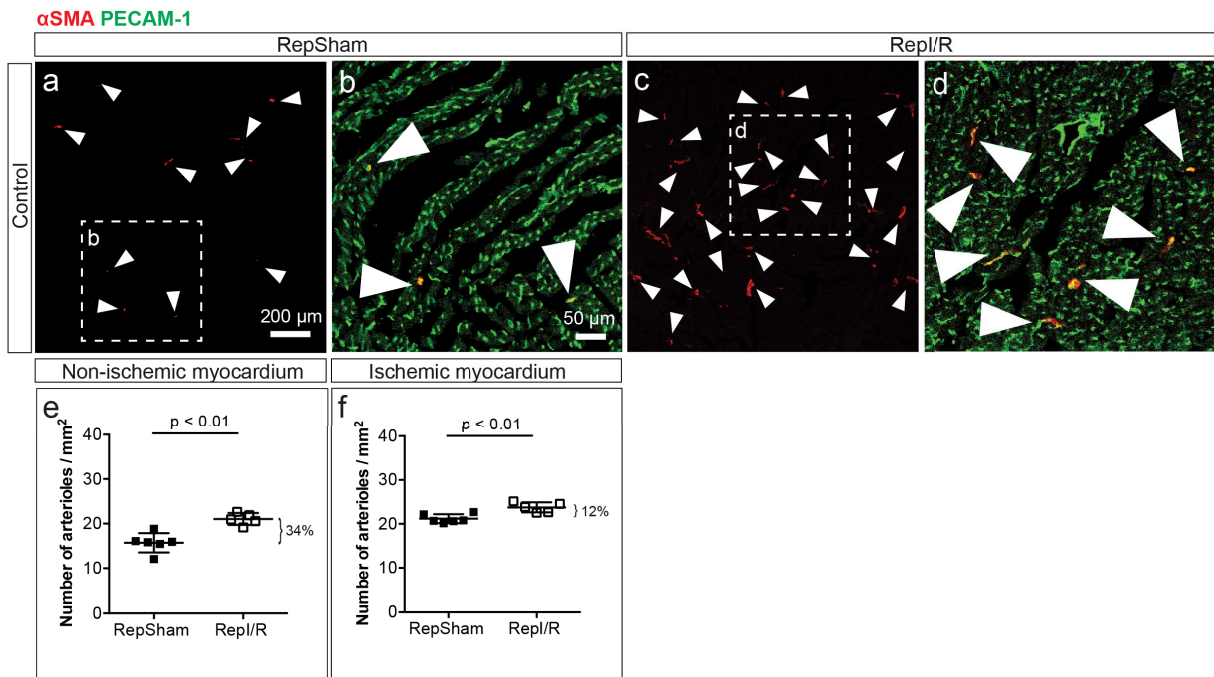


Figure 3.21: Repl/R treatment induces arteriole number increase in the ischemic and the non-ischemic myocardium of control mice.

(a-d) Representative immunofluorescence images of the non-ischemic myocardium of control mouse hearts treated with (a, b) RepSham or (c, d) Repl/R procedure. Dotted squares indicate zoom in of sections. Sections were stained for endothelial cells (PECAM-1, green) and smooth muscle cells (α SMA, red). Arrows indicate arterioles by co-staining of PECAM-1 and α SMA. (e, f) Quantification of arterioles per mm² in (e) the non-ischemic and (f) the ischemic myocardium. Reported values are means \pm SEM with RepSham n = 6 and Repl/R n = 5 mice. Statistical significance was determined using unpaired two-tailed Students t-test. Carina Henning and Anna Branopolski performed the presented experiment.

Furthermore, analysis of arteriole formation was investigated in *Itgb1*^{IECKO} mice. Here, the treatment with Repl/R was not able to trigger arteriole formation in the non-ischemic myocardium (Fig. 3.22 a-e). However, in contrast to blocking antibody treated mice, Repl/R procedure was capable to induce arteriole growth in the ischemic myocardium (Fig. 3.22 f). Notably, this increase was only slightly but still significant. Therefore, these findings demonstrate that arteriole formation after Repl/R intervention is partially dependent on endothelial β 1 integrin and is mainly needed in the non-ischemic myocardium.

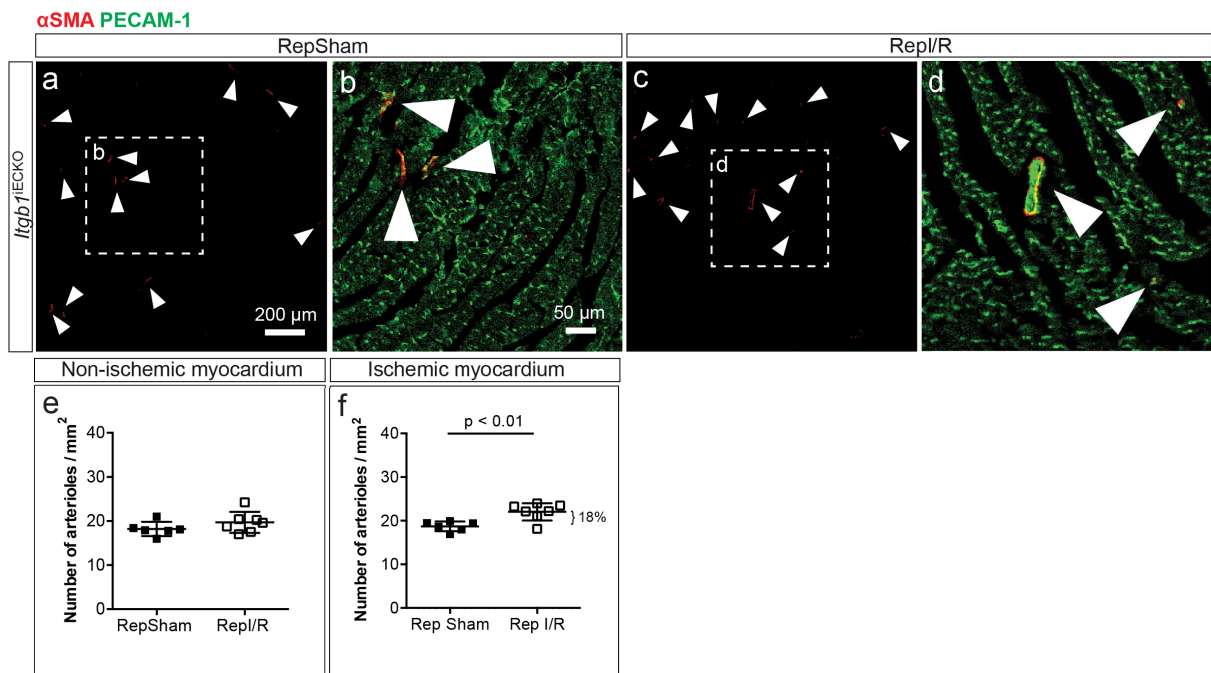
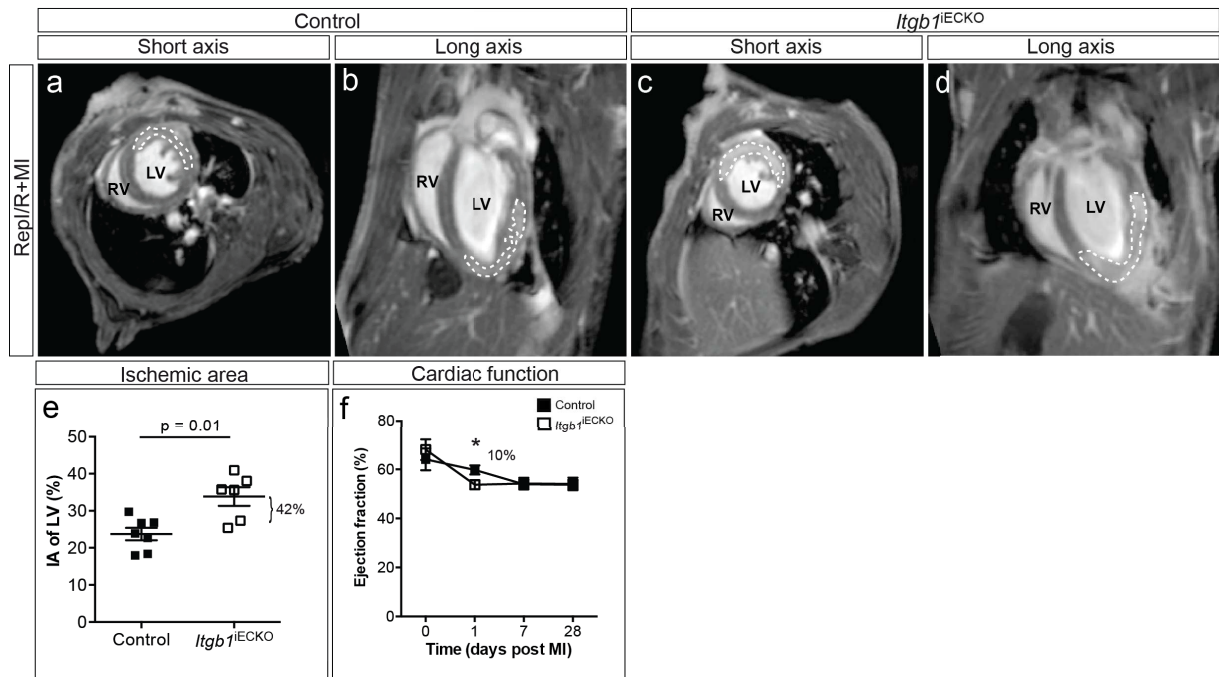


Figure 3.22: Repl/R-induced arteriole number increase in the non-ischemic myocardium is inhibited in *Itgb1*^{IECKO} mice.

(a-d) Representative immunofluorescence images of the non-ischemic myocardium of *Itgb1*^{IECKO} mouse hearts treated with (a, b) RepSham or (c, d) Repl/R procedure. Dotted squares indicate zoom in of sections. Sections were stained for endothelial cells (PECAM-1, green) and smooth muscle cells (α SMA, red). Arrows indicate arterioles by co-staining of PECAM-1 and α SMA. (e, f) Quantification of arterioles per mm² in (e) the non-ischemic and (f) the ischemic myocardium. Reported values are means \pm SEM with RepSham n = 6 and Repl/R n = 7 mice. Statistical significance was determined using unpaired two-tailed Students t-test. Carina Henning and Anna Branopolski performed the presented experiment.

3.4.4. Repl/R-induced cardiac protection is impaired by endothelial β 1 integrin deletion

To study the role of endothelial β 1 integrin in cardiac protection, a subsequent MI was performed after Repl/R procedure in control and *Itgb1*^{IECKO} mice. Notably, mice with EC-specific KO of β 1 integrin showed greater ischemic area, analyzed by LGE in MRI measurements compared to controls (Fig 3.23 a-e). Thus, Repl/R-induced ischemic area reduction and therefore infarction size reduction was abolished in these animals. This suggests that protection from MI, assessed by the analysis of ischemic area, is dependent on EC-specific β 1 integrin. Furthermore, cardiac function, shown by LV ejection fraction, was slightly decreased 1 d after MI in *Itgb1*^{IECKO} compared to controls. Further, 7 d and 28 d post MI changes between groups disappeared (Fig. 3.23 f). Taken together, results showed a mild decrease of Repl/R-induced cardioprotection by EC-specific β 1 integrin deletion. Therefore, findings indicate a partial dependency on endothelial β 1 integrin for protection from MI, as the cardioprotective influence of Repl/R treatment was not fully abolished.



3.5. Myocardial ischemia-induced hepatocyte growth factor secretion is regulated by $\beta 1$ integrin

Next, it was analyzed whether initial ischemia induction could stimulate the secretion of known cardiac EC produced growth factors with cardioprotective capacity. Furthermore, it was determined whether this secretion was dependent on $\beta 1$ integrin.

Notably, growth factors were reported to have an essential role in tissue growth and survival, and they were released by ischemia and mechanical stimulus (Lorenz et al., 2018; Rafii et al., 2016). For instance, endothelin-1 and neuregulin-1, secreted from cardiac ECs, are important for cardiac function, protection, regeneration and survival (Hedhli et al., 2011; Noireaud and Andriantsitohaina, 2014; Rafii et al., 2016). Furthermore, the release of hepatocyte growth factor (HGF) might be relevant for the signaling of cardioprotection too. It was reported that HGF has a critical role in cardiac function, protection and repair from myocardial injury, as it could act as pro-survival factor for cardiomyocytes and stimulates vascular growth in form of angiogenesis under MI (Gallo et al., 2014; Nakamura et al., 2000).

Furthermore, in relation to integrin signaling, it was shown that mechanical stretching of human hepatic ECs induces proliferation and survival of human hepatocytes in a $\beta 1$ integrin dependent manner (Lorenz et al., 2018). Therefore, HGF could be important for signaling ischemia-induced cardioprotection via $\beta 1$ integrin.

To investigate the secretion of growth factor by myocardial ischemia, mice underwent a short left ventricular ischemia stimulation of 15 min with subsequent reperfusion of 1 d. Afterwards, plasma and ischemic heart tissue were checked for endothelin-1 and neuregulin-1 secretion (Fig. 3.24 a-d). In the here performed experiment, short and single myocardial ischemia did not change endothelin-1 or neuregulin-1 protein expression in the plasma (Fig. 3.24 a, b) as well as in the ischemic myocardium (Fig. 3.24 c, d) compared to sham mice.

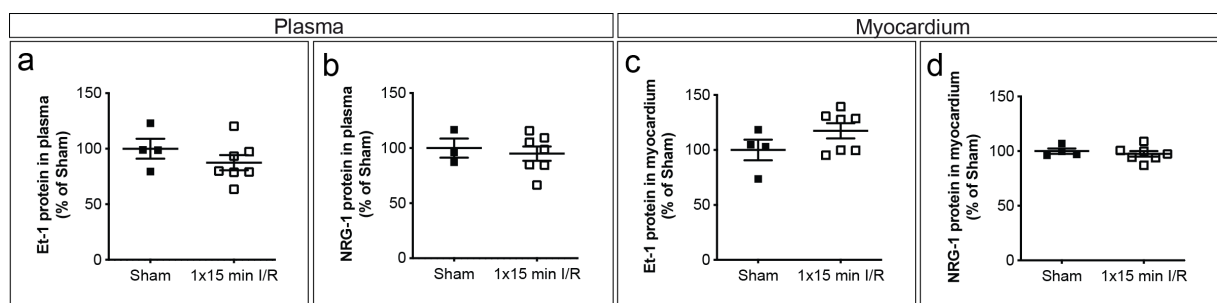


Figure 3.24: Endothelin-1 and neuregulin-1 secretion is not influenced by short myocardial ischemia reperfusion.

(a-d) Quantification of percentage of protein concentration in ELISA analysis after 15 min ischemia reperfusion versus sham procedure for (a, c) endothelin-1 (Et-1) and (b, d) neuregulin-1 (NRG-1) in (a, b) plasma samples and (c, d) ischemic myocardium. Reported values are means \pm SEM with sham n = 3-4 and 1x15 min I/R n = 7 mice. Statistical significance was determined using unpaired two-tailed Students t-test. Carina Henning performed the presented experiment.

However, analysis of HGF in the myocardium showed an increase of protein content (Fig. 3.25 a), which was still present after $\beta 1$ -B-AB treatment, but no longer significant (Fig. 3.25 b). Furthermore, investigation in mice with EC-specific $\beta 1$ integrin deletion showed similar results. Here, in control mice HGF protein content was strongly increased in the myocardium by ischemia reperfusion (Fig. 3.25 c) but clearly limited in *Itgb1*^{IECKO} mice (Fig. 3.25 d).

In conclusion, short myocardial ischemia reperfusion of 15 min could not stimulate endothelin-1 or neuregulin-1 protein expression, but was sufficient to trigger HGF protein expression, which was to some extent dependent on $\beta 1$ integrin function.

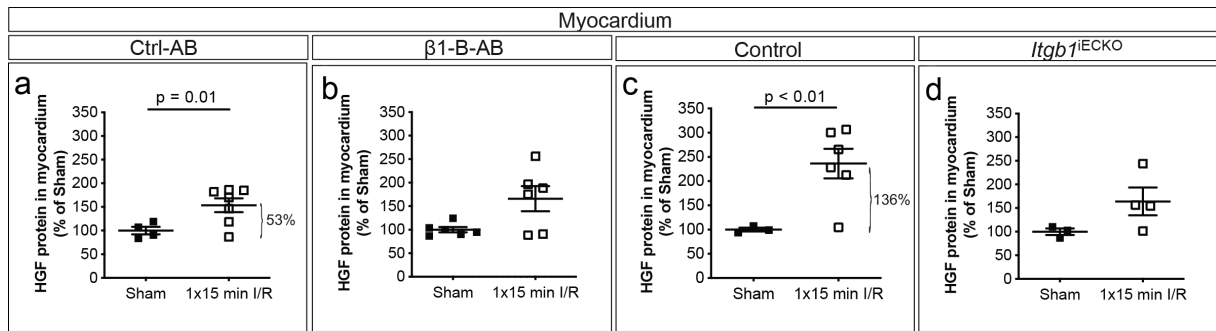


Figure 3.25: Ischemia-induced HGF secretion is diminished by $\beta 1$ integrin blockage and EC-specific $\beta 1$ integrin KO.

(a-d) Quantification of percentage of protein concentration in ELISA analysis after 15 min ischemia reperfusion versus sham procedure for hepatocyte growth factor (HGF) in the ischemic myocardium of mice treated with (a) ctrl-AB or (b) $\beta 1$ -B-AB as well as in (c) control and (d) *Itgb1*^{IECKO} mice. Reported values are means \pm SEM with sham n = 3-6 and 1x15 min I/R n = 4-7 mice. Statistical significance was determined using unpaired two-tailed Students t-test. Carina Henning performed the presented experiment.

3.6. Role of $\beta 1$ integrin in permanent myocardial ischemia

As described in the previous experiments and in line with literature, short periods of myocardial ischemia can initiate cardiac vessel growth, indicated by increased proliferation of cardiac ECs and arteriole formation. Furthermore, those ischemic events lead to cardiac protection in form of improved cardiac function and reduced infarction size after MI. Notably, these effects were influenced by $\beta 1$ integrin. Therefore, these results suggest functional $\beta 1$ integrin to be relevant for myocardial ischemia-induced signaling, vascular remodeling and further protection from myocardial damage.

Similar to the permanent occlusion in the hindlimb ischemia model, the LAD in mouse hearts can also be fully occluded and is investigated as model for patients with acute STEMI, not receiving proper reperfusion (Lindsey et al., 2018). However, in the past this pathological model was further used to induce vascular adaptation by collateralization in postnatal and adult mouse hearts (Das et al., 2019; Zhang and Faber, 2015).

To strengthen the results from Repl/R intervention and to increase the clinical relevance, this myocardial ischemia model was used and investigated in the context of $\beta 1$ integrin dependency. In contrast to Repl/R, here the LAD was constantly occluded by a surgical knot, resulting in left ventricular ischemia and the reperfusion of the myocardium with fresh blood and nutrients was inhibited (Fig. 3.26 a). Before and in regular time periods after LAD occlusion, $\beta 1$ -B-AB or ctrl-AB were i.v. injected in the same amount as for Repl/R or RepSham intervention (Fig. 3.26 b I). Additionally, endothelium-specific KO of $\beta 1$ integrin (*Itgb1*^{IECKO}) was induced by tamoxifen injections before permanent LAD occlusion and compared to their tamoxifen-treated controls (Fig. 3.26 b II). In both experimental approaches, mouse hearts were checked for vascular adaptation processes and changes in cardiac function.

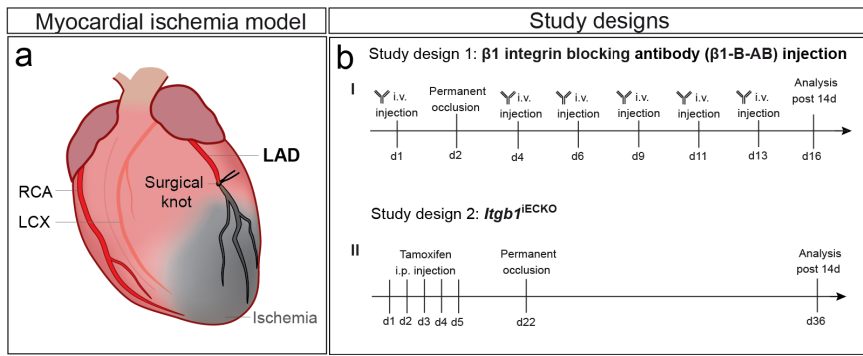


Figure 3.26: Illustration of the myocardial ischemia model for permanent LAD occlusion and the study design.

(a) Schematic illustration of a mouse heart with permanent LAD occlusion by surgical knot and the coronary arteries, including the right coronary artery (RCA), the left circumflex artery (LCX) and left anterior descending artery (LAD). (b) Visualization of study design 1 for (I) i.v. antibody treatment (control (ctrl-AB) or $\beta 1$ integrin blocking antibodies ($\beta 1$ -B-AB)) and study design 2 for (II) EC-specific KO of $\beta 1$ integrin (control or *Itgb1*^{IECKO} mice). Image (a) was drafted by Carina Henning and illustrated by Yousun Koh.

3.6.1. Permanent myocardial ischemia-induced vascular adaptation is regulated by endothelial $\beta 1$ integrin

To analyze the vascular morphology and the subsequent changes by total LAD occlusion, mouse hearts were retrograde perfused over the thoracic aorta with Microfil® compound. After perfusion and curing, the coronary vessels, mainly the larger artery branches, which include the RCA, the LCX and the LAD, were visualized (Fig. 3.27 a). However, also smaller branches, arteries and arterioles in a resolution of around 10 μm were detectable (Fig. 3.27 b).

Upon LAD occlusion and subsequent Microfil® perfusion, the myocardial area supplied by the LAD stayed totally unperfused underneath the surgical knot (Fig. 3.27 c, d). In line with a previous study, this observation indicated no pre-existing anastomotic vessels in mouse hearts, if so filling of the affected myocardium, should have been detectable, even to a small extent (Zhang and Faber, 2015). Due to permanent LAD occlusion over time, adult mouse hearts initiate vascular adaptation likely to compensate and to minimize myocardial damage of constant ischemia (Zhang and Faber, 2015). Therefore, the hearts were analyzed for morphologic changes of the coronary system after occlusion. To investigate the role of $\beta 1$ integrin, mice were additionally treated with blocking AB or $\beta 1$ integrin was deleted in the endothelium.

Here, 14 d after coronary artery occlusion mice treated with ctrl-AB showed clear regrowth of blood vessels or revascularization and perfusion of the ischemic myocardial area compared to direct Microfil® perfusion upon artery occlusion (Fig. 3.27 c-f). However, these characteristics of vascular adaptation were reduced in mice treated with $\beta 1$ -B-AB

(Fig. 3.27 g, h). Less vessels in the infarcted area were observed and vessel density was limited compared to ctrl-AB treated mice.

Furthermore, vascular adaptation was checked in EC-specific $\beta 1$ integrin deficient mice. Notably, control mice showed a similar response to total LAD occlusion as wt mice treated with ctrl-AB. The ischemic myocardial area exhibited vascularization and perfusion (Fig. 3.27 i, j), whereas in *Itgb1*^{IECKO} mouse hearts vascularization and perfusion of the infarcted myocardium was mostly abolished (Fig. 3.27 k, l). Furthermore, it was observed that the left ventricular wall was dilated and thinned.

Concluding these observations, the mouse myocardium is capable to react to permanent perfusion deficiency with revascularization of the infarcted myocardium. It is likely that the induced vascularization and subsequent perfusion reduces myocardial damage and contributes to tissue healing (Zhang and Faber, 2015). Notably, those processes were found to be strongly dependent on $\beta 1$ integrin function, especially in the endothelium.

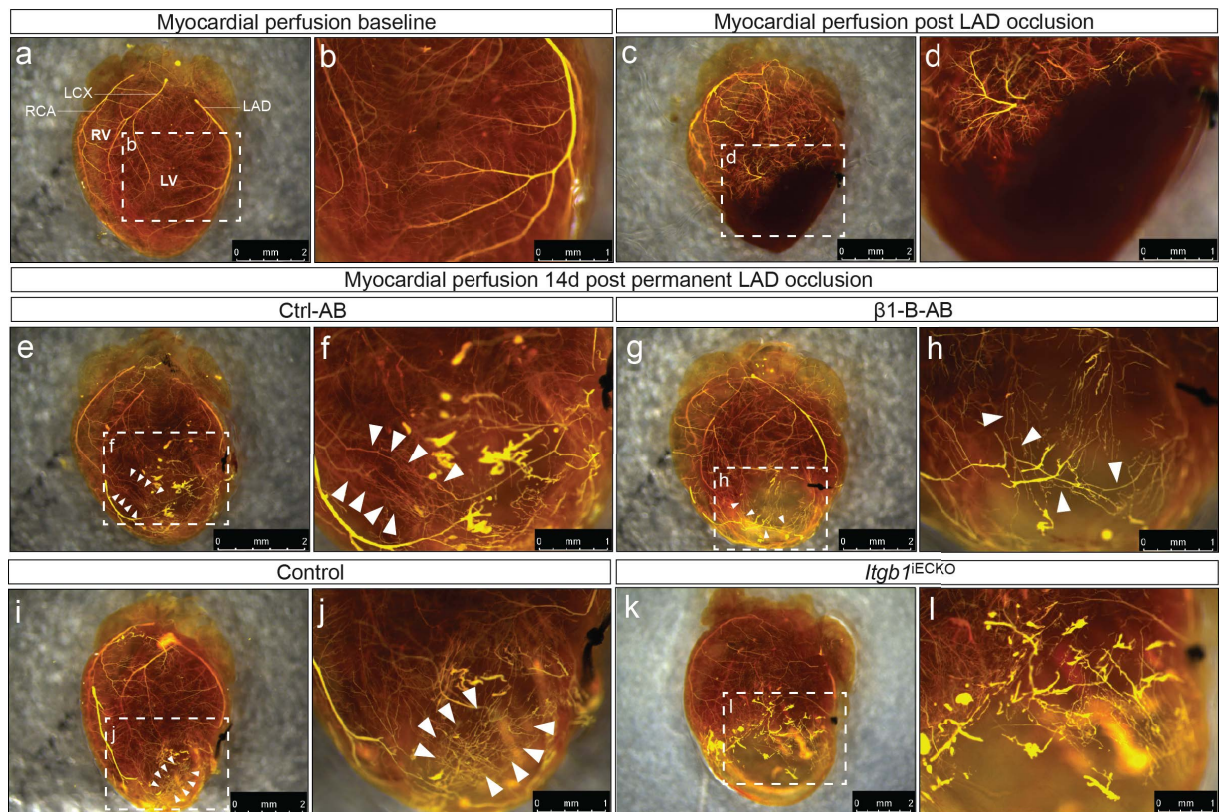


Figure 3.27: Revascularization after permanent LAD occlusion is impaired by $\beta 1$ integrin inhibition and EC-specific deletion.

(a-l) Representative brightfield images of mouse hearts after perfusion with Microfil® compound and optical clearing to image the coronary vasculature under (a, b) baseline condition, (c, d) directly after LAD occlusion and (e-l) 14 d after permanent LAD occlusion. (a) Orientation of the heart is indicated by the left ventricle (LV) and the right ventricle (RV) and the coronary branches, including the RCA, the LCX and the LAD. (e-l) Mice were treated either with (e, f) ctrl-AB or (g, h) $\beta 1$ -B-AB or changes were visualized in tamoxifen treated (i, j) control or (k, l) *Itgb1*^{IECKO} mice. Dotted squares indicate zoom in of images. Carina Henning performed the presented experiment.

3.6.2. Maintenance of cardiac function and survival after permanent myocardial ischemia requires endothelial $\beta 1$ integrin

Next, cardiac function was examined upon permanent LAD occlusion and in response to $\beta 1$ integrin dysfunction. Therefore, function of the heart was examined in echocardiography by imaging and analyzing the parasternal long axis. Here, the left ventricular end-diastolic and end-systolic volume as well as the ejection fraction, before and regularly after coronary artery occlusion, were determined.

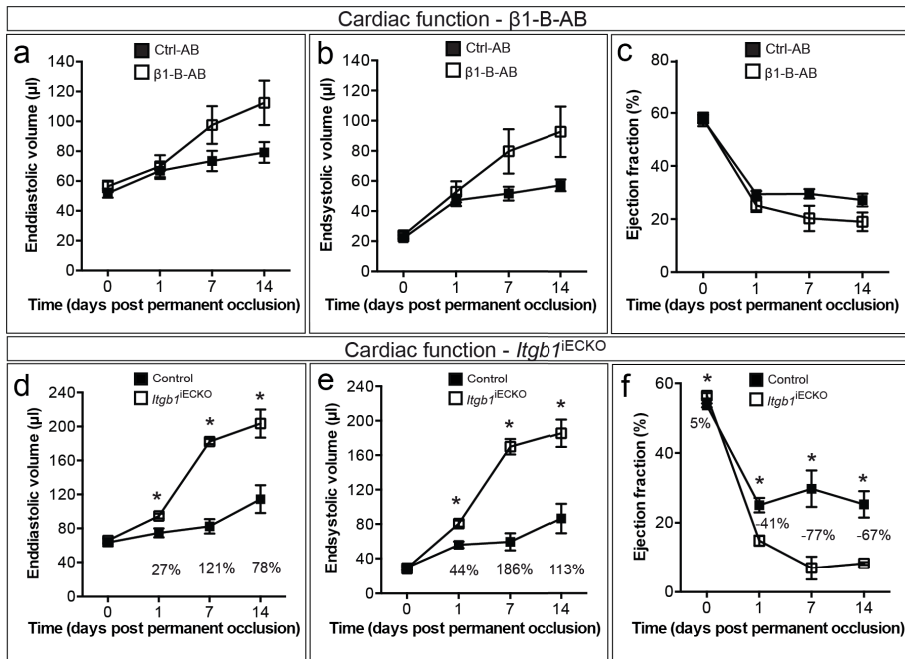


Figure 3.28: Cardiac function after permanent LAD occlusion is sensitive to pharmacological $\beta 1$ integrin inhibition and strongly declined by EC-specific deletion.

(a-f) Quantification of cardiac function by (a, d) end-diastolic, (b, e) end-systolic volume and (c, f) percentage of left ventricular ejection fraction before and within 14 d after permanent LAD occlusion. (a-c) Mice were treated either with ctrl-AB or $\beta 1$ -B-AB or changes were analyzed in (d-f) tamoxifen treated control or $Itgb1^{iECKO}$ mice. Reported values are means \pm SEM with (a-c) ctrl-AB n = 5 and $\beta 1$ -B-AB n = 5 as well as (d-f) control mice n = 5 and $Itgb1^{iECKO}$ mice 0d: n = 5, 1 d: n = 4, 7 d: n = 2, 14 d: n = 2. Statistical significance was determined using unpaired two-tailed Students t-test; hereby listed *p-values are (d) 1 d = 0.02; 7 d < 0.01; 14 d = 0.03 (e) 1 d < 0.01; 7 d < 0.01; 14 = 0.02 (f) 0 d = 0.03; 1 d < 0.01; 7 d = 0.02; 14 d = 0.01. Carina Henning and Aysel Ayhan performed the presented experiment.

After analysis, results revealed an impairment of cardiac function by permanent LAD occlusion in the next 14 d, tendentially greater in mice treated with $\beta 1$ -B-AB compared to mice with ctrl-AB (Fig. 3.28 a-c). Furthermore, this effect was even stronger in gene deficient mice. Here, LAD occlusion resulted in severe cardiac dysfunction, which was substantially larger in $Itgb1^{iECKO}$ mice. These findings were indicated by a huge increase of the end-diastolic and the end-systolic volume in $Itgb1^{iECKO}$ mice compared to their controls (Fig. 3.28 d, e). Furthermore,

this increase led to a strong decrease of the ejection fraction in *Itgb1*^{IECKO} mice related to control mice (Fig. 3.28 f).

In conclusion, these findings suggest the essential role of endothelial $\beta 1$ integrin for the maintenance of cardiac function and heart homeostasis upon acute MI.

Interestingly, most of the *Itgb1*^{IECKO} mice died in the first 4 d after artery occlusion, whereas all control mice survived the procedure (Fig. 3.29 e). Quantification of the survival rate in a Kaplan-Meier curve demonstrated a 60% reduction of survival in *Itgb1*^{IECKO} mice. Examination of hearts from dead *Itgb1*^{IECKO} mice revealed myocardial rupture as possible cause of cardiac death. Brightfield overview and transversal cross-section images showed that the apex region of the heart was thinned and ripped, indicated by black arrows in the figure (Fig. 3.29 a-d).

Taken together, results from total coronary artery occlusion, resulting in a severe MI, indicate endothelial $\beta 1$ integrin as crucial for revascularization of the infarcted myocardium, maintenance of cardiac function and protection from fatal myocardial rupture.

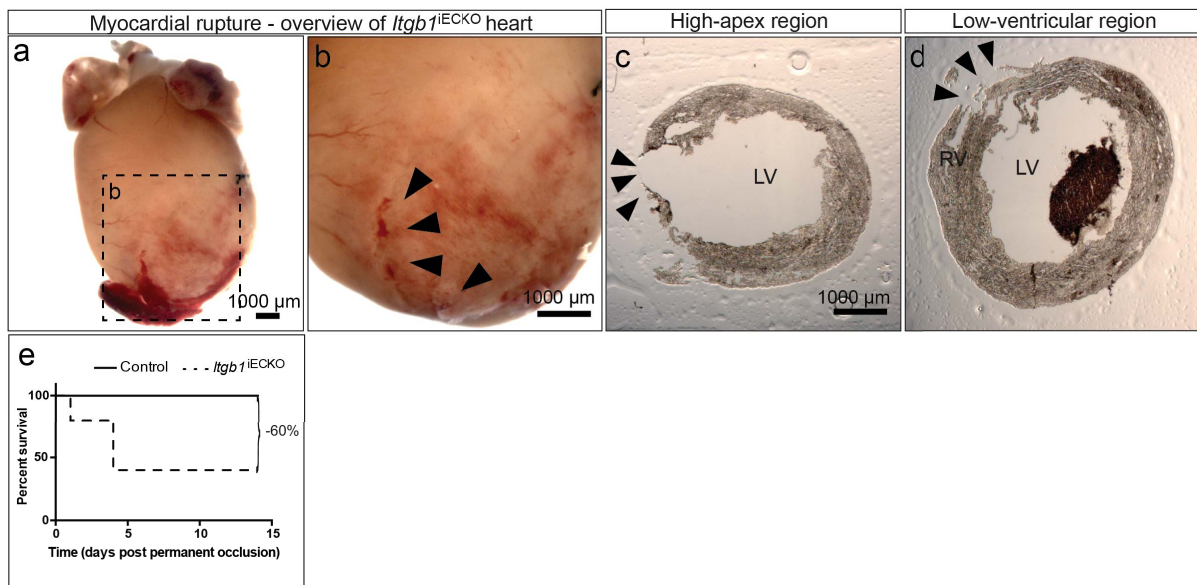


Figure 3.29: Myocardial rupture and subsequent cardiac death after permanent LAD occlusion is strongly dependent on endothelial $\beta 1$ integrin.

(a-d) Representative brightfield images of hearts from *Itgb1*^{IECKO} mice after permanent LAD occlusion in (a, b) overview and (c, d) transversal cross-section images. Arrows show position of myocardial rupture, (b) dotted square indicates zoom in of (a) image without coagulated blood. For orientation the LV and the RV are shown in (c, d). (e) Quantification of the survival rate in a Kaplan-Meier curve of control mice n = 6 and *Itgb1*^{IECKO} mice 0 d: n = 5, 1 d: n = 4 and from 4 d: n = 2. Statistical significance was determined using log-rank test (Mantel-Cox test) with listed p-value = 0.03. Carina Henning performed the presented experiment.

4. Discussion

Some parts of the discussion are substantially described in the publication (Henning et al., 2019) and in the manuscript (Henning et al., 2020, in preparation), which is prepared for publication in a peer-reviewed journal.

4.1. Role of $\beta 1$ integrin in transmission of hemodynamic changes

The recognition of hemodynamic changes by the endothelium is of huge impact, as it initiates short- and long-term vascular adaptation in the affected organs or tissues. In pathological conditions, like in CVDs, the endothelial function, and therefore the sense and transfer of blood flow changes, is impaired or disrupted. In clinical practice and also in research studies, measurement of the FMD offers an effective tool to give insights in the endothelial function, and the impairment correlates with the presence of CVDs. Until now, the mechanism behind is not fully understood but eNOS, which functions as a vasodilatory molecule, as well as KLF2, PECAM-1, VE-cadherin or VEGFR2/3 seem to play an important role (Baeyens et al., 2016; Heiss et al., 2015; Henning et al., 2019).

To gain knowledge in the here described clinically important condition, the relevance of endothelial $\beta 1$ integrin functionality was determined. The receptor subunit $\beta 1$ integrin is a member of the largest group of integrins, characterized as ECM, or rather BM receptor, and is known to transfer mechanical forces (Humphrey et al., 2014; Ingber, 1991; Planas-Paz et al., 2012; Ross et al., 2013; Schwartz, 2010). For instance, mechanosensing by $\beta 1$ integrin was sufficient to release angiocrine signals, important for liver growth and survival, and its impairment in hepatic stellate cells could affect liver regeneration (Lorenz et al., 2018; Rohn et al., 2020). Therefore, it is conceivable that $\beta 1$ integrin could also transmit mechanical forces initiated by artery occlusion. Indeed, data from FMD described in this thesis showed endothelial $\beta 1$ integrin to be essential for the transmission of hemodynamic changes. Here, results demonstrate that EC-specific depletion of $\beta 1$ integrin did not inhibit shear stress generation, which was indicated by unchanged flow velocity behavior, but the endothelial response to shear stress, FMD, was inhibited. In conclusion, upon EC-specific $\beta 1$ integrin deletion, shear stress transfer into the FA was interrupted, the subsequent FMD response was suppressed and normal endothelial function diminished, which was also the case when $\beta 1$ integrin was blocked by antibody application (Henning et al., 2019). Some studies before also gave hints that integrins were involved in the signaling of vasodilation. For instance, the subunit $\alpha 1$ integrin was found to be important to transmit the signal of blood flow to eNOS by activation via peptidase inhibitor 3 kinase (PI3-kinase) and protein kinase B (Akt) (Loufrani et al., 2008). Furthermore, it was demonstrated that the EC-specific activation of $\alpha 5\beta 1$ integrin contributed

to coronary artery dilation, isolated from pigs (Hein et al., 2001), and that the binding of $\beta 3$ integrin to the ECM was important for shear stress-induced porcine coronary artery dilation (Muller et al., 1997). In addition to this, the here presented results demonstrate for the first time that endothelial $\beta 1$ integrin is essential for *in vivo* mouse FMD. This suggests that endothelial $\beta 1$ integrin is strongly needed for triggering *in vivo* vessel vasodilation, which is fundamental for physiological and pathological vascular adaptation also in humans. Therefore, targeting $\beta 1$ integrin in a clinically relevant manner could improve endothelial function and vascular response to artery occlusion.

When focusing more on the appearance of integrins, the apical EC surface is directly exposed to blood flow changes, but integrin receptor expression is mainly present on the basal or abluminal side of the EC membrane. Conceivably, shear stress by blood flow changes is signaled over the apical surface of the endothelium via the cytoskeleton to the connected integrin receptors. The integrin receptors sense this tension and bind to the ECM (Katsumi et al., 2004; Yang and Rizzo, 2013). However, it was also shown that integrins were additionally expressed on the apical surface, although to a small extent, but with the ability of mechanical response (Matthews et al., 2006; Xanthis et al., 2019). Apically expressed $\beta 1$ integrin was activated, and integrin inhibition caused a reduction in shear stress-induced PI3-kinase, Akt and eNOS signaling (Yang and Rizzo, 2013). Own data by immunostaining showed the expression of luminal and apical $\beta 1$ integrin simultaneously (Henning et al., 2019). Furthermore, the importance of $\beta 1$ integrin for eNOS activation and presence was shown *in vitro*, as human artery ECs expressed less phosphorylated and total eNOS upon $\beta 1$ integrin knockdown (Henning et al., 2019). Even if both surface sides contribute to the sensing of mechanical forces, further investigations are needed to determine the molecular mechanism and the signaling way from the apical to the basal EC side.

Interestingly, a recently published study showed endothelial $\beta 1$ integrin not only to be critical in terms of force guiding, but also as key regulator in direction-determined flow sensing (Xanthis et al., 2019). This was indicated by specific activation of $\beta 1$ integrin in response to unidirectional, but not bidirectional flow, in an *in vitro* flow system and in murine aorta samples (Xanthis et al., 2019). To determine similar observations *in vivo*, the use of an ultrasound-based method is not limited to discover endothelial function, it can also be used for the detection of flow direction under physiological or pathological conditions. However, analyzing smaller vessels like collaterals in the hindlimb or coronary arteries may turn out challenging due to resolution limitations. Thus, measurements of flow changes by ultrasound are practicable, but limited to bigger vessels. To analyze vascular adaptation of smaller arteries, illuminated laser speckle flowmetry (LSF) might be a useful tool instead. With this method, researchers could already show increases in blood flow velocity and shear stress in hindlimb

collaterals in mice (Meisner et al., 2013). They could detect collateral segments with reversed blood flow after FA ligation. More precisely, they observed morphological cell adaptation, as indicated by EC repolarization in the new direction of blood flow. Furthermore, the luminal diameter and the wall area was enhanced in segments with reversed blood flow in comparison to collateral segments without reversed blood flow (Heuslein and Blackman, 2015; Meisner et al., 2013).

This imaging technique and the knowledge about $\beta 1$ integrin as key regulator also in flow direction might help to improve the understanding of $\beta 1$ integrin activation *in vivo* and in the transmission of hemodynamic changes in smaller vessels. Therefore, using LSF could give insights into blood flow behavior in mice with $\beta 1$ integrin inhibition, and might explain their impairment of hindlimb collateralization. Derived from FMD measurements, it is likely that $\beta 1$ integrin inhibition will not influence flow velocity after FA ligation in collaterals, but limits the transmission of shear stress into the endothelium. Therefore, it is assumed that vascular adaptation cannot occur, meaning collateralization is abolished, and flow velocity in the collaterals will stay constant, which should be detectable by LSF measurements. This would prove further that endothelial $\beta 1$ integrin is crucial for transmitting shear stress-induced adult collateralization, as essential mechanism to compensate full main artery occlusion.

4.2. Role of $\beta 1$ integrin in vascular adaptation

Chronic or transient rise in blood flow causes vascular adaptation in the long-term, meaning pre-existing collaterals expand, enlarge and become functional. Furthermore, new arterioles can also develop by arterialization of capillaries (Faber et al., 2014; Heil and Schaper, 2004; Mac Gabhann and Peirce, 2010; Schaper, 2009; Simons and Eichmann, 2015; Simons and Ware, 2003). Whatever process is occurring, $\beta 1$ integrin seems to be involved in this structural modification of the blood vasculature. For instance, research showed $\beta 1$ integrin to be upregulated in rabbit hindlimb collaterals after FA ligation (Cai et al., 2009). Additionally, endothelial $\beta 1$ integrin was demonstrated to be important for the growth of stable, non-leaky blood vessels, for vascular remodeling in response to carotid artery ligation and for vascular leakage in endotoxemia (Hakanpaa et al., 2018; Lei et al., 2008; Yamamoto et al., 2015).

All these findings support a central role of $\beta 1$ integrin in connection to the vascular system. Nevertheless, and especially with regard to clinically relevant adult blood vessel remodeling, which might be beneficial for patients with CVDs, $\beta 1$ integrin importance should be further investigated. Therefore, different *in vivo* mouse models, which reflect the conditions of human CVDs were used in this thesis for further evaluation of $\beta 1$ integrin.

4.2.1. Impact of β 1 integrin for cardiac endothelial cell proliferation

One important step of arterial adaptation and remodeling is characterized by increased proliferation of vascular derived cells, like ECs (Meier et al., 2013; Schaper, 2009; van Royen et al., 2009). Also, integrins were shown to be involved in a variety of physiological and pathological processes that contain cell proliferation (Avraamides et al., 2008; Lorenz et al., 2018; Silva et al., 2008; Somanath et al., 2009). To analyze the relevance of β 1 integrin for vascular formation, the previously described Repl/R procedure was used to trigger cardiac EC proliferation in different regions of the myocardium and in relation to β 1 integrin inhibition. Therefore, β 1 integrin signaling was suppressed by pharmacological as well as genetic manipulation. Interestingly, in both regions, meaning in the ischemic and in the non-ischemic myocardium, proliferation of ECs was increased in control mice. Furthermore, this increase was stronger in the ischemic region, but still detectable in the non-ischemic one, and mostly abolished by β 1 integrin inhibition in both regions.

Based on ischemia induction, the affected myocardial region turns hypoxic, which was identified by hypoxia staining in this area. Studies before showed β 1 integrin to be upregulated by hypoxia via activation of HIF-1 α in fibroblasts (Keely et al., 2009). In relation to cell growth, this integrin subunit was also relevant for hypoxia-induced embryonic stem cell proliferation (Lee et al., 2011). Furthermore, α 5 β 1 integrin was also shown to hold a proliferating capacity in brain ECs under hypoxic conditions (Li et al., 2012). Taken together, findings from literature and this thesis indicate hypoxia as one effective trigger for β 1 integrin-related EC proliferation in the ischemic region.

Interestingly, results from the non-ischemic myocardium demonstrated that cardiac EC proliferation was inducible independently from local hypoxia. However, this proliferating capacity was indeed dependent on endothelial β 1 integrin. This suspects a second trigger to be crucial for Repl/R-induced ECs proliferation. As in the previous section discussed, changes in hemodynamics during or shortly after artery occlusion can lead to a shear stress increase in the surrounding vasculature. More precisely, a pressure gradient arises between the area proximal and distal to the stenosed artery, a scenario mainly validated in other organs (Meier et al., 2013). Therefore, it is imaginable that those gradients increase shear stress in regions unaffected by hypoxia, but recognized by mechanosensitive receptors like β 1 integrin, targeting pathways for EC proliferation. This could explain why EC proliferation in these regions was abolished after inhibition or depletion. In this context, also others researchers could show the requirement of β 1 integrin for cell stretch-induced lymphatic EC proliferation (Planas-Paz et al., 2012).

In summary, the here presented results indicate endothelial $\beta 1$ integrin to be essential for ischemia-induced cardiac EC proliferation, which is driven by both, hypoxia and potential shear stress alterations in the surrounding myocardial vasculature. However, to prove the latter, further investigations in shear stress experiments with cardiac ECs are needed.

4.2.2. Impact of $\beta 1$ integrin for arteriole and capillary formation

As EC proliferation is revealed as one of the first steps of vascular remodeling, further structural changes in arteriole or capillary formation should be detectable. Therefore, morphological alterations in the blood vasculature were analyzed next. Again, ischemia was induced by ligation of the FA, by transient occlusions of the LAD (Repl/R) or by permanent occlusion of the LAD. Although vascular changes were analyzed by different evaluation methods, results from all ischemia models showed successful induction of vessel adaptation. In more detail, first it was demonstrated that HI resulted in an increase in arteriole number in the thigh and a rise in capillary density in the calf of mouse hindlimbs, similarly as in previous work (Limbourg et al., 2009). Comparable to the myocardial ischemia model, FA ligation leads to decreased perfusion and development of hypoxic regions in the hindlimb. While the thigh recovers within a few days, the calf stays mainly unperfused (Henning et al., 2019). Notably, different forces are relevant for vascular adaptation. Here, the thigh is mainly affected by shear stress increase, which contributes to an enlargement of pre-existing collaterals and a rise in arteriole number (arteriogenesis). This reflects a pathological reaction to compensate the blockage by increasing perfusion to the ischemic calf. Therefore, absence of perfusion and subsequent hypoxia in the calf triggers the increase of capillary density (angiogenesis), which improves blood supply of the muscles (Heil et al., 2006; Heil and Schaper, 2004; Limbourg et al., 2009; Schaper, 2009). Importantly, both processes are relevant to balance artery occlusion, meaning arteriogenesis provides an increase of perfusion, and angiogenesis improves immediate blood supply to the affected tissue (Limbourg et al., 2009; Simons and Ware, 2003).

Regarding to this, data showed endothelial $\beta 1$ integrin to be crucial for both processes. Interestingly, induction of gene deficiency alone did not affect arteriole or capillary quantity and was not able to initiate EC apoptosis. This indicates that the observed results were not caused by changes in vascular viability upon EC-specific $\beta 1$ integrin depletion, but rather due to the crucial role of $\beta 1$ integrin in processing a vascular adaptive stimulus (Henning et al., 2019). Furthermore, expression and functionality of $\beta 1$ integrin was also essential for blood vessel remodeling in the murine heart. The Repl/R procedure, mimicking short episodes of ischemia like in patients with CAD and total LAD occlusion, comparable to an acute myocardial infarction

(AMI), was previously used to induce cardiac vessel growth (Das et al., 2019; Lavine et al., 2013; Zhang and Faber, 2015). The here presented data showed similar results, as cardiac vessel growth was clearly induced, but possibly different to the hindlimb situation, as mice lack pre-existing collaterals in the heart (Zhang and Faber, 2015). One plausible scenario for this finding might be *de novo* formation of arterioles by arterialization of capillaries, including mural cell coverage and further vessel expansion (Faber et al., 2014; Mac Gabhann and Peirce, 2010; Simons and Eichmann, 2015).

According to the presented results, Repl/R procedure did not induce collateral formation, indicated by interconnecting bigger arteries, however an increase in arteriole formation was detectable in the ischemic and non-ischemic myocardium. Conceivably, arteriole formation might be considered as initial step for developing collaterals, as they mature from smaller arteries and occur in different regions of the myocardium (Faber et al., 2014; Lavine et al., 2013; Meier et al., 2013; van Royen et al., 2001). However, full coronary artery occlusion for several days was sufficient to induce *de novo* collateral formation in the infarcted myocardium, also shown by previous work (Das et al., 2019; Zhang and Faber, 2015). By comparing both models, ischemia duration is decisive for manifestation of cardiac vessel growth. Meaning, long-lasting ischemia impact to the myocardium, triggers vascular adaptation more effectively, likely to reduce a massive organ damage or loss of function compared to short ischemia influence.

Furthermore, data showed ischemia-induced hypoxia is necessary for arteriole formation and vascularization in the ischemic myocardium. However, similar to the explanation from EC proliferation studies, it is not the only force, as arteriole formation also occurs in the non-ischemic myocardium. As previously discussed, hemodynamic changes in the surrounding blood vessels might trigger vascular adaptation additionally, even if vessels have to develop *de novo* and do not remodel from pre-existing ones. For instance, patients with coronary occlusions showed an increased collateral flow index, and from measurements in dogs it is known that coronary artery occlusion increases blood flow and shear stress in the coronary circulation, considered as trigger for collateral remodeling, also in the heart (Guan et al., 2016; Jamaïyar et al., 2019; Meier et al., 2013; Schwartz et al., 1983). Nevertheless, measurements in mouse hearts are needed to prove this, since they lack native collaterals and due to the small size of the heart generated forces might behave differently.

Furthermore, focusing on the relevance of $\beta 1$ integrin, its inhibition or EC-specific depletion impaired vascular adaptation independent of the myocardial ischemia model. Both models indicate the central role of this specific transmembrane receptor in the process of adult coronary modification, especially for long-term adaptation during constant myocardial ischemia. However, one exception was detectable, in which EC-specific $\beta 1$ integrin depletion did not fully block arteriole formation in the ischemic myocardium, even though EC proliferation

was inhibited. Upon ischemia induction and therefore tissue injury, a subsequent inflammatory response occurs, additionally known to be relevant for vascular growth and remodeling (Heil and Schaper, 2004; Medzhitov, 2008; Swirski and Nahrendorf, 2018). To some extent, latter response might be able to trigger arteriole formation independently of EC proliferation and presence of $\beta 1$ integrin on ECs. In the past, it was shown that ECs from sprouting capillaries can rearrange for the formation of arteries, and that arterial ECs can migrate towards capillaries to reassemble to arteries, which was essential for collateralization (Das et al., 2019; Pitulescu et al., 2017). However, those events were analyzed in postnatal or neonatal studies and not completely isolated from EC proliferation. It was also mentioned that the mechanism of adult cardiac collateralization might be different to some extent (Das et al., 2019). Currently, a statement how arteriole formation in the injured myocardium is plausible without or with reduced EC proliferation and $\beta 1$ integrin existence cannot be made. Therefore, further investigations are strongly needed.

As integrins are heterodimeric transmembrane receptors, connected over ligand-binding to collagen, fibronectin and laminin to the ECM (Moreno-Layseca et al., 2019), further investigations in the relevance of different heterodimers might be interesting. For instance, an increase in vascular fibronectin and simultaneous $\alpha 5\beta 1$ integrin expression was shown in spinal cord blood vessel remodeling by chronic mild hypoxia and in growing collaterals by hindlimb ischemia (Cai et al., 2009; Halder et al., 2018). Furthermore, in preliminary data, laminin- $\beta 6$ integrin was shown to be crucial for coronary collateral growth in rats (Joseph et al., 2018). Interestingly, eNOS might be related to $\beta 1$ integrin signaling as well, since eNOS KO mice show a similar phenotype of impaired vascular remodeling upon HI, and KD of $\beta 1$ integrin in human ECs demonstrate a decrease in total and phosphorylated eNOS protein expression (Dai and Faber, 2010; Henning et al., 2019; Yu et al., 2005).

Besides, targeting $\beta 1$ integrin by miR-223 showed inhibition of bFGF- and VEGF-induced growth factor receptor phosphorylation and Akt activation (Shi et al., 2013). The interaction of $\beta 1$ integrin and growth factor receptors, like VEGFRs was further revealed by others, and also promotes the release of angiocrine factors, like HGF (Lorenz et al., 2018; Planas-Paz et al., 2012). Here, vascular growth-related and cardioprotective HGF expression (Gallo et al., 2014; Nakamura et al., 2000) was negatively influenced by $\beta 1$ integrin inhibition or endothelium-specific deletion, indicating a potential dependency. However, to understand the pathway behind $\beta 1$ integrin dependent vascular remodeling, possible interaction partners need to be further addressed.

4.3. Role of β 1 integrin in cardioprotection

In line with previous work, protection from MI was induced by Repl/R procedure, as demonstrated by reduced infarction size and improved cardiac function (Lavine et al., 2013). After pointing out the essential role of β 1 integrin globally and in the endothelium for adult vascular adaptation, the relevance of this specific integrin for cardioprotection was investigated next. A few previously performed studies determined the role of β 1 integrin in the adult mouse heart. For instance, global heterozygous depletion of β 1 integrin impaired cardiac outcome after MI (Krishnamurthy et al., 2006) and the overexpression of α 7 β 1D in cardiomyocyte reduced infarction size after I/R (Okada et al., 2013). Another study showed β 1 integrin expression to be upregulated especially in the zone of inflammation and fibrosis (Sun et al., 2003). Furthermore, the role of EC-specific β 1 integrin in mouse hearts was investigated in lipopolysaccharide (LPS)-induced vascular leakage (Hakanpaa et al., 2018). Additionally, the here presented data showed that pharmacological inhibition of β 1 integrin abolished Repl/R-induced cardioprotection. This was indicated by infarction size and cardiac function analysis. In the scenario of Repl/R procedure, the effects of antibody treatment were stronger compared to EC-specific genetic manipulation. This suggests that β 1 integrin is required on other cell types, like SMCs, cardiomyocytes or immune cells, such as monocytes and macrophages that produce cytokines, matrix metalloproteases (MMPs) and growth factors for cardiac health and remodeling after MI (Fung and Helisch, 2012; Lavine et al., 2013; Raffetto and Khalil, 2008).

In contrast, findings from EC-specific β 1 integrin deficient mice after full coronary artery occlusion were stronger and distinct compared to those from mice with pharmacological inhibition of β 1 integrin. Permanent artery occlusion of the LAD results in a severe acute myocardial infarction (AMI), damaging the myocardium irreversibly, but is also sufficient to trigger new collateral growth. These newly formed vessels likely balance the occlusion, minimize the tissue damage and finally reduce the absolute infarction impact, even if it takes some days after AMI (Zhang and Faber, 2015). In the process of *de novo* collateralization, endothelial β 1 integrin integrity is essential, which was indicated by massive impairment in cardiac function and increased lethality in EC-specific β 1 integrin KO mice compared to controls. Therefore, endothelial β 1 integrin was shown to be crucial for prevention of heart failure and cardiac death. Morphological and histological analysis of hearts from dead mice suggested myocardial rupture as presumable cause of death.

In general, myocardial or cardiac rupture is identified as a laceration of the heart, for instance affecting the ventricles or the septum. After an AMI, the occurrence of cardiac rupture represents one of the most severe and fatal consequences (Honda et al., 2014; Matteucci et al., 2019). In postmortem examination it was shown that in up to 30.7% of all sudden deaths after AMI, myocardial rupture was detectable (Hutchins et al., 2002) and responsible for around 10% to 20% of all in-hospital deaths upon AMI (Gao et al., 2005). In the worst case, complete

transmural rupture causes hemopericardium, in which blood enriches in the pericardial sac and contributes to fast death, as body blood perfusion is no longer guaranteed (Honda et al., 2014). As AMI decreases myocardial wall resistance, it is presumed that rupture occurs due to permanent stretching of the infarcted and weakened myocardial wall (Gao et al., 2005). The activation of MMPs and the degradation of collagen that stabilizes cardiomyocytes, play an essential role, leading to destabilization of the injured myocardium with likelihood to rupture (Gao et al., 2005).

From previous work, it is known that endothelial $\beta 1$ integrin is essential for VE-cadherin localization and stabilization of newly built blood vessels (Yamamoto et al., 2015). Therefore, in the model of permanent LAD occlusion, growth of new blood vessels is strongly declined, and injured vessels stay eventually leaky due to the absence of endothelial $\beta 1$ integrin. Consequently, perfusion of the infarcted myocardium is inhibited, necrosis of the tissue is stronger processed, and healing and remodeling of the myocardium are impaired, which increases the occurrence of cardiac wall rupture. In conclusion, the subunit $\beta 1$ integrin specifically expressed by the endothelium is urgently needed for protecting the heart from AMI-induced cardiac death. However, further research is required to determine the exact mechanism behind as well as investigations in the restriction of the phenotype to this specific subunit and cell type.

4.4. Clinical relevance of targeting $\beta 1$ integrin

As CVDs reflect the leading cause of deaths worldwide, research and investigations are of huge importance to receive novel insights into the mechanisms involved. Therefore, findings are essential to improve current therapeutic measures, but also to develop new drug treatments and medical applications against CVDs. Besides current prevention strategies, like healthy lifestyles changes or medical treatment of hypertension or hyperlipidemia, triggering an endogenous growth of blood vessels might be another promising approach. In this context, the formation of a functional collateral network can protect from severe CVDs, such as MI or acute peripheral artery occlusion (Faber et al., 2014; Gloekler and Seiler, 2007; McDermott et al., 2014; Seiler, 2010). Furthermore, artery constriction or narrowing leads also to shear stress alteration and hypoxic conditions in the affected organs, which can trigger short- and long-term vascular remodeling. This mechanism enables to adapt and to balance the pathological situation. Therefore, understanding the mechanism behind this endogenous protection system could lead to the discovery of possible target molecules for improving the treatment and the prevention of CVDs.

Interestingly, the here presented data revealed $\beta 1$ integrin to be involved in the process of such a cardioprotective vascular adaptation, and identified this transmembrane receptor as possible target for therapeutic application. Vascular adaptation in consequence of an ischemic injury includes infiltration of immune cells, proliferation of vascular cells as well as degradation and rearrangement of the ECM (Meier et al., 2013; van Royen et al., 2009). Hereby, function of $\beta 1$ integrin is critical for all processes, meaning dysfunction can lead to an insufficient remodeling of the vasculature and consequently of the entire injured myocardium. Most importantly, integrins enable cross-talk via mechanotransduction between the ECM or BM and the cytoskeleton (Humphrey et al., 2014; Hynes, 2002; Ingber, 1991; Lorenz et al., 2018; Moreno-Layseca et al., 2019; Planas-Paz et al., 2012; Ross et al., 2013; Schwartz, 2010; Sun et al., 2019). Particularly therefore and shown in this thesis, $\beta 1$ integrin presence and function is needed for cardioprotective vascular adaptation, mainly triggered by ischemia-induced hypoxia and potential hemodynamic changes. Furthermore, these findings might be beneficial for patients with CVDs, but can also help to understand other physiological or pathological conditions dealing with signaling via the ECM and vascular remodeling. For instance, aging and the metabolic disorder diabetes mellitus are also associated with alterations in the ECM (Goldin et al., 2006; Meschiari et al., 2017; Safar, 2018). Conceivably, those changes might be responsible for the increase in arterial stiffness, the impairment of endothelial function and the decrease in cardioprotective collateralization. This finally contributes to a higher cardiovascular risk with potential threat of cardiac rupture after AMI for individuals with diabetes mellitus compared to healthy ones (Dincer et al., 2006; Meyer et al., 2008; Nesto and Zarich, 1998; Ruitter et al., 2010; Safar, 2018; Shen et al., 2018). In this case, targeting $\beta 1$ integrin to balance those changes in the ECM, and therefore improving endogenous vascular adaptation, might be beneficial to reduce cardiovascular risk in patients with diabetes mellitus as well.

Overall, based on the shown findings and the corresponding literature, endothelial $\beta 1$ integrin might be a possible target molecule for treating patients with CVDs, or humans exhibiting diabetes mellitus who suffer from CVDs as comorbidity. In this scenario, endothelial $\beta 1$ integrin could be stimulated and activated by specific pharmacological treatment. Such a stimulation might improve endothelial function and contribute to cardioprotective blood vascular growth. Finally, in the long-term $\beta 1$ integrin stimulation could reduce fatal consequences from AMI, like cardiac rupture or furthermore is able to decrease the occurrence of myocardial ischemia in general. Nevertheless, even if potential exists, further research is strongly needed to investigate the mechanism behind and to develop potential pharmacological treatments in prevention or in consequence of an infarction injury.

4.5. Conclusion

In summary, the here presented data provide clear evidence for the essential role of endothelial $\beta 1$ integrin for artery vasodilation and therefore for endothelial function as well as for ischemia-induced vascular growth and cardioprotection. These findings were shown by using three different clinically relevant *in vivo* adult mouse models of ischemia injury, in which $\beta 1$ integrin signaling was targeted by pharmacological and genetic manipulation. Triggers like changes in hemodynamics and hypoxia exposure were applied to stimulate endothelial $\beta 1$ integrin in the hindlimb and the heart. Here, $\beta 1$ integrin integrity was equally important for acute vascular adaptation as well as for chronic adaptation with cardioprotective properties.

In detail, clinically comparable and relevant FMD measurements showed endothelial $\beta 1$ integrin-mediated mechanotransduction to be essential for vasodilation of the endothelium. Furthermore, shown in models aiming prolonged ischemia induction, $\beta 1$ integrin was also needed for chronic vascular adaptation in the hindlimb and the heart. Focusing on the findings in the myocardium, the murine heart represents an ideal model to perform research on CADs due to its similarity to the human situation (Fig. 4.1 a). By transient LAD occlusions, also named Repl/R procedure (Fig. 4.1 b), vascular growth was successfully initiated, indicated by morphological changes in form of cardiac EC proliferation and formation of arterioles. Interestingly, changes were detectable in the ischemic and non-ischemic myocardium, which indicates hypoxia not to be the only stimulus. It is conceivable that changes in hemodynamics during and shortly after LAD occlusion trigger these vascular changes as well. Furthermore, Repl/R finally caused a protection from MI in form of reduced infarction size and improved cardiac function. Most importantly, those adaptation processes of the murine hearts were mainly dependent on $\beta 1$ integrin signaling, pointing out the relevant role of this specific subunit for cardioprotection from ischemic injury (Fig. 4.1 c). With the application of another mouse model, the observed results became even more significant. Here, permanent LAD occlusion (Fig. 4.1 d) induced the revascularization of the infarcted myocardial region, potentially to minimize tissue damage and to support myocardial healing. In this process, the presence of endothelial $\beta 1$ integrin was absolutely critical, as mice showed an impaired revascularization, declined cardiac function and increased lethality by cardiac rupture, when $\beta 1$ integrin was knocked out in ECs. Therefore, findings indicate endothelial $\beta 1$ integrin to be essential for the preservation of heart function and the protection from cardiac death after AMI (Fig. 4.1 e).

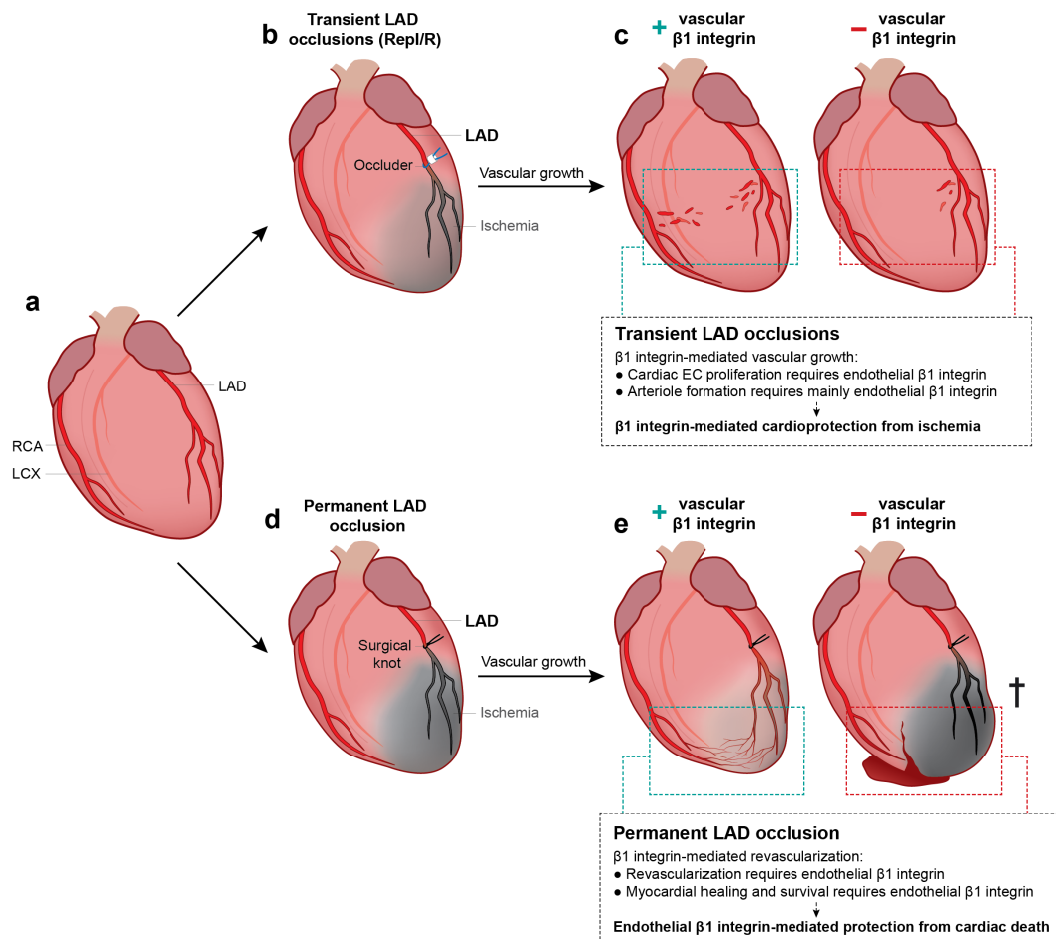
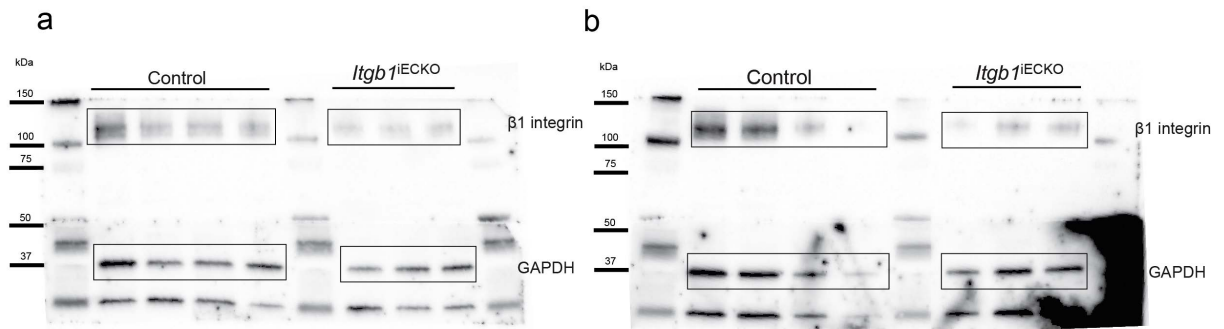


Figure 4.1: Schematic summary of $\beta 1$ integrin importance in myocardial ischemia models.

(a) Illustration of a mouse heart with coronary arteries and branches similar to the human heart, including the right coronary artery (RCA), the left circumflex artery (LCX) and the left anterior descending artery (LAD). The induction of (b) transient LAD occlusions (Repl/R) should mimics ischemic events in patients with CADs. (c) Note that the following Repl/R-induced blood vascular growth and cardioprotection is mainly dependent on $\beta 1$ integrin. The induction of (d) permanent LAD occlusion should images the scenario under acute myocardial infarction (AMI). (e) Permanent LAD occlusion-induced revascularization and protection from cardiac death is dependent on endothelial $\beta 1$ integrin. Image was drafted by Carina Henning and illustrated by Yousun Koh.

Finally, all findings together indicate the substantial role of endothelial $\beta 1$ integrin, for adult vascular remodeling and adaptation as well as for cardioprotection in response to pathological ischemia injury. Furthermore, those results suggest endothelial $\beta 1$ integrin as potential target molecule to stimulate peripheral and myocardial blood vascular growth, which might be beneficial for patients with PVDs or CADs.

Supplementary information



Supplementary figure 1: Uncropped Western blot for $\beta 1$ integrin protein expression analysis.

(a, b) Images of uncropped Western Blot from Fig. 3.18 to determine tamoxifen-induced *Itgb1* gene deletion, presenting protein bands for cardiac endothelial $\beta 1$ integrin (top) and GAPDH (bottom) as housekeeping protein. Controls 1-4 and *Itgb1*^{IECKO} 1-3 are visualized in (b) and controls 5-8 and *Itgb1*^{IECKO} 4-6 are visualized in (a), highlighted by a black frame.

Reference

- Abaci, A., Oguzhan, A., Kahraman, S., Eryol, N.K., Unal, S., Arinc, H., and Ergin, A. (1999). Effect of diabetes mellitus on formation of coronary collateral vessels. *Circulation* 99, 2239-2242.
- Abrams, J. (2005). Clinical practice. Chronic stable angina. *N Engl J Med* 352, 2524-2533.
- Aird, W.C. (2007a). Phenotypic heterogeneity of the endothelium: I. Structure, function, and mechanisms. *Circ Res* 100, 158-173.
- Aird, W.C. (2007b). Phenotypic heterogeneity of the endothelium: II. Representative vascular beds. *Circ Res* 100, 174-190.
- Ambrose, J.A., and Singh, M. (2015). Pathophysiology of coronary artery disease leading to acute coronary syndromes. *F1000Prime Rep* 7, 08.
- Aвраамидес, C.J., Garmy-Susini, B., and Varner, J.A. (2008). Integrins in angiogenesis and lymphangiogenesis. *Nat Rev Cancer* 8, 604-617.
- Axnick, J. (2016). β 1 integrin-dependent mechanotransduction induces angiocrine signaling required to promote liver growth and survival. In Institute of Metabolic Physiology (Heinrich-Heine-University Düsseldorf).
- Baeyens, N., Bandyopadhyay, C., Coon, B.G., Yun, S., and Schwartz, M.A. (2016). Endothelial fluid shear stress sensing in vascular health and disease. *J Clin Invest* 126, 821-828.
- Baldwin, H.S. (1996). Early embryonic vascular development. *Cardiovasc Res* 31 *Spec No*, E34-45.
- Balla, C., Pavasini, R., and Ferrari, R. (2018). Treatment of Angina: Where Are We? *Cardiology* 140, 52-67.
- Banchi, A. (1904). Morfologia delle arteriae coronariae cordis. *Arch Ital Anat Embriol* 3, 87-164.
- Baroldi, G., Mantero, O., and Scomazzoni, G. (1956). The collaterals of the coronary arteries in normal and pathologic hearts. *Circ Res* 4, 223-229.
- Benedito, R., Roca, C., Sorensen, I., Adams, S., Gossler, A., Fruttiger, M., and Adams, R.H. (2009). The notch ligands Dll4 and Jagged1 have opposing effects on angiogenesis. *Cell* 137, 1124-1135.
- Bergheanu, S.C., Bodde, M.C., and Jukema, J.W. (2017). Pathophysiology and treatment of atherosclerosis : Current view and future perspective on lipoprotein modification treatment. *Neth Heart J* 25, 231-242.
- Bilazarian, S.D., Faxon, D.P., and Jacobs, A.K. (1991). Coronary sinus retroperfusion: a critical review. *Coronary Artery Disease* 2, 640-648.
- Billinger, M., Kloos, P., Eberli, F.R., Windecker, S., Meier, B., and Seiler, C. (2002). Physiologically assessed coronary collateral flow and adverse cardiac ischemic events: a follow-up study in 403 patients with coronary artery disease. *J Am Coll Cardiol* 40, 1545-1550.
- Bonetti, P.O., Lerman, L.O., and Lerman, A. (2003). Endothelial dysfunction: a marker of atherosclerotic risk. *Arterioscler Thromb Vasc Biol* 23, 168-175.

- Bonner, F., Jacoby, C., Temme, S., Borg, N., Ding, Z., Schrader, J., and Fogel, U. (2014). Multifunctional MR monitoring of the healing process after myocardial infarction. *Basic Res Cardiol* 109, 430.
- Brand, T. (2003). Heart development: molecular insights into cardiac specification and early morphogenesis. *Developmental Biology* 258, 1-19.
- Breier, G. (2000). Angiogenesis in embryonic development - A review. *Placenta* 21, S11-S15.
- Cai, W.-J., Li, M.B., Wu, X., Wu, S., Zhu, W., Chen, D., Luo, M., Eitenmüller, I., Kampmann, A., Schaper, J., *et al.* (2009). Activation of the integrins $\alpha 5\beta 1$ and $\alpha v\beta 3$ and focal adhesion kinase (FAK) during arteriogenesis. *Mol Cell Biochem* 322, 161-169.
- Cai, W.J., and Schaper, W. (2008). Mechanisms of arteriogenesis. *Acta Bioch Bioph Sin* 40, 681-692.
- Campbell, N.A., Reece, J.B., Urry, L.A., Cain, M.L., Wasserman, S.A., Minorsky, P.V., and Jackson, R.B. (2009). *Biologie*, 8 edn (Pearson Education Deutschland GmbH).
- Carlson, T.R., Hu, H., Braren, R., Kim, Y.H., and Wang, R.A. (2008). Cell-autonomous requirement for beta1 integrin in endothelial cell adhesion, migration and survival during angiogenesis in mice. *Development* 135, 2193-2202.
- Carmeliet, P. (2000). Mechanisms of angiogenesis and arteriogenesis. *Nat Med* 6, 389-395.
- Carmeliet, P., and Jain, R.K. (2011). Molecular mechanisms and clinical applications of angiogenesis. *Nature* 473, 298-307.
- Chalothorn, D., and Faber, J.E. (2010). Formation and maturation of the native cerebral collateral circulation. *J Mol Cell Cardiol* 49, 251-259.
- Charakida, M., Masi, S., Luscher, T.F., Kastelein, J.J.P., and Deanfield, J.E. (2010). Assessment of atherosclerosis: the role of flow-mediated dilatation. *European Heart Journal* 31, 2854-U2824.
- Chomczynski, P., and Sacchi, N. (1987). Single-step method of RNA isolation by acid guanidinium thiocyanate-phenol-chloroform extraction. *Anal Biochem* 162, 156-159.
- Clark, W.M., Lessov, N.S., Dixon, M.P., and Eckenstein, F. (1997). Monofilament intraluminal middle cerebral artery occlusion in the mouse. *Neurol Res* 19, 641-648.
- Clayton, J.A., Chalothorn, D., and Faber, J.E. (2008). Vascular endothelial growth factor-A specifies formation of native collaterals and regulates collateral growth in ischemia. *Circ Res* 103, 1027-1036.
- Cohen, M., and Rentrop, K.P. (1986). Limitation of myocardial ischemia by collateral circulation during sudden controlled coronary artery occlusion in human subjects: a prospective study. *Circulation* 74, 469-476.
- Collaborators, G.B.D.C.o.D. (2018). Global, regional, and national age-sex-specific mortality for 282 causes of death in 195 countries and territories, 1980-2017: a systematic analysis for the Global Burden of Disease Study 2017. *Lancet* 392, 1736-1788.
- Conway, E.M., Collen, D., and Carmeliet, P. (2001). Molecular mechanisms of blood vessel growth. *Cardiovasc Res* 49, 507-521.

- Dai, X., and Faber, J.E. (2010). Endothelial nitric oxide synthase deficiency causes collateral vessel rarefaction and impairs activation of a cell cycle gene network during arteriogenesis. *Circ Res* 106, 1870-1881.
- Das, S., Goldstone, A.B., Wang, H., Farry, J., D'Amato, G., Paulsen, M.J., Eskandari, A., Hironaka, C.E., Phansalkar, R., Sharma, B., *et al.* (2019). A Unique Collateral Artery Development Program Promotes Neonatal Heart Regeneration. *Cell* 176, 1128-1142 e1118.
- Dewald, O., Frangogiannis, N.G., Zoerlein, M.P., Duerr, G.D., Taffet, G., Michael, L.H., Welz, A., and Entman, M.L. (2004). A murine model of ischemic cardiomyopathy induced by repetitive ischemia and reperfusion. *Thorac Cardiovasc Surg* 52, 305-311.
- Di Angelantonio, E., Kaptoge, S., Pennells, L., De Bacquer, D., Cooney, M.T., Kavousi, M., Stevens, G., Riley, L., Savin, S., Altay, S., *et al.* (2019). World Health Organization cardiovascular disease risk charts: revised models to estimate risk in 21 global regions. *Lancet Glob Health* 7, E1332-E1345.
- Dincer, I., Ongun, A., Turhan, S., Ozdol, C., Ertas, F., and Erol, C. (2006). Effect of statin treatment on coronary collateral development in patients with diabetes mellitus. *American Journal of Cardiology* 97, 772-774.
- Eitenmuller, I., Volger, O., Kluge, A., Troidl, K., Barancik, M., Cai, W.J., Heil, M., Pipp, F., Fischer, S., Horrevoets, A.J.G., *et al.* (2006). The range of adaptation by collateral vessels after femoral artery occlusion. *Circulation Research* 99, 656-662.
- Erkens, R., Kramer, C.M., Luckstadt, W., Panknin, C., Krause, L., Weidenbach, M., Dirzka, J., Krenz, T., Mergia, E., Suvorava, T., *et al.* (2015). Left ventricular diastolic dysfunction in Nrf2 knock out mice is associated with cardiac hypertrophy, decreased expression of SERCA2a, and preserved endothelial function. *Free Radical Bio Med* 89, 906-917.
- Faber, J.E., Chilian, W.M., Deindl, E., van Royen, N., and Simons, M. (2014). A brief etymology of the collateral circulation. *Arterioscler Thromb Vasc Biol* 34, 1854-1859.
- Fassler, R., and Meyer, M. (1995). Consequences of lack of beta 1 integrin gene expression in mice. *Genes Dev* 9, 1896-1908.
- Ference, B.A., Ginsberg, H.N., Graham, I., Ray, K.K., Packard, C.J., Bruckert, E., Hegele, R.A., Krauss, R.M., Raal, F.J., Schunkert, H., *et al.* (2017). Low-density lipoproteins cause atherosclerotic cardiovascular disease. 1. Evidence from genetic, epidemiologic, and clinical studies. A consensus statement from the European Atherosclerosis Society Consensus Panel. *European Heart Journal* 38, 2459-2472.
- Fujita, M., and Sasayama, S. (2010). Coronary collateral growth and its therapeutic application to coronary artery disease. *Circ J* 74, 1283-1289.
- Fujita, M., Sasayama, S., Ohno, A., Nakajima, H., and Asanoi, H. (1987). Importance of angina for development of collateral circulation. *Br Heart J* 57, 139-143.
- Fulton, W.F. (1956). Chronic generalized myocardial ischaemia with advanced coronary artery disease. *Br Heart J* 18, 341-354.
- Fulton, W.F. (1963). Arterial Anastomoses in the Coronary Circulation. I. Anatomical Features in Normal and Diseased Hearts Demonstrated by Stereoarteriography. *Scott Med J* 8, 420-434.
- Fulton, W.F. (1964). The Time Factor in the Enlargement of Anastomoses in Coronary Artery Disease. *Scott Med J* 9, 18-23.

- Fung, E., and Helisch, A. (2012). Macrophages in collateral arteriogenesis. *Front Physiol* 3, 353.
- Fuster, V., Alexander, R.W., O'Rourke, R.A., Roberts, R., King III, S.B., and Wellens, H.J.J. (2001). *Hurst's The Heart*, 10 edn (The McGraw-Hill Companies Inc.).
- Fuster, V., Kelly, B.B., and Vedanthan, R. (2011). Promoting global cardiovascular health: moving forward. *Circulation* 123, 1671-1678.
- Gallo, S., Sala, V., Gatti, S., and Crepaldi, T. (2014). HGF/Met Axis in Heart Function and Cardioprotection. *Biomedicines* 2, 247-262.
- Gao, X.M., Xu, Q., Kiriazis, H., Dart, A.M., and Du, X.J. (2005). Mouse model of post-infarct ventricular rupture: time course, strain- and gender-dependency, tensile strength, and histopathology. *Cardiovascular Research* 65, 469-477.
- Gloekler, S., and Seiler, C. (2007). Cardiology patient page. Natural bypasses can save lives. *Circulation* 116, e340-341.
- Goldin, A., Beckman, J.A., Schmidt, A.M., and Creager, M.A. (2006). Advanced glycation end products: sparking the development of diabetic vascular injury. *Circulation* 114, 597-605.
- Goldstein, J.L., and Brown, M.S. (2015). A Century of Cholesterol and Coronaries: From Plaques to Genes to Statins. *Cell* 161, 161-172.
- Guan, Y., Cai, B., Liu, Z., Ye, F., Deng, P., Cai, W.J., Schaper, J., and Schaper, W. (2016). The Formation of Aberrant Collateral Vessels during Coronary Arteriogenesis in Dog Heart. *Cells Tissues Organs* 201, 118-129.
- Haberkorn, S.M., Jacoby, C., Ding, Z., Keul, P., Bonner, F., Polzin, A., Levkau, B., Schrader, J., Kelm, M., and Fogel, U. (2017). Cardiovascular Magnetic Resonance Relaxometry Predicts Regional Functional Outcome After Experimental Myocardial Infarction. *Circ Cardiovasc Imaging* 10.
- Habib, G.B., Heibig, J., Forman, S.A., Brown, B.G., Roberts, R., Terrin, M.L., and Bolli, R. (1991). Influence of coronary collateral vessels on myocardial infarct size in humans. Results of phase I thrombolysis in myocardial infarction (TIMI) trial. The TIMI Investigators. *Circulation* 83, 739-746.
- Hakanpaa, L., Kiss, E.A., Jacquemet, G., Miinalainen, I., Lerche, M., Guzman, C., Mervaala, E., Eklund, L., Ivaska, J., and Saharinen, P. (2018). Targeting beta1-integrin inhibits vascular leakage in endotoxemia. *Proc Natl Acad Sci U S A* 115, E6467-E6476.
- Halder, S.K., Kant, R., and Milner, R. (2018). Chronic mild hypoxia promotes profound vascular remodeling in spinal cord blood vessels, preferentially in white matter, via an alpha5beta1 integrin-mediated mechanism. *Angiogenesis* 21, 251-266.
- Hansson, G.K., and Hermansson, A. (2011). The immune system in atherosclerosis. *Nat Immunol* 12, 204-212.
- Hansson, G.K., and Libby, P. (2006). The immune response in atherosclerosis: a double-edged sword. *Nat Rev Immunol* 6, 508-519.
- He, L., Huang, X., Kanisicak, O., Li, Y., Wang, Y., Li, Y., Pu, W., Liu, Q., Zhang, H., Tian, X., *et al.* (2017). Preexisting endothelial cells mediate cardiac neovascularization after injury. *J Clin Invest* 127, 2968-2981.

- Heaps, C.L., and Parker, J.L. (2011). Effects of exercise training on coronary collateralization and control of collateral resistance. *J Appl Physiol* (1985) *111*, 587-598.
- Hedhli, N., Huang, Q., Kalinowski, A., Palmeri, M., Hu, X., Russell, R.R., and Russell, K.S. (2011). Endothelium-derived neuregulin protects the heart against ischemic injury. *Circulation* *123*, 2254-2262.
- Heil, M., Eitenmuller, I., Schmitz-Rixen, T., and Schaper, W. (2006). Arteriogenesis versus angiogenesis: similarities and differences. *J Cell Mol Med* *10*, 45-55.
- Heil, M., and Schaper, W. (2004). Influence of mechanical, cellular, and molecular factors on collateral artery growth (arteriogenesis). *Circ Res* *95*, 449-458.
- Hein, T.W., Platts, S.H., Waitkus-Edwards, K.R., Kuo, L., Mousa, S.A., and Meininger, G.A. (2001). Integrin-binding peptides containing RGD produce coronary arteriolar dilation via cyclooxygenase activation. *Am J Physiol Heart Circ Physiol* *281*, H2378-2384.
- Heiss, C., Rodriguez-Mateos, A., and Kelm, M. (2015). Central role of eNOS in the maintenance of endothelial homeostasis. *Antioxid Redox Signal* *22*, 1230-1242.
- Heiss, C., Sievers, R.E., Amabile, N., Momma, T.Y., Chen, Q., Natarajan, S., Yeghiazarians, Y., and Springer, M.L. (2008). In vivo measurement of flow-mediated vasodilation in living rats using high-resolution ultrasound. *Am J Physiol-Heart C* *294*, H1086-H1093.
- Henning, C., Branopolski, A., Schuler, D., Dimitroulis, D., Huelsemann, P., Nicolaus, C., Sansone, R., Ludolf Postma, J., Eberhard, D., Le Noble, F., *et al.* (2019). Requirement of beta1 integrin for endothelium-dependent vasodilation and collateral formation in hindlimb ischemia. *Sci Rep* *9*, 16931.
- Herlitz, J., Karlson, B.W., Richter, A., Liljeqvist, J.A., Wiklund, O., and Hjalmarson, A. (1993). Occurrence of angina pectoris prior to acute myocardial infarction and its relation to prognosis. *Eur Heart J* *14*, 484-491.
- Heuslein, and Blackman, B.R. (2015). Mechanisms of Amplified Arteriogenesis in Collateral Artery Segments Exposed to Reversed Flow Direction (vol 35, pg 2354, 2015). *Arterioscl Throm Vas* *35*, E58-E58.
- Hinkel, R., Howe, A., Renner, S., Ng, J., Lee, S., Klett, K., Kaczmarek, V., Moretti, A., Laugwitz, K.L., Skroblin, P., *et al.* (2017). Diabetes Mellitus-Induced Microvascular Destabilization in the Myocardium. *J Am Coll Cardiol* *69*, 131-143.
- Hoefer, I.E., den Adel, B., and Daemen, M.J.A.P. (2013). Biomechanical factors as triggers of vascular growth. *Cardiovascular Research* *99*, 276-283.
- Honda, S., Asaumi, Y., Yamane, T., Nagai, T., Miyagi, T., Noguchi, T., Anzai, T., Goto, Y., Ishihara, M., Nishimura, K., *et al.* (2014). Trends in the clinical and pathological characteristics of cardiac rupture in patients with acute myocardial infarction over 35 years. *J Am Heart Assoc* *3*, e000984.
- Humphrey, J.D., Dufresne, E.R., and Schwartz, M.A. (2014). Mechanotransduction and extracellular matrix homeostasis. *Nat Rev Mol Cell Bio* *15*, 802-812.
- Hutchins, K.D., Skurnick, J., Lavenhar, M., and Natarajan, G.A. (2002). Cardiac rupture in acute myocardial infarction - A reassessment. *Am J Foren Med Path* *23*, 78-82.
- Hwang, J.Y. (2017). Doppler ultrasonography of the lower extremity arteries: anatomy and scanning guidelines. *Ultrasonography* *36*, 111-119.

Hynes, R.O. (2002). Integrins: bidirectional, allosteric signaling machines. *Cell* 110, 673-687.

Ibanez, B., Aletras, A.H., Arai, A.E., Arheden, H., Bax, J., Berry, C., Bucciarelli-Ducci, C., Croisille, P., Dall'Armellina, E., Dharmakumar, R., *et al.* (2019). Cardiac MRI Endpoints in Myocardial Infarction Experimental and Clinical Trials JACC Scientific Expert Panel. *Journal of the American College of Cardiology* 74, 238-256.

Ingason, A.B., Goldstone, A.B., Paulsen, M.J., Thakore, A.D., Truong, V.N., Edwards, B.B., Eskandari, A., Bollig, T., Steele, A.N., and Woo, Y.J. (2018). Angiogenesis precedes cardiomyocyte migration in regenerating mammalian hearts. *J Thorac Cardiovasc Surg* 155, 1118-1127 e1111.

Ingber, D. (1991). Integrins as mechanochemical transducers. *Current Opinion in Cell Biology* 3, 841-848.

Insull, W. (2009). The Pathology of Atherosclerosis: Plaque Development and Plaque Responses to Medical Treatment. *Am J Med* 122, S3-S14.

Jamaiyar, A., Juguilon, C., Dong, F., Cumpston, D., Enrick, M., Chilian, W.M., and Yin, L. (2019). Cardioprotection during ischemia by coronary collateral growth. *Am J Physiol Heart Circ Physiol* 316, H1-H9.

Jamaiyar, A., Juguilon, C., Richardson, D., Gadd, J., Wang, T., Enrick, M., Goodner, R., Chilian, W.M. and Yin, L. (2020). Sprouting Angiogenesis Contributes to Coronary Collateral Growth Induced by Repetitive Ischemia in Adult Mice. *The FASEB Journal* 34, 1-1.

Joseph, G., D'Addario, C., McEvoy, K., Jadhav, R., Hutcheson, B., and Rocic, P. (2018). Laminin- $\beta 6$ integrin Interaction is Crucial for Coronary Collateral Growth. *The FASEB Journal* 32, 899.895-899.895.

Katsumi, A., Orr, A.W., Tzima, E., and Schwartz, M.A. (2004). Integrins in mechanotransduction. *J Biol Chem* 279, 12001-12004.

Keely, S., Glover, L.E., MacManus, C.F., Campbell, E.L., Scully, M.M., Furuta, G.T., and Colgan, S.P. (2009). Selective induction of integrin beta1 by hypoxia-inducible factor: implications for wound healing. *FASEB J* 23, 1338-1346.

Kingma, J.G. (2018). Myocardial Infarction: An Overview of STEMI and NSTEMI Physiopathology and Treatment. *World Journal of Cardiovascular Diseases* 08, 498-517.

Knuuti, J., Wijns, W., Saraste, A., Capodanno, D., Barbato, E., Funck-Brentano, C., Prescott, E., Storey, R.F., Deaton, C., Cuisset, T., *et al.* (2020). 2019 ESC Guidelines for the diagnosis and management of chronic coronary syndromes The Task Force for the diagnosis and management of chronic coronary syndromes of the European Society of Cardiology (ESC). *European Heart Journal* 41, 407-477.

Kodama, K., Kusuoka, H., Sakai, A., Adachi, T., Hasegawa, S., Ueda, Y., Mishima, M., Hori, M., Kamada, T., Inoue, M., *et al.* (1996). Collateral channels that develop after an acute myocardial infarction prevent subsequent left ventricular dilation. *J Am Coll Cardiol* 27, 1133-1139.

Krishnamurthy, P., Subramanian, V., Singh, M., and Singh, K. (2006). Deficiency of beta1 integrins results in increased myocardial dysfunction after myocardial infarction. *Heart* 92, 1309-1315.

Lammert, E., and Zeeb, M. (2014). *Metabolism of Human Diseases, Vol 1* (Springer Wien Heidelberg New York Dordrecht London).

- Lange, V. (2013). *Kardiologie*, 3 edn (Urban & Fischer: Elsevier GmbH, München).
- Lavine, K.J., Kovacs, A., Weinheimer, C., and Mann, D.L. (2013). Repetitive myocardial ischemia promotes coronary growth in the adult mammalian heart. *J Am Heart Assoc* 2, e000343.
- Lee, S.H., Lee, Y.J., and Han, H.J. (2011). Role of hypoxia-induced fibronectin-integrin beta1 expression in embryonic stem cell proliferation and migration: Involvement of PI3K/Akt and FAK. *J Cell Physiol* 226, 484-493.
- Legate, K.R., Montanez, E., Kudlacek, O., and Fassler, R. (2006). ILK, PINCH and parvin: the tIPP of integrin signalling. *Nat Rev Mol Cell Bio* 7, 20-31.
- Lei, L., Liu, D., Huang, Y., Jovin, I., Shai, S.Y., Kyriakides, T., Ross, R.S., and Giordano, F.J. (2008). Endothelial expression of beta1 integrin is required for embryonic vascular patterning and postnatal vascular remodeling. *Mol Cell Biol* 28, 794-802.
- Li, L., Welser-Alves, J., van der Flier, A., Boroujerdi, A., Hynes, R.O., and Milner, R. (2012). An angiogenic role for the alpha5beta1 integrin in promoting endothelial cell proliferation during cerebral hypoxia. *Exp Neurol* 237, 46-54.
- Libby, P. (2013). Mechanisms of Acute Coronary Syndromes and Their Implications for Therapy. *New Engl J Med* 368, 2004-2013.
- Libby, P., Buring, J.E., Badimon, L., Hansson, C.K., Deanfield, J., Bittencourt, M.S., Tokgozoglu, L., and Lewis, E.F. (2019). Atherosclerosis. *Nat Rev Dis Primers* 5.
- Limbourg, A., Korff, T., Napp, L.C., Schaper, W., Drexler, H., and Limbourg, F.P. (2009). Evaluation of postnatal arteriogenesis and angiogenesis in a mouse model of hind-limb ischemia. *Nat Protoc* 4, 1737-1746.
- Lindsey, M.L., Bolli, R., Canty, J.M., Du, X.J., Frangogiannis, N.G., Frantz, S., Gourdie, R.G., Holmes, J.W., Jones, S.P., Kloner, R.A., *et al.* (2018). Guidelines for experimental models of myocardial ischemia and infarction. *Am J Physiol-Heart C* 314, H812-H838.
- Liu, F., and McCullough, L.D. (2014). The middle cerebral artery occlusion model of transient focal cerebral ischemia. *Methods Mol Biol* 1135, 81-93.
- Livak, K.J., and Schmittgen, T.D. (2001). Analysis of relative gene expression data using real-time quantitative PCR and the 2^{-Delta Delta C(T)} Method. *Methods* 25, 402-408.
- Lorenz, L., Axnick, J., Buschmann, T., Henning, C., Urner, S., Fang, S., Nurmi, H., Eichhorst, N., Holtmeier, R., Bodis, K., *et al.* (2018). Mechanosensing by beta1 integrin induces angiocrine signals for liver growth and survival. *Nature* 562, 128-132.
- Loufrani, L., Retailleau, K., Bocquet, A., Dumont, O., Danker, K., Louis, H., Lacolley, P., and Henrion, D. (2008). Key role of alpha(1)beta(1)-integrin in the activation of PI3-kinase-Akt by flow (shear stress) in resistance arteries. *Am J Physiol Heart Circ Physiol* 294, H1906-1913.
- Lu, L., Liu, M., Sun, R.R., Zheng, Y., and Zhang, P.Y. (2015). Myocardial Infarction: Symptoms and Treatments. *Cell Biochemistry and Biophysics* 72, 865-867.
- Lucitti, J.L., Mackey, J.K., Morrison, J.C., Haigh, J.J., Adams, R.H., and Faber, J.E. (2012). Formation of the collateral circulation is regulated by vascular endothelial growth factor-A and a disintegrin and metalloprotease family members 10 and 17. *Circ Res* 111, 1539-1550.
- Lusis, A.J. (2000). Atherosclerosis. *Nature* 407, 233-241.

- Mac Gabhann, F., and Peirce, S.M. (2010). Collateral capillary arterialization following arteriolar ligation in murine skeletal muscle. *Microcirculation* 17, 333-347.
- Manari, A., Albiero, R., and De Servi, S. (2009). High-risk non-ST-segment elevation myocardial infarction versus ST-segment elevation myocardial infarction: same behaviour and outcome? *J Cardiovasc Med (Hagerstown)* 10 Suppl 1, S13-16.
- Marwick, T.H. (2018). Ejection Fraction Pros and Cons: JACC State-of-the-Art Review. *J Am Coll Cardiol* 72, 2360-2379.
- Matteucci, M., Fina, D., Jiritano, F., Meani, P., Blankesteyn, W.M., Raffa, G.M., Kowaleski, M., Heuts, S., Beghi, C., Maessen, J., *et al.* (2019). Treatment strategies for post-infarction left ventricular free-wall rupture. *Eur Heart J Acute Cardiovasc Care* 8, 379-387.
- Matthews, B.D., Overby, D.R., Mannix, R., and Ingber, D.E. (2006). Cellular adaptation to mechanical stress: role of integrins, Rho, cytoskeletal tension and mechanosensitive ion channels. *J Cell Sci* 119, 508-518.
- McCorry, L.K., Zdanowicz, M.M., and Gonnella, C.Y. (2019). *Essentials of Human Physiology and Pathophysiology for Pharmacy and Allied Health, Vol 1* (Taylor & Francis).
- McDermott, M.M., Carr, J., Liu, K., Kramer, C.M., Yuan, C., Tian, L., Criqui, M.H., Guralnik, J.M., Ferrucci, L., Zhao, L., *et al.* (2014). Collateral vessel number, plaque burden, and functional decline in peripheral artery disease. *Vasc Med* 19, 281-288.
- Medzhitov, R. (2008). Origin and physiological roles of inflammation. *Nature* 454, 428-435.
- Meier, P., Schirmer, S.H., Lansky, A.J., Timmis, A., Pitt, B., and Seiler, C. (2013). The collateral circulation of the heart. *BMC Med* 11, 143.
- Meisner, J.K., Niu, J., Sumer, S., and Price, R.J. (2013). Trans-illuminated laser speckle imaging of collateral artery blood flow in ischemic mouse hindlimb. *J Biomed Opt* 18, 096011.
- Meschiari, C.A., Ero, O.K., Pan, H., Finkel, T., and Lindsey, M.L. (2017). The impact of aging on cardiac extracellular matrix. *Geroscience* 39, 7-18.
- Meyer, M.F., Lieps, D., Schatz, H., and Pfohl, M. (2008). Impaired flow-mediated vasodilation in type 2 diabetes: lack of relation to microvascular dysfunction. *Microvasc Res* 76, 61-65.
- Miquerol, L., Thireau, J., Bideaux, P., Sturny, R., Richard, S., and Kelly, R.G. (2015). Endothelial plasticity drives arterial remodeling within the endocardium after myocardial infarction. *Circ Res* 116, 1765-1771.
- Misfeldt, A.M., Boyle, S.C., Tompkins, K.L., Bautch, V.L., Labosky, P.A., and Baldwin, H.S. (2009). Endocardial cells are a distinct endothelial lineage derived from Flk1+ multipotent cardiovascular progenitors. *Dev Biol* 333, 78-89.
- Möbius-Winkler, S., Uhlemann, M., Adams, V., Sandri, M., Erbs, S., Lenk, K., Mangner, N., Mueller, U., Adam, J., Grunze, M., *et al.* (2016). Coronary Collateral Growth Induced by Physical Exercise. *Circulation* 133, 1438-1448.
- Moorman, A., Webb, S., Brown, N.A., Lamers, W., and Anderson, R.H. (2003). Development of the heart: (1) formation of the cardiac chambers and arterial trunks. *Heart* 89, 806-814.
- Moreno-Layseca, P., Icha, J., Hamidi, H., and Ivaska, J. (2019). Integrin trafficking in cells and tissues. *Nat Cell Biol* 21, 122-132.

- Moyes, C.D., and Schulte, P.M. (2008). *Tierphysiologie*, Vol 1 (Pearson Education Deutschland GmbH.).
- Muller, J.M., Chilian, W.M., and Davis, M.J. (1997). Integrin signaling transduces shear stress-dependent vasodilation of coronary arterioles. *Circ Res* 80, 320-326.
- Murray, C.D. (1926). The Physiological Principle of Minimum Work: I. The Vascular System and the Cost of Blood Volume. *Proc Natl Acad Sci U S A* 12, 207-214.
- Nakamura, T., Mizuno, S., Matsumoto, K., Sawa, Y., Matsuda, H., and Nakamura, T. (2000). Myocardial protection from ischemia/reperfusion injury by endogenous and exogenous HGF. *J Clin Invest* 106, 1511-1519.
- Nesto, R.W., and Zarich, S. (1998). Acute myocardial infarction in diabetes mellitus: lessons learned from ACE inhibition. *Circulation* 97, 12-15.
- Niiyama, H., Huang, N.F., Rollins, M.D., and Cooke, J.P. (2009). Murine model of hindlimb ischemia. *J Vis Exp*.
- Noireaud, J., and Andriantsitohaina, R. (2014). Recent insights in the paracrine modulation of cardiomyocyte contractility by cardiac endothelial cells. *Biomed Res Int* 2014, 923805.
- Nossuli, T.O., Lakshminarayanan, V., Baumgarten, G., Taffet, G.E., Ballantyne, C.M., Michael, L.H., and Entman, M.L. (2000). A chronic mouse model of myocardial ischemia-reperfusion: essential in cytokine studies. *Am J Physiol Heart Circ Physiol* 278, H1049-1055.
- Okada, H., Lai, N.C., Kawaraguchi, Y., Liao, P., Copps, J., Sugano, Y., Okada-Maeda, S., Banerjee, I., Schilling, J.M., Gingras, A.R., *et al.* (2013). Integrins protect cardiomyocytes from ischemia/reperfusion injury. *Journal of Clinical Investigation* 123, 4294-4308.
- Perlman, R.L. (2016). Mouse models of human disease An evolutionary perspective. *Evol Med Public Hlth*, 170-176.
- Persson, A.B., and Buschmann, I.R. (2011). Vascular growth in health and disease. *Front Mol Neurosci* 4, 14.
- Piek, J.J., van Liebergen, R.A., Koch, K.T., Peters, R.J., and David, G.K. (1997). Clinical, angiographic and hemodynamic predictors of recruitable collateral flow assessed during balloon angioplasty coronary occlusion. *J Am Coll Cardiol* 29, 275-282.
- Piepoli, M.F., Hoes, A.W., Agewall, S., Albus, C., Brotons, C., Catapano, A.L., Cooney, M.T., Corra, U., Cosyns, B., Deaton, C., *et al.* (2016). 2016 European Guidelines on cardiovascular disease prevention in clinical practice. *Rev Esp Cardiol (Engl Ed)* 69, 939.
- Pitulescu, M.E., Schmidt, I., Giaimo, B.D., Antoine, T., Berkenfeld, F., Ferrante, F., Park, H., Ehling, M., Biljes, D., Rocha, S.F., *et al.* (2017). Dll4 and Notch signalling couples sprouting angiogenesis and artery formation. *Nat Cell Biol* 19, 915-927.
- Planas-Paz, L., Strilic, B., Goedecke, A., Breier, G., Fassler, R., and Lammert, E. (2012). Mechanoinduction of lymph vessel expansion. *EMBO J* 31, 788-804.
- Pohl, T., Seiler, C., Billinger, N., Herren, E., Wustmann, K., Mehta, H., Windecker, S., Eberli, F.R., and Meier, B. (2001). Frequency distribution of collateral flow and factors influencing collateral channel development - Functional collateral channel measurement in 450 patients with coronary artery disease. *Journal of the American College of Cardiology* 38, 1872-1878.

- Potente, M., Gerhardt, H., and Carmeliet, P. (2011). Basic and therapeutic aspects of angiogenesis. *Cell* 146, 873-887.
- Potocnik, A.J., Brakebusch, C., and Fassler, R. (2000). Fetal and adult hematopoietic stem cells require beta1 integrin function for colonizing fetal liver, spleen, and bone marrow. *Immunity* 12, 653-663.
- Pugsley, M.K., and Tabrizchi, R. (2000). The vascular system. An overview of structure and function. *J Pharmacol Toxicol Methods* 44, 333-340.
- Raffetto, J.D., and Khalil, R.A. (2008). Matrix metalloproteinases and their inhibitors in vascular remodeling and vascular disease. *Biochem Pharmacol* 75, 346-359.
- Rafii, S., Butler, J.M., and Ding, B.S. (2016). Angiocrine functions of organ-specific endothelial cells. *Nature* 529, 316-325.
- Reardon, C.M., O'Ceallaigh, S., and O'Sullivan, S.T. (2004). An anatomical study of the superficial inferior epigastric vessels in humans. *Br J Plast Surg* 57, 515-519.
- Roffi, M., Patrono, C., Collet, J.P., Mueller, C., Valgimigli, M., Andreotti, F., Bax, J.J., Borger, M.A., Brotons, C., Chew, D.P., *et al.* (2016). 2015 ESC Guidelines for the management of acute coronary syndromes in patients presenting without persistent ST-segment elevation Task Force for the Management of Acute Coronary Syndromes in Patients Presenting without Persistent ST-Segment Elevation of the European Society of Cardiology (ESC). *European Heart Journal* 37, 267-+.
- Rohn, F., Kordes, C., Buschmann, T., Reichert, D., Wammers, M., Poschmann, G., Stuhler, K., Benk, A.S., Geiger, F., Spatz, J.P., *et al.* (2020). Impaired integrin alpha5 /beta1 -mediated hepatocyte growth factor release by stellate cells of the aged liver. *Aging Cell*, e13131.
- Rosenthal, N., and Brown, S. (2007). The mouse ascending: perspectives for human-disease models. *Nature Cell Biology* 9, 993-999.
- Ross, T.D., Coon, B.G., Yun, S., Baeyens, N., Tanaka, K., Ouyang, M., and Schwartz, M.A. (2013). Integrins in mechanotransduction. *Curr Opin Cell Biol* 25, 613-618.
- Ruiter, M.S., van Golde, J.M., Schaper, N.C., Stehouwer, C.D., and Huijberts, M.S. (2010). Diabetes impairs arteriogenesis in the peripheral circulation: review of molecular mechanisms. *Clin Sci* 119, 225-238.
- Safar, M.E. (2018). Arterial stiffness as a risk factor for clinical hypertension. *Nature Reviews Cardiology* 15, 97-105.
- Schaper, W. (2009). Collateral circulation: past and present. *Basic Res Cardiol* 104, 5-21.
- Schaper, W., and Scholz, D. (2003). Factors regulating arteriogenesis. *Arterioscler Thromb Vasc Biol* 23, 1143-1151.
- Schierling, W., Troidl, K., Mueller, C., Troidl, C., Wustrack, H., Bachmann, G., Kasprzak, P.M., Schaper, W., and Schmitz-Rixen, T. (2009). Increased intravascular flow rate triggers cerebral arteriogenesis. *J Cereb Blood Flow Metab* 29, 726-737.
- Schuler, D., Sansone, R., Freudemberger, T., Rodriguez-Mateos, A., Weber, G., Momma, T.Y., Goy, C., Altschmied, J., Haendeler, J., Fischer, J.W., *et al.* (2014). Measurement of Endothelium-Dependent Vasodilation in Mice-Brief Report. *Arterioscler Thromb Vas* 34, 2651-U2176.

- Schwartz, J.S., Cohn, J.N., and Bache, R.J. (1983). Effects of coronary occlusion on flow in the distribution of a neighboring stenotic coronary artery in the dog. *Am J Cardiol* 52, 189-195.
- Schwartz, M.A. (2010). Integrins and extracellular matrix in mechanotransduction. *Cold Spring Harb Perspect Biol* 2, a005066.
- Seiler, C. (2010). The human coronary collateral circulation. *Eur J Clin Invest* 40, 465-476.
- Seiler, C., Stoller, M., Pitt, B., and Meier, P. (2013). The human coronary collateral circulation: development and clinical importance. *Eur Heart J* 34, 2674-2682.
- Serini, G., Napione, L., Arese, M., and Bussolino, F. (2008). Besides adhesion: new perspectives of integrin functions in angiogenesis. *Cardiovasc Res* 78, 213-222.
- Shen, Y., Ding, F.H., Dai, Y., Wang, X.Q., Zhang, R.Y., Lu, L., and Shen, W.F. (2018). Reduced coronary collateralization in type 2 diabetic patients with chronic total occlusion. *Cardiovasc Diabetol* 17.
- Shi, L., Fisslthaler, B., Zippel, N., Fromel, T., Hu, J., Elgheznawy, A., Heide, H., Popp, R., and Fleming, I. (2013). MicroRNA-223 antagonizes angiogenesis by targeting beta1 integrin and preventing growth factor signaling in endothelial cells. *Circ Res* 113, 1320-1330.
- Shriki, J.E., Shinbane, J.S., Rashid, M.A., Hindoyan, A., Withey, J.G., DeFrance, A., Cunningham, M., Oliveira, G.R., Warren, B.H., and Wilcox, A. (2012). Identifying, characterizing, and classifying congenital anomalies of the coronary arteries. *Radiographics* 32, 453-468.
- Silva, R., D'Amico, G., Hodivala-Dilke, K.M., and Reynolds, L.E. (2008). Integrins: the keys to unlocking angiogenesis. *Arterioscler Thromb Vasc Biol* 28, 1703-1713.
- Simons, M., and Eichmann, A. (2015). Molecular controls of arterial morphogenesis. *Circ Res* 116, 1712-1724.
- Simons, M., and Ware, J.A. (2003). Therapeutic angiogenesis in cardiovascular disease. *Nat Rev Drug Discov* 2, 863-871.
- Somanath, P.R., Ciocea, A., and Byzova, T.V. (2009). Integrin and growth factor receptor alliance in angiogenesis. *Cell Biochem Biophys* 53, 53-64.
- Stephens, L.E., Sutherland, A.E., Klimanskaya, I.V., Andrieux, A., Meneses, J., Pedersen, R.A., and Damsky, C.H. (1995). Deletion of beta 1 integrins in mice results in inner cell mass failure and peri-implantation lethality. *Genes Dev* 9, 1883-1895.
- Sun, M., Opavsky, M.A., Stewart, D.J., Rabinovitch, M., Dawood, F., Wen, W.H., and Liu, P.P. (2003). Temporal response and localization of integrins beta1 and beta3 in the heart after myocardial infarction: regulation by cytokines. *Circulation* 107, 1046-1052.
- Sun, Z., Costell, M., and Fassler, R. (2019). Integrin activation by talin, kindlin and mechanical forces. *Nat Cell Biol* 21, 25-31.
- Swift, H., and Bordoni, B. (2020). Anatomy, Bony Pelvis and Lower Limb, Femoral Artery. In *StatPearls (Treasure Island (FL))*.
- Swirski, F.K., and Nahrendorf, M. (2018). Cardioimmunology: the immune system in cardiac homeostasis and disease. *Nat Rev Immunol* 18, 733-744.

- Talman, V., and Kivela, R. (2018). Cardiomyocyte-Endothelial Cell Interactions in Cardiac Remodeling and Regeneration. *Front Cardiovasc Med* 5, 101.
- Tang, J., Zhang, H., He, L.J., Huang, X.Z., Li, Y., Pu, W.J., Yu, W., Zhang, L.B., Cai, D.Q., Lui, K.O., *et al.* (2018). Genetic Fate Mapping Defines the Vascular Potential of Endocardial Cells in the Adult Heart. *Circulation Research* 122, 984-993.
- Tanjore, H., Zeisberg, E.M., Gerami-Naini, B., and Kalluri, R. (2008). Beta1 integrin expression on endothelial cells is required for angiogenesis but not for vasculogenesis. *Dev Dyn* 237, 75-82.
- Thoma, R. (1893). *Untersuchungen über die Histogenese und Histomechanik des Gefäßsystems*. Stuttgart: F Enke.
- Thygesen, K., Alpert, J.S., Jaffe, A.S., Simoons, M.L., Chaitman, B.R., White, H.D., and Writing Group on behalf of the Joint, E.S.C.A.A.H.A.W.H.F.T.F.f.t.U.D.o.M.I. (2012). Third universal definition of myocardial infarction. *Glob Heart* 7, 275-295.
- Treuting, P., and Dintzis, S. (2012). *Comparative Anatomy and Histology, a mouse and human atlas*, 1 edn (Elsevier Inc.).
- Urner, S., Kelly-Goss, M., Peirce, S.M., and Lammert, E. (2018). Mechanotransduction in Blood and Lymphatic Vascular Development and Disease. *Adv Pharmacol* 81, 155-208.
- Urner, S., Planas-Paz, L., Hilger, L.S., Henning, C., Branopolski, A., Kelly-Goss, M., Stanczuk, L., Pitter, B., Montanez, E., Peirce, S.M., *et al.* (2019). Identification of ILK as a critical regulator of VEGFR3 signalling and lymphatic vascular growth. *EMBO J* 38.
- van Royen, N., Piek, J.J., Buschmann, I., Hoefler, I., Voskuil, M., and Schaper, W. (2001). Stimulation of arteriogenesis; a new concept for the treatment of arterial occlusive disease. *Cardiovascular Research* 49, 543-553.
- van Royen, N., Piek, J.J., Schaper, W., and Fulton, W.F. (2009). A critical review of clinical arteriogenesis research. *J Am Coll Cardiol* 55, 17-25.
- Villa, A.D., Sammut, E., Nair, A., Rajani, R., Bonamini, R., and Chiribiri, A. (2016). Coronary artery anomalies overview: The normal and the abnormal. *World J Radiol* 8, 537-555.
- Virani, S.S., Alonso, A., Benjamin, E.J., Bittencourt, M.S., Callaway, C.W., Carson, A.P., Chamberlain, A.M., Chang, A.L.R., Cheng, S.S., Delling, F.N., *et al.* (2020). Heart Disease and Stroke Statistics-2020 Update: A Report From the American Heart Association. *Circulation* 141, E139-E596.
- Wang, Y.D., Nakayama, M., Pitulescu, M.E., Schmidt, T.S., Bochenek, M.L., Sakakibara, A., Adams, S., Davy, A., Deutsch, U., Luthi, U., *et al.* (2010). Ephrin-B2 controls VEGF-induced angiogenesis and lymphangiogenesis. *Nature* 465, 483-U108.
- Welters, A., Kluppel, C., Mrugala, J., Wormeyer, L., Meissner, T., Mayatepek, E., Heiss, C., Eberhard, D., and Lammert, E. (2017). NMDAR antagonists for the treatment of diabetes mellitus-Current status and future directions. *Diabetes Obes Metab* 19 Suppl 1, 95-106.
- Wolf, D., and Ley, K. (2019). Immunity and Inflammation in Atherosclerosis. *Circ Res* 124, 315-327.
- Wustmann, K., Zbinden, S., Windecker, S., Meier, B., and Seiler, C. (2003). Is there functional collateral flow during vascular occlusion in angiographically normal coronary arteries? *Circulation* 107, 2213-2220.

- Xanthis, I., Souilhol, C., Serbanovic-Canic, J., Roddie, H., Kalli, A.C., Fragiadaki, M., Wong, R., Shah, D.R., Askari, J.A., Canham, L., *et al.* (2019). beta 1 integrin is a sensor of blood flow direction. *J Cell Sci* 132.
- Xin, M., Olson, E.N., and Bassel-Duby, R. (2013). Mending broken hearts: cardiac development as a basis for adult heart regeneration and repair. *Nat Rev Mol Cell Biol* 14, 529-541.
- Yamamoto, H., Ehling, M., Kato, K., Kanai, K., van Lessen, M., Frye, M., Zeuschner, D., Nakayama, M., Vestweber, D., and Adams, R.H. (2015). Integrin beta1 controls VE-cadherin localization and blood vessel stability. *Nat Commun* 6, 6429.
- Yang, B., and Rizzo, V. (2013). Shear Stress Activates eNOS at the Endothelial Apical Surface Through beta1 Containing Integrins and Caveolae. *Cell Mol Bioeng* 6, 346-354.
- Yu, E., Malik, V.S., and Hu, F.B. (2018). Cardiovascular Disease Prevention by Diet Modification: JACC Health Promotion Series. *J Am Coll Cardiol* 72, 914-926.
- Yu, J., deMuinck, E.D., Zhuang, Z., Drinane, M., Kauser, K., Rubanyi, G.M., Qian, H.S., Murata, T., Escalante, B., and Sessa, W.C. (2005). Endothelial nitric oxide synthase is critical for ischemic remodeling, mural cell recruitment, and blood flow reserve. *Proc Natl Acad Sci U S A* 102, 10999-11004.
- Zbinden, R., Zbinden, S., Meier, P., Hutter, D., Billinger, M., Wahl, A., Schmid, J.P., Windecker, S., Meier, B., and Seiler, C. (2007). Coronary collateral flow in response to endurance exercise training. *Eur J Cardiovasc Prev Rehabil* 14, 250-257.
- Zbinden, R., Zbinden, S., Windecker, S., Meier, B., and Seiler, C. (2004). Direct demonstration of coronary collateral growth by physical endurance exercise in a healthy marathon runner. *Heart* 90, 1350-1351.
- Zernecke, A., Shagdarsuren, E., and Weber, C. (2008). Chemokines in Atherosclerosis An Update. *Arterioscl Throm Vas* 28, 1897-1908.
- Zhang, H., Chalothorn, D., and Faber, J.E. (2019). Collateral Vessels Have Unique Endothelial and Smooth Muscle Cell Phenotypes. *Int J Mol Sci* 20.
- Zhang, H., and Faber, J.E. (2015). De-novo collateral formation following acute myocardial infarction: Dependence on CCR2(+) bone marrow cells. *J Mol Cell Cardiol* 87, 4-16.
- Zhou, P., and Pu, W.T. (2016). Recounting Cardiac Cellular Composition. *Circ Res* 118, 368-370.
- Zimarino, M., D'Andreamatteo, M., Waksman, R., Epstein, S.E., and De Caterina, R. (2014). The dynamics of the coronary collateral circulation. *Nat Rev Cardiol* 11, 191-197.
- Zovein, A.C., Luque, A., Turlo, K.A., Hofmann, J.J., Yee, K.M., Becker, M.S., Fassler, R., Mellman, I., Lane, T.F., and Iruela-Arispe, M.L. (2010). beta 1 Integrin Establishes Endothelial Cell Polarity and Arteriolar Lumen Formation via a Par3-Dependent Mechanism. *Developmental Cell* 18, 39-51.

Publications

Some parts (Fig. 3.1 - Fig. 3.6) of this dissertation were substantially used for the following publication:

Henning C*, Branopolski A*, Schuler D*, Dimitroulis D, Hülsemann P, Nicolaus C, Sanson R, Ludolf Postma J, Eberhard D, Le Noble F, Kelm M, Lammert E*, Heiss C*: **Requirement of β 1 integrin for endothelium-dependent vasodilation and collateral formation in hindlimb ischemia.** *Sci Rep* 9, 16931, doi:10.1038/s41598-019-53137-x (2019).

* equally contributed

Weblink: <https://www.nature.com/articles/s41598-019-53137-x>

Name of the journal: Nature Scientific reports

Author position: first author

Impact factor (2018): 4.525

Contribution of Carina Henning in detail: Carina Henning contributed to the writing of the manuscript, to the preparation of the figures, to the performing of the experiments and reviewed the final manuscript.

Finally, Carina Henning together with the other first authors Anna Branopolski and Dr. Dominik Schuler, contributed equally to this publication with approximately 25%.

Approximately 50% of the main figures from the publication were used for this dissertation.

Some parts of this dissertation are planned to be used for a publication:

Henning C*, Branopolski A*, Follert P, Aysel Ayhan, Flögel U, Kelm M, Heiss C*, Lammert E*: **Endothelial β 1 integrin-mediated cardiac vascular growth, protection from myocardial infarction, and prevention of heart failure.** Publication in preparation (2020).

* equally contributed

Other publications:

Urner S, Planas-Paz L, Hilger LS, Henning C, Branopolski A, Kelly-Goss M, Stanczuk L, Pitter B, Montanez E, Peirce SM, Makinen T, Lammert, E: **Identification of ILK as a critical regulator of VEGFR3 signalling and lymphatic vascular growth.** *EMBO J* 38, doi:10.15252/embj.201899322 (2018).

Lorenz L, Axnick J, Buschmann T, Henning C, Urner S, Fang S, Nurmi H, Eichhorst N, Holtmeier R, Bodis K, Hwang JH, Mussig K, Eberhard D, Stypmann J, Kuss O, Roden M, Alitalo K, Häussinger D, Lammert E: **Mechanosensing by β 1 integrin induces angiocrine signals for liver growth and survival.** *Nature* 562, 128-132, doi:10.1038/s41586-018-0522-3 (2017).

Welters A, Klüppel C, Mrugala J, Wörmeyer L, Meissner T, Mayatepek E, Heiss C, Eberhard D, Lammert E: **NMDAR antagonists for the treatment of diabetes mellitus-Current status and future directions.** *Diabetes Obes Metab* 19 Suppl 1, 95-106, doi:10.1111/dom.13017 (2017).

Abbreviations

AAR	area at risk
Akt	protein kinase B
BCA	bicinchoninic acid
bFGF	basic fibroblast growth factor
BM	basement membrane
bp	base pair
BrdU	5-bromo-20-deoxyuridine
BSA	bovine serum albumin
CAD	coronary artery diseases
CCL2/5	C-C chemokine ligand type 2/5
<i>Cdh5</i>	cadherin 5 gene
CHD	coronary heart diseases
CK-MB	creatine kinase
Control	<i>Cdh5-Cre^{ERT2}</i> mice
ctrl-AB	control antibody
CVD	cardiovascular diseases
CWS	circumferential wall stress
CX3CL1	chemokine (C-X3-C motif) ligand 1
CXCL10	C-X-C motif chemokine ligand 10
DAPI	4',6-diamidino-2-phenylindole
EC	endothelial cells
ECG	electrocardiography
ECM	extracellular matrix
EDTA	ethylenediaminetetraacetic acid
EDV	end-diastolic volume
EF	ejection fraction
ELISA	enzyme-linked immunosorbent assay
eNOS	endothelial nitric oxide synthase
ESV	end-systolic volume
Et-1	endothelin-1
FA	femoral artery
FISP	fast gradient echo cine sequence with steady state precession
FMD	flow mediated vasodilation
FSS	fluid shear stress

GAPDH	glyceraldehyde 3-phosphate dehydrogenase
HDL	high-density lipoprotein
HGF	hepatocyte growth factor
HI	hindlimb ischemia
HIF-1 α	hypoxia inducible factor-1 α
HP-FITC-MAb	hypoxyprobe-fluorescein isothiocyanate-monoclonal antibody
<i>Hprt1</i>	hypoxanthine phosphoribosyltransferase 1 gene
HRP	horseradish peroxidase
i.p.	intraperitoneal
i.v.	intravenously
ICAM 1	intercellular adhesion molecule 1
IHD	ischemic heart diseases
ILK	integrin-linked protein kinase
INF	infarction size
IR	ischemia reperfusion
<i>Itgb1</i>	β 1 integrin gene
<i>Itgb1</i> ^{iECKO}	<i>Cdh5</i> -Cre ^{ERT2} ; homozygous <i>Itgb1</i> -KO mice
KLF2	Kruppel-like factor 2
KO	knockout
LAD	left anterior descending artery
LCA	left coronary artery
LCX	left circumflex artery
LDL	low-density lipoprotein
LGE	late gadolinium enhancement
LSF	trans-illuminated laser speckle flowmetry
LV	left ventricle
MACS	magnetic-activated cell sorting
MCP-1	monocyte chemotactic protein
MI	myocardial infarction
MRI	magnetic resonance imaging
NRG-1	neuregulin-1
NSTEMI	non-ST elevation myocardial infarction
O.C.T	optimum cutting temperature
PBS (Ca ²⁺ , Mg ²⁺)	phosphate buffered saline plus Ca ²⁺ and Mg ²⁺
PCR	polymerase chain reaction
PDGF-B	platelet derived growth factor subunit B
PE	polyethylene

PECAM-1	platelet endothelial cell adhesion molecule
PFA	paraformaldehyde
PI3-kinase	peptidase inhibitor 3 kinase
PINCH	particularly interesting Cys-His-rich protein
PVD	peripheral vascular disease
PVDF	polyvinylidene fluoride
RCA	right coronary artery
Repl/R	repetitive ischemia reperfusion
RepSham	repetitive sham
RIPA	radioimmunoprecipitation assay
ROI	region-of-interest
<i>Rplp0</i>	ribosomal protein lateral stalk subunit P0
rpm	revolutions per minute
RT	room temperature
RV	right ventricle
s	seconds
SDS-PAGE	sodium dodecyl sulfate-polyacrylamide gel electrophoresis
SEM	standard error of the mean
STEMI	ST elevation myocardial infarction
TGF- β 1	transforming growth factor beta 1
tMCAO	transient middle cerebral artery occlusion
TTC	triphenyl tetrazolium chloride
VCAM 1	vascular cell adhesion molecule 1
VEGF A	vascular endothelial growth factor A
VEGFR2/3	vascular endothelial growth factor receptor 2/3
wt	wild type
α -SMA	α -smooth muscle actin
β 1-B-AB	β 1 integrin blocking antibody
<i>β2m</i>	beta-2-microglobulin gene

List of figures

Figure 1.1: Schematic illustration of the cardiovascular system.	4
Figure 1.2: General structure of blood vessels.....	7
Figure 1.3: Schematic image of the coronary vasculature.	9
Figure 1.4: Schematic illustration of coronary collaterals.	13
Figure 1.5: Integrin receptor.	19
Figure 3.1: Endothelial cell-specific deletion of <i>Itgb1</i> causes no changes in flow velocity, but impairs FMD response upon short femoral artery (FA) occlusion.....	37
Figure 3.2: Illustration of hindlimb ischemia experiments.....	38
Figure 3.3: Hindlimb ischemia-induced arteriole vessel growth in the thigh is reduced in mice with endothelial cell-specific deletion of <i>Itgb1</i>	39
Figure 3.4: Hindlimb ischemia did not induce angiogenesis in the thigh of control and KO mice with endothelial cell-specific deletion of <i>Itgb1</i>	40
Figure 3.5: Hindlimb ischemia slightly induces arteriole vessel growth in the calf of control mice, but not in KO mice with endothelial cell-specific deletion of <i>Itgb1</i>	41
Figure 3.6: Hindlimb ischemia-induced angiogenesis in the calf is reduced in mice with endothelial cell-specific deletion of <i>Itgb1</i>	42
Figure 3.7: Illustration of the closed-chest myocardial ischemia model to induce transient, repetitive myocardial ischemia reperfusion (Repl/R).....	43
Figure 3.8: Illustration of Repl/R study design and area of interest for histological analysis.	44
Figure 3.9: LAD occlusion causes hypoxia and therefore ischemia in the left ventricle of the myocardium.....	44
Figure 3.10: Repl/R treatment induces EC proliferation in the ischemic and the non-ischemic myocardium.....	46
Figure 3.11: Repl/R-induced EC proliferation in the myocardium is inhibited by $\beta 1$ integrin blocking antibody treatment.....	47
Figure 3.12: Repl/R treatment induces arteriole number increase in the ischemic and the non-ischemic myocardium.	48
Figure 3.13: Repl/R-induced arteriole number increase in the myocardium is inhibited by $\beta 1$ integrin blocking antibody treatment.	49
Figure 3.14: Repl/R treatment contributes to infarction size reduction upon myocardial infarction.....	50
Figure 3.15: Repl/R-induced infarction size reduction is inhibited by $\beta 1$ integrin blocking antibody treatment.....	51
Figure 3.16: Repl/R treatment reduces the ischemic area and preserves cardiac function after MI.....	52

Figure 3.17: Repl/R-induced myocardial protection from MI is sensitive to $\beta 1$ integrin blocking antibody treatment.....	53
Figure 3.18: Tamoxifen-induced endothelial cell-specific deletion of <i>Itgb1</i> in cardiac ECs from adult mice.....	54
Figure 3.19: Repl/R treatment induces EC proliferation in the ischemic and the non-ischemic myocardium of control mice.....	55
Figure 3.20: Repl/R-induced EC proliferation in the myocardium is inhibited in <i>Itgb1</i> ^{iECKO} mice.....	56
Figure 3.21: Repl/R treatment induces arteriole number increase in the ischemic and the non-ischemic myocardium of control mice.....	57
Figure 3.22: Repl/R-induced arteriole number increase in the non-ischemic myocardium is inhibited in <i>Itgb1</i> ^{iECKO} mice.....	58
Figure 3.23: Repl/R-induced myocardial protection is partially impaired in <i>Itgb1</i> ^{iECKO} mice.....	59
Figure 3.24: Endothelin-1 and neuregulin-1 secretion is not influenced by short myocardial ischemia reperfusion.....	60
Figure 3.25: Ischemia-induced HGF secretion is diminished by $\beta 1$ integrin blockage and EC-specific $\beta 1$ integrin KO.....	61
Figure 3.26: Illustration of the myocardial ischemia model for permanent LAD occlusion and the study design.....	62
Figure 3.27: Revascularization after permanent LAD occlusion is impaired by $\beta 1$ integrin inhibition and EC-specific deletion.....	63
Figure 3.28: Cardiac function after permanent LAD occlusion is sensitive to pharmacological $\beta 1$ integrin inhibition and strongly declined by EC-specific deletion.....	64
Figure 3.29: Myocardial rupture and subsequent cardiac death after permanent LAD occlusion is strongly dependent on endothelial $\beta 1$ integrin.....	65
Figure 4.1: Schematic summary of $\beta 1$ integrin importance in myocardial ischemia models.....	77
Supplementary figure 1: Uncropped Western blot for $\beta 1$ integrin protein expression analysis.....	78

Declaration

Hereby, I declare that I wrote the presented dissertation independently and without impermissible external sources as stated under the compliance with “Grundsätze zur Sicherung guter wissenschaftlicher Praxis an der Heinrich-Heine-Universität”. Further on, I declare that I did not submitted the presented dissertation or a similar form of it to another academic institute and I did not complete another promotion attempt.

Düsseldorf,

Carina Henning

Eidesstattliche Erklärung

Hiermit erkläre ich an Eides Statt, dass ich die vorgelegte Dissertation eigenständig und ohne fremde Hilfe außer der dargelegten Quellen unter der Beachtung „Grundsätze zur Sicherung guter wissenschaftlicher Praxis an der Heinrich-Heine-Universität” angefertigt habe. Weiterhin versichere ich, dass ich die vorgelegte Dissertation oder eine ähnliche Form davon noch nicht bei einem anderen akademischen Institut eingereicht habe und bisher auch noch keinen Promotionsversuch unternommen habe.

Düsseldorf, den

Carina Henning

Danksagung

An diesem Punkt möchte ich mich herzlich bei meinem Doktorvater Ecki bedanken, der mir die Möglichkeit gegeben hat, meine Arbeit in seinem Institut anfertigen zu können. Vielen Dank für die andauernde Unterstützung, für die konstruktiven Gespräche, für die hilfreichen Ratschläge und den wissenschaftlichen Austausch. Ich bin dankbar dafür, dass ich so viel von ihm lernen durfte und er mich stets motiviert hat meine Ziele zu erreichen.

Weiterhin möchte ich mich auch bei Ulrich Flögel bedanken, für die Übernahme des Zweitgutachters, aber natürlich auch für seine große Hilfsbereitschaft und Unterstützung in wissenschaftlicher Hinsicht. Er hatte immer ein großes Gehör für meine Fragen, Bitten oder außergewöhnlichen Ideen.

Auch würde ich mich gerne bei Christian Heiss bedanken, als tollen Mentor und für seiner große Unterstützung, egal wie sehr er zeitlich eingespannt war.

Natürlich möchte ich mich auch bei allen aktuellen und ehemaligen Mitgliedern des Instituts für Stoffwechselphysiologie bedanken, für die so angenehme und kollegiale Arbeitsatmosphäre. Alle hatten immer ein offenes Ohr, haben mich bei Fragen und Problemen unterschützt und mich in meinem wissenschaftlichen, aber auch menschlichen Denken bereichert. Besonders bedanken möchte ich mich bei Anna für die tolle jahrelange Zusammenarbeit, den regen wissenschaftlichen Austausch, aber auch fürs Zuhören und zur Seite stehen allgemein. Sie ist nicht nur eine Kollegin für mich geworden, sondern auch eine gute Freundin. Auch den restlichen Mitgliedern will ich so sehr danke sagen, jedem von ihnen. Bitte fühlt euch alle angesprochen, auch wenn ich niemanden persönlich nenne.

Weiterhin würde ich mich gerne bei allen Mitgliedern des Forschungslabors für Kardiologie, Pneumologie und Angiologie bedanke. Vielen Dank, dass ihr mich so herzlich und freundschaftlich in euer Labor aufgenommen habt und mir mit Rat und Tat zur Seite standet.

Auch möchte ich dem SFB 1116 herzlich danken, ein Teil von diesem besonderen Programm gewesen sein zu dürfen. Der Austausch und die Kooperationen mit den anderen Instituten waren sehr bereichernd, in wissenschaftlicher wie auch in menschlicher Hinsicht.

Abschließend möchte ich mich natürlich bei meiner Familie und meinen Freunden bedanken, besonders bei meinem Vater und meinem Ehemann, ihr habt mich immer unterstützt, egal in welcher Lebenslage. Vielen Dank, dass ihr immer für mich da seid und an mich glaubt, wo immer mein Weg noch hinführen mag.